2012

Combinatorial analysis of tumorigenic microRNAs driving prostate cancer

William Budd
Virginia Commonwealth University

Combinatorial analysis of tumorigenic microRNAs driving prostate cancer

A dissertation submitted in partial fulfillment for the degree of Doctor of Philosophy at Virginia Commonwealth University.

by

William Thomas Budd
Masters of Science Virginia Commonwealth University 2010

Director: Zendra Zehner; PhD
Department of Biochemistry and Molecular Biology and Massey Cancer Center

Virginia Commonwealth University
Richmond, Virginia
July 2012

Acknowledgement

I would like to dedicate this work to many people that have supported me on my journey to become a scientist. First of all, my wife Lori, without her support and patience none of this work would have been possible. My children Preston and Marina made many sacrifices along the way. They gave up many evenings and weekends due to my work in the lab. Also, I would like to dedicate this work to my grandfather William Paris. He has been a tremendous influence in my life and taught me that if you are willing to work hard anything is possible. It is often said that it takes a village to raise a child and in my case that statement could not be any truer. Several individuals stepped up to help me out during a tough part of my life. Willie Amos, himself a cancer survivor, offered me a place to stay when I had no where else to go and gave me advice, guidance, and support. My "adopted" parents Phillip and Helen Skipper have been an active part of my life since my teen years. Mr. Skipper is a survivor of prostate cancer.

Scientifically, none of this would have been possible without my advisor Zendra Zehner. Dr Zehner has guided me intellectually throughout my years in her lab. She has also supported me emotionally when dealing with situations that developed in other aspects of life. Her advice and guidance were indispensable to my success. Walter Holmes, Danail Bonchev, Andrew Yeudall and Joy Ware were other members of my committee that offered guidance and support during project development. Members of the lab helped with various aspects of the research. Danielle Weaver assisted with the

networks analysis and proteomics. Sarah Seasholls helped with the miRNA arrays and the individual assays. Combinatorial analyses such as this are the future of science and they are only possible if working as a team. Unfortunately, there is not enough room to thank everyone that deserves recognition but be assured that I realize many people contributed to the development of this project.

Table of Contents

List of Tables

List of Figures

List of Abbreviations

3'-UTR	3'-untranslated region
5'-UTR	5'-untranslated region
ANOVA	Analysis of variance test
BCL-6	B-cell lymphoma 6
BPH	Benign prostatic hypertrophy
CaP	Prostate Cancer
CDK	Cyclin dependent kinases
CDKN1A	Cyclin dependent kinase inhibitor 1A
cDNA	Copy DNA
CT	Cycle threshold
EEC	Endometrial endometroid carcinomas
EGF	Epidermal growth factor
EGFR	Epidermal growth factor receptor
EMT	Epithelial to mesenchymal transition
ER	Endoplasmic reticulum
FBS	Fetal bovine serum
FFPE	Formalin fixed paraffin embedded
GRB2	Growth factor receptor bound protein 2
H&E	Hematoxylin and eosin
IR	Infrared
ITS	Insulin, transferrin, selenium
LCM	Laser capture microdissection
LNA	Locked nucleic acid
LOH	Loss of heterozygosity
MAPK-14	Mitogen-activated protein kinase 14
miR	MicroRNA
miRNA	MicroRNA
PBs	Processing bodies
PBS	Phosphate buffered saline
PCD2	Programmed cell death 2
PCR	Polymerase chain reaction
PERL	Pattern extraction and reporting language
PIN	Prostatic intraepithelial neoplasia
PSA	Prostate specific antigen
PTEN	Phosphatase and tensin homog
qRT-PCR	Quantitative real time PCR
RISC	RNA induced silencing complex

RPMA	Reverse phase protein microarrays
RPMI	Roswell Park Memorial Insitute medium
RT	Reverse transcription
UV	Ultraviolet
VEGFA	Vascular endothelial growth factor
XBP1	X-box binding protein 1

Abstract

COMBINATORIAL ANALYSIS OF TUMORIGENIC MICRORNAS DRIVING PROSTATE CANCER

By William T. Budd; PhD

A dissertation submitted in partial fulfillment for the degree of Doctor of Philosophy at Virginia Commonwealth University.

Virginia Commonwealth University, 2012

Major Director: Zendra Zehner; PhD Biochemistry and Molecular Biology

Prostate cancer is the leading non-cutaneous malignancy affecting men in the United States. One in every six men will be affected by prostate cancer. Due to the high incidence of prostate cancer, there is a need to develop biomarkers capable of identifying tumors from benign prostatic lesions. miRNAs are small molecules that regulate protein translation and impact cellular integrity when dysregulated. It is widely thought that miRNAs have the potential to serve as biomarkers.

This study utilizes a unique combinatorial analysis of miRNA dysregulation to identify key miRNAs involved in prostate tumor initiation, progression and metastasis. Numerous dysregulated miRNAs potentially influence cancer development. A unique bioinformatically driven, network based approach was used to rank potential miRNAs that drive tumor progression. This study showed that miRNAs preferentially regulate highly connected proteins and transcription factors that affect numerous downstream

targets. Thus dysregulation of a single highly connected miRNA could severely impact homeostatic maintenance of the tissue.

In combination with miRNA profiling of a cancer cell progression model, the utilization of laser captured microdissection was used to separate cancer specific microRNA portraits from background differences arising from stroma cells, lymphocytes, and remaining normal epithelial cells. Integration of miRNA profiles with information gathered using networks biology and targeted proteomics resulted in the identification of a key miRNA that affects prostate cancer development and may be useful as a novel biomarker for identification/ staging of prostate cancer.

Human miR-125b was identified as a potential miRNA suppressor of tumor formation. Previous work has identified miR-125-b as the post-transcriptional regulator of the ErbB2/ ErbB3 growth factor receptor family. Loss of miR-125b drives up expression of ErbB2/ ErbB3 activating downstream PI3K/AKT and RAS oncogene pathways. The level of miR-125b decreases 3-5-fold between benign and tumor epithelium. Further, miR-125b decreases during the development of prostatic intraepithelial neoplasia, which is regarded as an early indicator of prostate cancer. Thus miR-125b may be an ideal marker of early changes indicative of cancer. Restoration of miR-125b into highly tumorigenic, metastatic cells reduces mobility and invasion of underlying tissues. Taken together these data show miR-125b is a tumor suppressor in the healthy prostate.

Chapter 1

Introduction and Background

Background

Cancer is a highly heterogeneous, multifactorial disease that results from numerous genetic mutations, aberrant gene expression and miRNA dysregulation [1]. Prostate cancer (CaP) is the most frequently diagnosed visceral carcinoma and the second leading cause of cancer related deaths of men in the United States [2]. An estimated 241,000 men will be diagnosed in 2012 [3]. It is predicted that nearly 27,000 will eventually succumb to the disease and likely that one of every six men will develop CaP during their lifetime. The death rate increases significantly as the tumor becomes more poorly differentiated and treatment options decline as the tumor leaves the confines of the prostate [4]. Metastatic dissemination is the single most significant event occurring during prostate cancer progression. Despite the significance of metastasis, molecular events surrounding tumor progression and metastasis are poorly understood.

A variety of genetic and epigenetic factors such as age, race, heredity, diet, sexual frequency and physical activity are known to influence the development of prostate tumors [5]. Important ethnic differences exist in prostate cancer epidemiology. Diagnostic rates vary dramatically across racial subgroups with the Hispanic male having the lowest rate of CaP diagnosis (Figure 1-1) [3]. It is known that the diagnostic rate of prostate cancer in Hispanic men under estimates the actual number of Hispanic males with the disease as they are less likely than their Caucasian counterparts to participate in active screening by prostate specific antigen (PSA) analysis or digital rectal exam [6]. Even though it appears the overall diagnostic incidence of prostate cancer is slightly lower in African-Americans, the age specific death rate is nearly two times higher. It is hypothesized that the death rate is higher in African-Americans because they are more likely to be diagnosed at a higher

clinical stage of tumorigenesis than their Caucasian counterparts [7]. The single greatest predictor of death from prostate cancer is the stage at diagnosis; the higher the stage at the time of diagnosis the greater the likelihood of death. It is imperative that the underlying causes of ethnic differentiation be determined and the disparity eliminated.

A recent study published in *Cancer Causes and Control* showed that lifestyle habits did not significantly differ between African-American and white men [8]. The only potential variable that impacted prostate cancer diagnosis was education. The higher the education level of the patient, the more likely they were to participate in active screening methods and be diagnosed at an earlier stage. Men with graduate degrees have a lower death rate from prostate cancer than a man with a high school diploma or less (Figure 1-2). Although the discrepancy is highest in African-American men, the trend applies to men of every race. The most likely reasons for the educational variation are an increased awareness of one's health and better access to health care.

Diagnosing prostate cancer

Evidence clearly demonstrates that early detection of prostate tumors reduces the likelihood of death from the disease [9]. Although prostate cancer can only be definitively diagnosed by biopsy and histological examination, screening tools such as the prostate specific antigen (PSA) and digital rectal examination are useful in identifying patients that need biopsy. Prostate biopsy is not without risk. Bleeding and infection are commonly observed complications. The prostate biopsy is normally performed using a transrectal approach guided by ultrasound imaging. There is a large risk of infection as

Figure 1-1: Incidence and death varies among men of different ethnicities

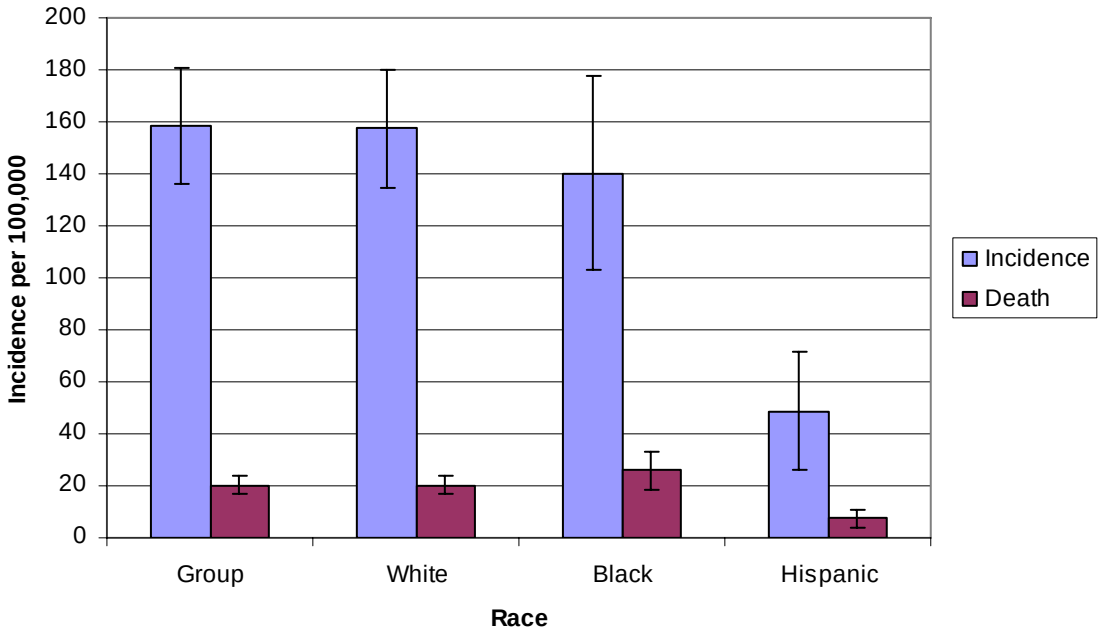

Figure 1-1: Incidence and death varies among men of different ethnicities

Analysis of data collected by the National Cancer Institute as part of the Surveilance, Epidemiology and End Results program [10]. Data were separated into groups by race and a table generated using Microsoft Excel.

Figure 1-2: Death rate from prostate cancer decreases with higher education

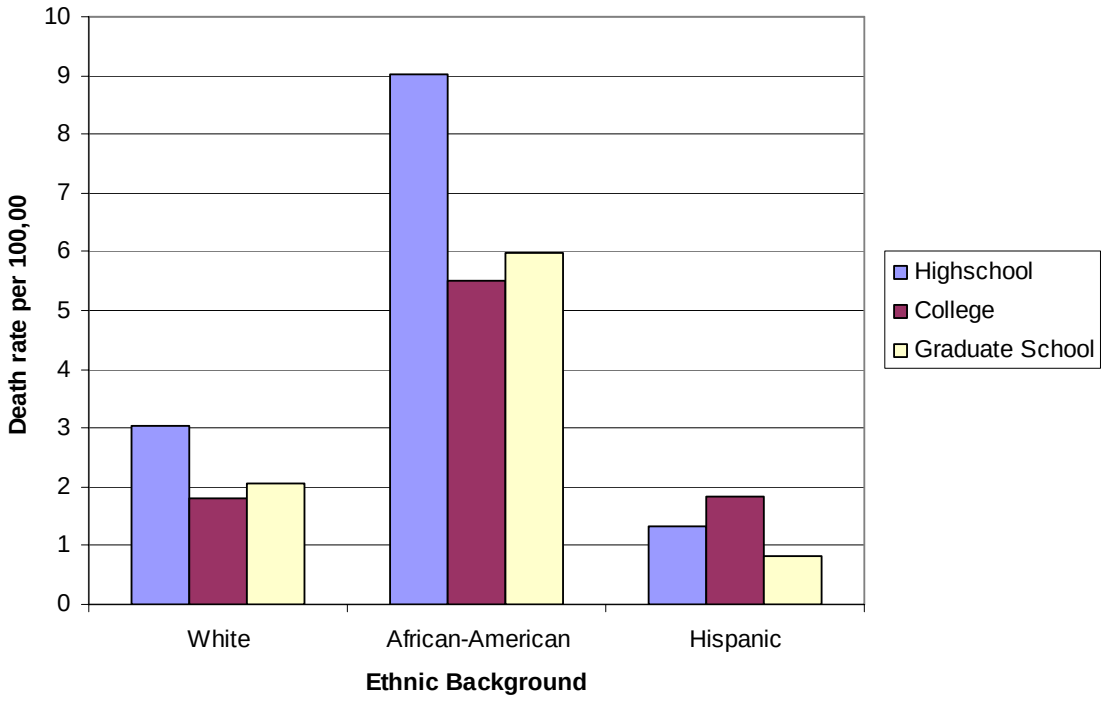

Figure 1-2: Death rate from prostate cancer co-varies with race and education

Analysis of data collected by the National Cancer Institute as part of the Surveillance, Epidemiology and End Results program [10]. Data was separated into groups by race and table generated using Microsoft Excel.

the needle passes from the rectum into the prostate. Many physicians minimize the incidence of infection through prophylactic antibiotic administration. The goal of active screening is to identify the population of patients that will receive the most benefit from biopsy.

Prior to the advent of the serum PSA test, it was estimated that only 25% of all prostate tumors were diagnosed and most were diagnosed at a later stage [9]. A physician cannot diagnose prostate cancer using a PSA analysis in isolation. PSA testing is only useful as a potential indicator of disease [11]. Studies show that in isolation the PSA is not a reliable indicator of disease and must be considered along with a digital rectal examination. The test is not as specific, many men have elevated PSA levels (>= 4.0 ng/ml) without any indication of cancer. It is estimated that 75% of elevated PSA assays are not caused by cancer. There are many causes of PSA elevation including benign prostatic hypertrophy (BPH) and infection.

Development of specific biomarkers to identify and stage prostate cancer

As PSA is not a specific indicator of prostate cancer, there exists a need to develop reliable biomarkers that can alert health care providers to the presence of early stage disease and distinguish indolent from aggressive tumors. Clearly, a great need exists for the development of more accurate biomarkers. In order to develop a more reliable marker for prostate cancer, one must understand the biological mechanism of tumor formation, progression and metastasis.

In recent years, microRNAs (miRNAs) have emerged as an important class of non-coding RNAs that influence post-transcriptional protein levels [12]. In the presence of

external cues and environmental stressors, miRNAs have the ability to induce rapid changes in the proteome allowing the cell to respond in a more precise and energy efficient manner [1]. Numerous cellular processes are affected by miRNA, including differentiation, growth/ hypertrophy, cell cycle control and apoptosis [13]. Mature miRNAs are ~ 22 nucleotides in length and regulate protein levels by binding mostly to the 3'-untranslated region (3'-UTR) of a messenger RNA, inducing translational repression or message cleavage. Aberrant expression of miRNAs contributes to the development of many pathological conditions including cancers of the breast, prostate, thyroid, and B-cell lymphomas [14]. Even though miRNAs have been casually observed to be associated with cancer of the prostate, there is not a clear consensus on specific miRNAs that contribute to oncogenesis. Dysregulated miRNAs may be useful as potential biomarkers for prostate cancer, as it has been shown that miRNAs can be exported from the cell and are found in most biological fluids.

Biogenesis of microRNA

The generation of miRNAs is a step wise process that results in the creation of a 22 nucleotide segment of RNA that is capable of inducing mRNA cleavage or translational repression. miRNA genes can be found as a component of a polycistronic transcript consisting of two to seven miRNAs under the control of a common promoter, exist in intergenic regions of the genome, or be found in an intron under the control of that gene's promoter [15, 16]. Creation of the pri-miRNA begins in the nucleus under the control of RNA polymerase II and ends with a several hundred nucleotide RNA molecule that possesses a characteristic stem loop structure. The pri-miRNA has a 5' cap and a

poly A tail on the 3' end (Figure 1-3) [17]. While in the nucleus, a ribonuclease like enzyme (Drosha) processes the pri-miRNA into a 70-100 nt fragment that retains the characteristic stem loop structure called a pre-miRNA. The pre-miRNA is exported into the cytoplasm by means of the nuclear export factor (Exportin V). Once in the cytoplasm, the loop of the pre-miRNA is cleaved and the stems are separated by Dicer into two 20-25 nt strands (mature miRNA). One of the strands accumulates and is incorporated into the RNA induced silencing complex (RISC).

miRNA function

Most eukaryotic genes are under the influence of at least one miRNA [18]. Many genes are controlled by multiple miRNAs. Dysregulation of a single miRNA can affect a multitude of proteins and potentially lead to a cancerous phenotype. MiRNAs regulate target messages via several mechanisms. Perfect binding between a miRNA and the target sequence will typically result in direct cleavage of the phosphodiester bond between nucleotides 10 and 11 of the target mRNA [19]. Message cleavage is carried out only by RISC complexes that contain Ago2 [20]. Incomplete complementarity of the miRNA to the 3'-UTR of the message is traditionally thought to result in translational inhibition [18]. Most mRNA degradation occurs through deadenylation, decapping and 5'-3' exonuclease degradation. Proteins needed for mRNA degradation have been shown to concentrate in cytoplasmic processing bodies (PBs). Experiments have shown that miRNAs and mRNA gene reporters also accumulate in these PBs, suggesting that co-localization of the miRNA/ mRNA may be another method of translational repression/ degradation.

Figure 1-3: Biogenesis of microRNA

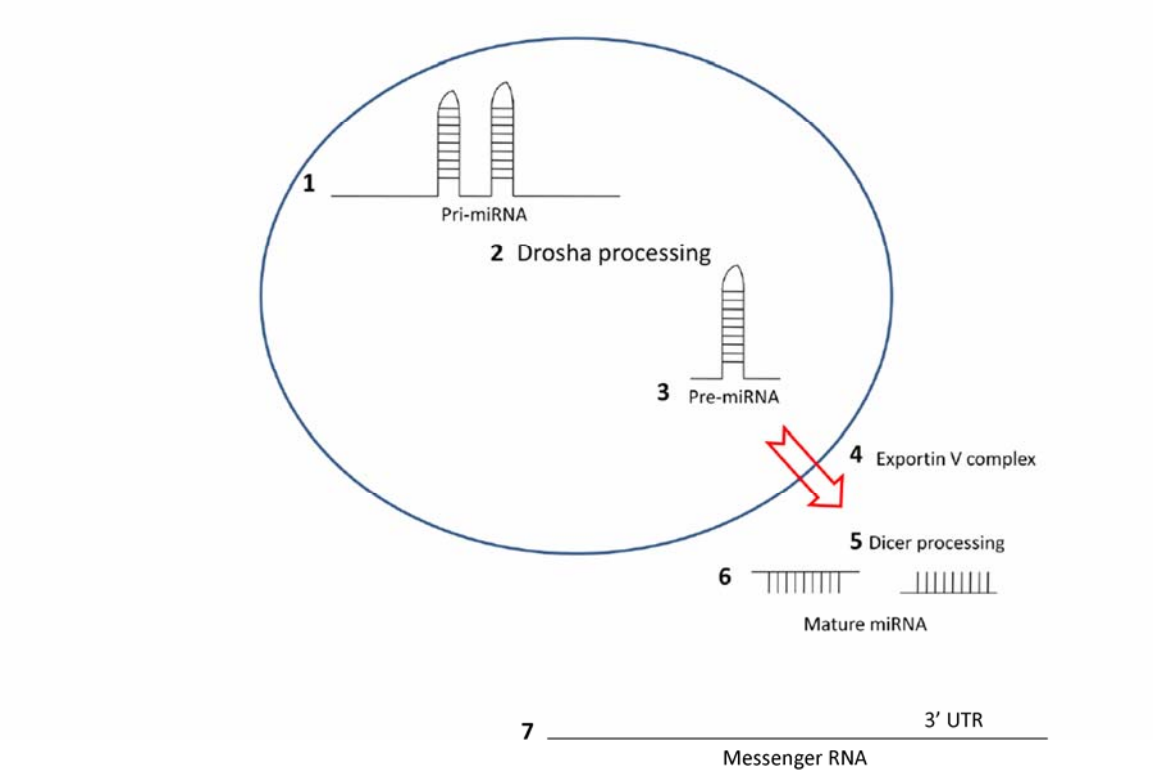

Figure 1-3: Biogenesis of miRNA

1. RNA polymerase II transcribes a 200- 700 nucleotide segment that is polyadenylated and 5' capped (pri-miRNA)
2. Ribonuclease enzyme (Drosha) processes the pri-miRNA into a 70-100 nt fragment known as the pre-miRNA
3. The pre-miRNA possesses a characteristic stem loop structure
4. Exportin V exports the pre-miRNA into the cytoplasm
5. The Dicer complex recognizes the characteristic stem loop structure and cleaves the pre-miRNA into a smaller RNA of approximately 22 nt (mature miRNA)
6. Each pre-cursor has the potential to generate two mature miRNA molecules
7. The mature miRNA recognizes complementary bases of the messenger RNA. The greatest numbers of proven interactions have been identified in the 3' UTR of message. However, interactions have been observed in the 5' UTR and within the coding sequence.

Many miRNA genes are dysregulated in cancer and influence tumor formation/ progression because they are located in regions of the genome that are commonly overexpressed or deleted [21]. Dysregulated miRNAs have been shown to contribute to oncogenesis by the loss of tumor suppressing miRNAs or increased expression of oncomiRs [22]. While tumor suppressing miRNAs are lost or reduced during oncogenesis, oncomiRs are amplified or overexpressed. Either loss of tumor suppressors or increased expression of oncomiRs ultimately results in increased cell growth, proliferation, invasiveness or metastasis. Aberrant expression of even a single miRNA has the potential to influence a large number of cellular processes as it is predicted that each miRNA has the potential to affect hundreds of proteins. Thus, dysregulation can destabilize homeostatic balance by affecting levels of a multitude of target proteins.

Genetically related prostate cancer progression model

Through the utilization of a unique genetically related prostate cancer cell progression model, we are able to identify miRNAs that likely contribute to prostate cancer initiation, progression and metastasis. Cell lines were derived through the immortalization of non-neoplastic prostate epithelium with SV40 large T antigen under the control of a SV40 promoter [23]. The parental (P69) cell line is poorly tumorigenic, and non-metastatic. P69 cells have a lower modal chromosome number than most other prostate cancer cell lines in use as these have been typically isolated from metastatic sites (LnCap, DU145, and PC3). An *in vivo* selection process was used to create cells with

Figure 1-4: Development of genetically related prostate cancer cell lines

Model for the development of a unique, genetically- related cancer progression model is presented. Human prostate epithelial cells immortalized with SV40 large T antigen were injected into a mouse and expanded using an *in vivo* selection process. At each passage, the cells acquired increased tumorigenic propensity as shown. The M12 subline possesses highly tumorigenic behavior and metastatic potential with 100% of mice injected suffering from disseminated cancerous lesions.

Figure 1-4: Development of genetically related prostate cancer cell lines

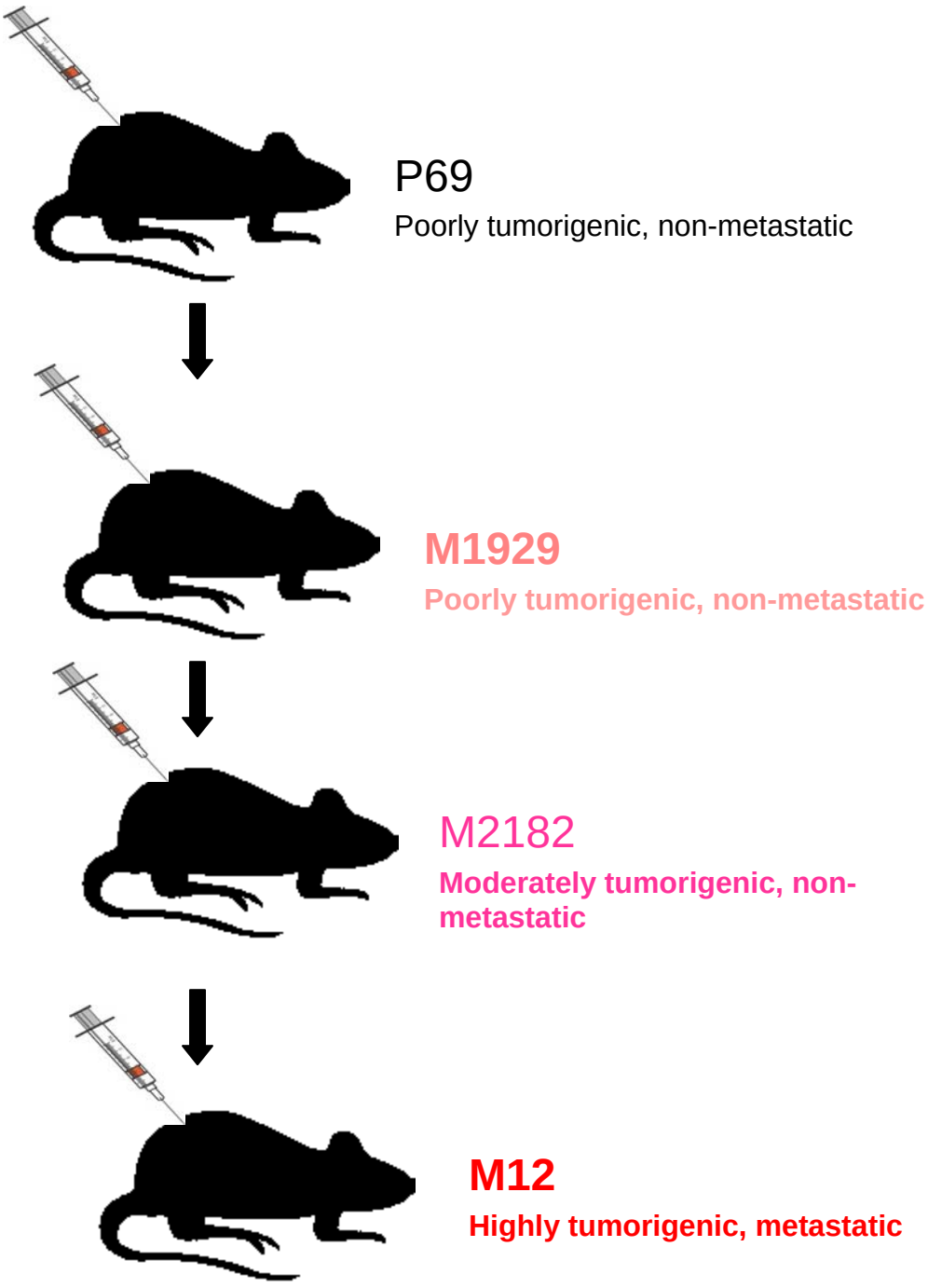

increased tumorigenicity and metastatic potential. After several rounds of *in vivo* selection following intra-prostatic and intra-peritoneal injections, a highly tumorigenic and metastatic variant (M12) was isolated. M12 cells routinely metastasize in nude, athymic mice following intra-prostatic/ intra-peritoneal injection and contain a chromosome 16:19 translocation. Restoration of chromosome 19 in M12 cells resulted in a variant that was less tumorigenic and non-metastatic (F6) [24]. These prostate cancer cell lines are unique as they are not derived from a primary tumor and are genetically related. They provide a model to study the molecular events that occur during prostate tumorigenesis and metastasis.

Identification of dysregulated miRNAs in prostate cancer cell progression model

Microarray technology has allowed researchers to simultaneously profile hundreds to thousands of molecules in a single assay [25]. The advent of array based profiling of miRNA expression is difficult because of the nature of the molecule [26]. miRNAs are on average only 22 nucleotides in length, vary dramatically in their abundance and melting temperature, and often only differ from one another by a single base. Despite the challenges, several technologies have been used with a modest degree of success [25]. Radiolabeled northern blots, bead based profiling methods, oligonucleotide arrays, and quantitative real time PCR applications have been utilized. Until recently, all of the methods described have been limited to samples for which one can obtain a relatively large amount of starting material.

The advent of locked nucleic acid technology has increased the sensitivity and specificity of miRNA based arrays [26, 27]. Locked nucleic acids have a reduced

conformational flexibility through the incorporation of a methylene bridge between the 4'- carbon atom and 2'- oxygen of the ribose ring [28]. Interspersion of locked nucleic acid nucleotides among non-locked nucleotides allows for fine tuning of the melting temperature of oligonucleotides. The inclusion of a single LNA base increases the melting temperature 2-10°C. LNA modified probes can be optimized in such a manner that a uniform melting temperature and normalized hybridization conditions can be established. LNA modified probes are ideal for profiling the entire miRnome as they have higher sensitivity and higher specificity than standard oligonucleotide probes. This technology allows researchers to profile precious tissue with a lower amount of starting RNA.

Several studies have reported numerous differences in miRNA expression that arise during cancer progression [25, 29, 30]. It remains to be determined for most of the miRNAs shown to be dysregulated, whether their aberrant expression is a cause or a consequence of cancer [31]. Evidence shows that aberrant expression of a single miRNA can induce oncogenic transformation [32]. Transgenic mice that overexpress miR-155 suffer a condition that mimics lymphoblastic leukemia. Although miR-155 has been shown to be causative in acute lymphoblastic leukemia, evidence for a potential role in prostate cancer is unclear.

Human-miR-21 has been described as the ubiquitous solid tumor oncomiR and is overexpressed in prostate, lung, pancreas, breast, stomach, and colon cancers [33]. Despite claims that increased miR-21 expression is observed in prostate cancer, it has been shown that knockdown of miR-21 does not affect proliferative or invasive properties in DU145 and PC3 cancer cell lines [34]. In matched human samples, there are approximately as many

men with prostate cancer that have increased miR-21 expression as those that do not. A role for miR-21 in the progression of CaP is not clear.

Attempts to identify a miRNA signature of prostate cancer using screens have failed to reveal a consistent pattern that can identify malignant epithelium from its normal counter part. The results are inconclusive and often contradictory. There are several potential reasons for disagreement among profiles. Improper study design, underestimated treatment of patients, underlying heterogeneity of the tissue, and platform inconsistencies are just a few of the reasons for potential disagreement among studies [35].

Identification of key signaling proteins affecting tumorigenesis

The advent of high throughput technologies has enabled researchers to identify hundreds of genetic mutations that lead to oncogene activation [36]. Previous researchers have shown that point mutations do not occur randomly in known oncogenes. Instead, there exist a relatively small number of codons that are affected disproportionately. There are many methods that can be utilized to discover somatic mutations that may be driving cancer progression. These mutations are often described as oncogenic "hits". Oncogenic mutations confer a survival advantage to the cell by aberrant influence of intracellular protein signaling pathways [37].

Common pathways that influence cancer progression are survival, growth, apoptosis, and cell cycle control pathways. Genetic sequencing and gene expression profiling cannot determine pathway activation. It has been shown that mRNA levels correlate poorly with the amount of an active protein. In order to determine the activation level of signaling proteins, proteomic technology is needed. Reverse phase protein

microarrays (RPMA) allow for the simultaneous evaluation of hundreds of proteins at a single time point [37].

RPMA was developed to interrogate a small number of cells and measure multiple analytes [37, 38]. RPMA arrays immobilize a protein analyte onto an array substrate and probe with an antibody. Potentially, hundreds of samples can be adhered to a single array. As only minute amounts are spotted onto the array, a sample can be extended across hundreds of slides. This approach allows researchers to profile hundreds of proteins across hundreds of samples and better characterize the intracellular signaling proteome.

Confirmation of microRNA dysregulation in human samples

Many studies have used human tissue obtained from prostatectomy or biopsy in an attempt to identify potential miRNA markers of cancer progression. For the most part, these studies have failed to identify miRNAs that can be used as biological markers for the diagnosis of prostate cancer let alone can be utilized to stage prostate tumors [39]. Nearly all of the published work using miRNA screens of human prostate tumors utilizes homogenized tissue following gross dissection. It is likely that the tissue being analyzed remains contaminated with other cell types such as stroma, blood vessel, nerves, smooth muscle or lymphocytes. In order to accurately profile a tissue's disease state, diseased cells must be removed from surrounding tissue and examined in a pure cell population [40].

Laser capture microdissection (LCM) is a technique that allows one to isolate pure cell populations from heterogeneous tissues [40]. LCM uses infrared and/or ultraviolet lasers to attach visualized cells to a thermolabile polymer cap. Not only can pure

populations of normal epithelium and stroma be separated from diseased tumor epithelium or activated stroma, but ultimately tumor cells at varying stages of disease can be individually captured. After dissection, the captured cells can be used to analyze all types of biological macromolecules, such as miRNAs, mRNA, or proteins can be isolated from these pure populations of captured cells.

Systems biological perspective

It is essential to have an understanding of the individual molecules that contribute to complex phenotypes such as cancer and metastasis [41]. However, complex systems are not just an assembly of genes, proteins, and other macromolecules. Emergent properties arise out of complex non-linear interactions amongst all the molecules in a cell. Traditional molecular biological and biochemical studies have uncovered many molecules that contribute tumorigenic properties upon dysregulation. Traditional reductionist approaches have viewed the human body as a collection of constituent parts [42]. The tradition of medicine has been to isolate and treat the defective component in isolation and hope the result is indicative of the whole. Unfortunately, complex phenotypes cannot be reduced to a single molecule as they discount the emergent properties that arise from the non-linear interaction of multiple components. The reductionist approach has been quite successful at treating many conditions but has failed to eradicate more complicated pathologies such as cancer. Cancer is the end result of numerous alterations in biochemical pathways and networks [43].

An alternative to the traditional reductionist philosophy is the concept of systems biology. Systems biologists seek to gather information about multiple types of molecules

(genes, proteins, RNA) in the cell and integrate the information in order to understand the perturbations underlying a given pathology from a systems level. High throughput technologies such as DNA microarray, genome sequencing, proteomics, and qRT-PCR profiling allow for the simultaneous acquisition of thousands data points. Integration of multiple data sources increases the likelihood of identifying key pathways involved in cancer initiation, progression and metastasis.

Complex interactions can be modeled as a biological network with the macromolecule represented as a node and interactions modeled as edges [1]. Network properties are described mathematically. An important indicator of molecular importance is node degree. A highly connected node is more likely to be essential and cause disease when dysregulated [44, 45].

Network properties identify key proteins affected by miRNA dysregulation

Traditionally, researchers using array based methods rank significance based on relative expression differences. This method assumes that the most differentially expressed miRNA is the most significant contributor to the observed phenotype. It is reasonable to hypothesize that small changes in some miRNAs may effect large changes in the tissue as some targets are more important than others. It is well known that highly connected proteins are more likely to be essential, and disease associated [44, 45]. Perturbations of these highly connected proteins are more likely to result in diseases such as cancer [1].

Hypothesis

This project utilizes a unique combinatorial approach to understand the impact of miRNA dysregulation upon prostate cancer progression. A novel isogenic prostate cancer cell progression model has been selected as it more closely mimics tumor progression as it occurs *in vivo*. I propose that miRNA profiling of these unique cell lines will better serve to identify miRNAs that contribute to cancer progression and metastasis. Arrays that utilize LNA™ modified probes are more advantageous than other array technologies currently in use as they are more sensitive and more specific. Differences in miRNA expression will be verified using quantitative real time PCR (qRT-PCR) with either TaqMan® probes or Exiqon® LNA™ probes.

miRNA significance will be ranked not just by expression differences but rather the identification of critical downstream protein nodes through the use of methods used in biological network analysis. As miRNAs affect protein levels, key signaling molecules will be measured using the RPMA format in conjunction with the George Mason University Center for Applied Proteomics and Molecular Medicine. Integration of miRNA profiles and proteomic data have the potential to increase the success of identifying novel miRNAs affecting tumorigenesis in the cancer progression model. It is our hypothesis that a combinatorial analysis of an RPMA profile and a miRNA array will reveal dysregulated miRNAs that affect significant downstream targets imparting an onocgenic advantage. The combination of the data revealed in the cancer cell line miRNA screens, RPMA proteomics along with information from our networks analysis will be used to rank the dysregulated miRNAs and each will be verified in human samples. We propose that the utilization of laser capture microdissection to obtain a pure

cell population from a heterogeneous prostate tumor sample will reveal miRNAs that can be used for diagnostic purposes. Overall, this combinatorial approach will reveal miRNAs that drive prostate cancer progression when dysregulated and may be useful as newer, more relevant biomarkers to identify and stage prostate cancer.

Specific aims of project

- Identify key microRNAs involved in prostate tumorigenesis using a systems biological approach.
- Using an Exiqon® miRNA screening platform with RNA collected from genetically related prostate cancer cell lines. Develop a list of prioritized miRNAs that affect key proteins involved in tumorigenesis of the prostate gland. .
- Measure the relative expression levels of the priority miRNAs determined in aim1 using microdissected tissue of malignant cells and benign cells obtained from flash frozen human prostate biopsy samples.
- Modify the expression of the differentially regulated miRNAs in a prostate cancer cell model and evaluate effects on tumorigenesis using a variety of *in vitro* analyses.
- Ultimately the effect of miRNA modulation on tumorigenic and metastatic properties will be evaluated in male, nude, athymic mice (Future Studies).

Chapter 2

Networks analysis reveals preferential miRNA regulation of highly connected protein nodes

Complex physiological processes can rarely be ascribed to a single molecule [46]. Instead, they arise out of the interaction and coordination of large numbers of proteins, nucleic acids, and other macromolecules. Healthy organisms intricately regulate thousands of components with remarkable fidelity and accuracy [1]. Protein-protein interactions are essential to many biological processes and mediate many of the reactions necessary to sustain life. A key strategy to understand the molecular workings of the cell is the systematic identification of crucial protein interactions [47].

These interactions can be modeled as a biological network with proteins represented as nodes and interactions among the proteins represented as edges. Topological features of the network can be described mathematically and used to infer molecular contribution to network/cellular stability. As observed, widespread miRNA dysregulation contributes to the development of many forms of cancer including cancer of the prostate. This work utilized a systems based, network approach to understand the impact of miRNA dysregulation on the overall stability of a protein-protein interaction network (Figure 2-1).

Identification of dysregulated miRNAs contributing to prostate cancer

MiRNAs associated with prostate cancer (111) were compiled from the miR2disease online resource [48]. Utilizing the built in search function for miRNAs associated with a specific disease, the database was queried using the term "prostate carcinoma" to identify miRNAs related to prostate tumorigenesis and included both causal and unspecified relationships. Using a PERL script, each miRNA was further

evaluated to extract information regarding its expression pattern and literature references for each dysregulated miRNA.

Proven targets of miRNAs associated with prostate cancer

A comprehensive record of proven miRNA/gene interactions was assembled from the Tarbase and miRecords repositories of experimentally supported miRNA targets downloaded in May 2011 [49, 50]. Utilizing a PERL script, multiple entries were eliminated and both resources were combined into a single non-redundant list. Dysregulated miRNAs contributing to prostate cancer were associated with validated targets using our comprehensive record.

Prostate gland transcriptome profiles were obtained from the Unigene database in order to build a protein-protein interaction network of prostate specific miRNA/ target interactions [51]. Transcripts that show any level of expression in the prostate gland were extracted and identifiers converted to HUGO gene symbols using a PERL script. By combining the information obtained from the miR2disease database, comprehensive miRNA/ target interactions and the list of expressed transcripts in the prostate, we compiled a total of 608 confirmed protein targets that are affected by miRNA dysregulation in the prostate.

Literature mined prostate protein-protein interaction network

The Agilent literature search (v2.76) tool was used in conjunction with Cytoscape 2.8 to infer two protein-protein interaction networks [52, 53]. The first was built using known prostate cancer miRNA targets. Each protein in the candidate list of 608 known prostate

cancer miRNA target proteins was used as a search term in the Agilent literature search tool and the search was controlled to limited interactions to Homo sapiens with a maximum of 10 hits per search string/ search engine. The second network was built in the same manner using 608 randomly chosen proteins that are expressed in the prostate gland according to the Unigene database but chosen without regard to known miRNA status [51]. Following network inference, visualization was accomplished using Cytoscape and topological network descriptors were estimated using CentiScaPe [54].

Randomization of prostate miRNA target protein-protein interaction network

The prostate cancer miRNA target network was shuffled 50,000 times using a degree preserving edge shuffle random network plugin developed by engineers at Syracuse University and implemented in Cytoscape. The plugin was downloaded (http://sites.google.com/site/randomnetworkplugin/Home) as a .jar file and installed in the Cytoscape package. The application was run across two processors and repeated 50,000 times to generate the best results.

Transcription factor analysis

Transcription factors were compiled from the TFCAT curated catalog of transcription factors [55]. Only genes determined to be transcription factors were downloaded and the default choice was selected for the remaining download filtering options. The file was exported into a tab delimited text file and a PERL script utilized to remove any redundant proteins. After filtering, there were a total of 3419 transcription factors.

Transcription factors targeted by miRNAs dysregulated during tumorigenesis of the prostate were compiled by intersecting the list of miRNA targets with the table of transcription factors using PERL. The process was repeated using the list of randomly associated proteins.

Statistical analysis

Differences in network distributions were evaluated using an Analysis of Variance test (ANOVA) with significance set at probability <= 0.05. All statistical analyses were performed using JMP 8.0 (Statistical Analysis Software Cary, NC). The distribution of node degree for the prostate miRNA targeted network and the randomly selected prostate protein network were created using the R Project for Statistical Computing (http://www.r-project.org/).

Figure 2-1: Outline of process to determine network properties of miRNA targets

MiRNAs contributing to the development of prostate carcinoma were downloaded from miR2Disease and associated with proven targets. A protein-protein interaction network was inferred using literature references with Agilent Literature Search. Network properties were calculated using CentiScape and pathway enrichment was estimated using Agilent.

Figure 2-1: Outline of process to determine network properties of miRNA targets

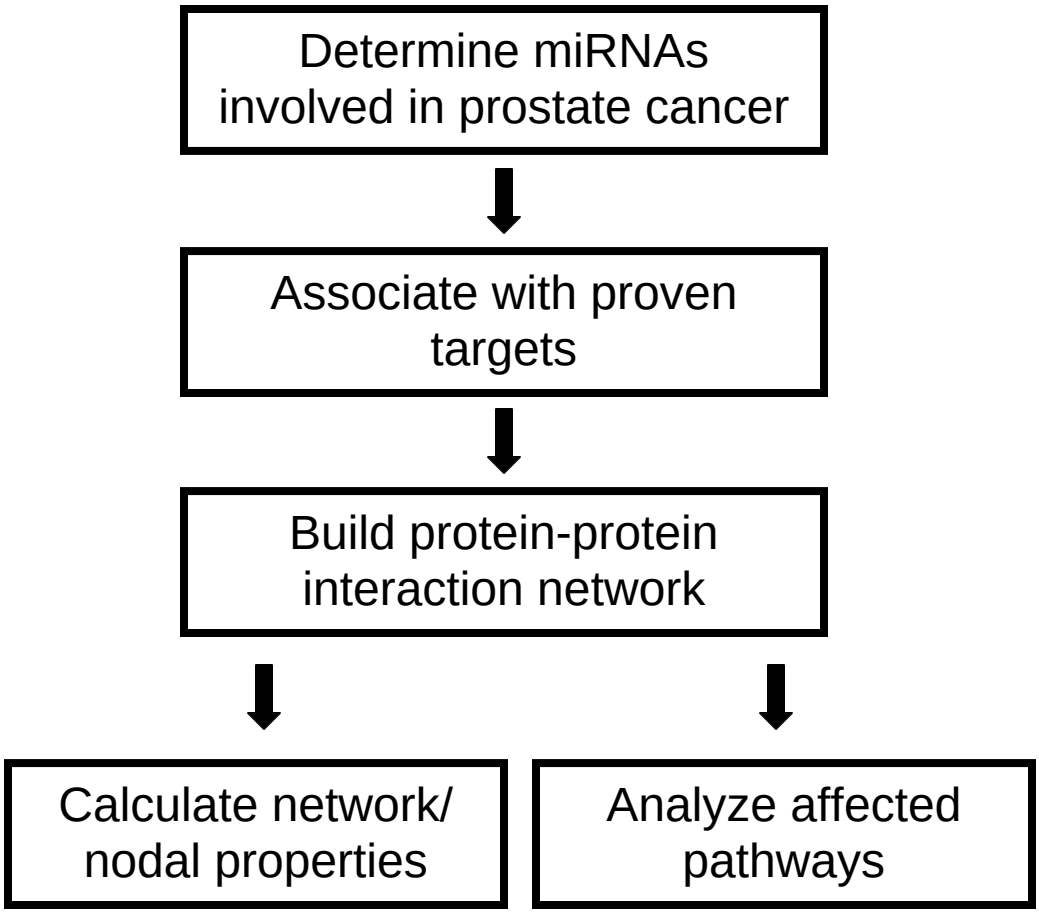

Analysis of miRNA contributions to prostate tumorigenesis

Dysregulation of miRNAs may result in tumor formation and progression through the increased expression of oncomiRs or decreased expression of tumor suppressors. Mir2disease is a manually curated database which associates experimentally supported miRNA dysregulation with disease [48]. Consideration of only experimentally proven miRNA/ disease associations will not reveal every miRNA that is involved in prostate cancer. However, this approach is more favorable than approaches that consider putative interactions as they suffer from an inherent lack of sensitivity evidenced by large numbers of false positive predictions. A search of the miR2disease database reveal a total of 111 miRNAs that contribute to prostate tumorigenesis and cancer progression when significantly dysregulated. It remains to be determined whether or not miRNA dysregulation is the cause of tumorigenesis, a consequence of tumorigenesis or both. Previous authors had observed a global decrease of miRNA expression levels during tumorigenesis leading to the hypothesis that most miRNAs function as tumor suppressors [56]. Our analysis using the miR2diease database finds that there are approximately as many oncomiRs as tumor suppressing miRNAs. Sixty microRNAs showed increased expression levels (oncomiRs) in tumor samples compared to normal tissue whereas 51 miRNAs decreased in tumor samples (tumor suppressors) (Figure 2-2).

Figure 2-2: microRNA dysregulation in prostate cancer

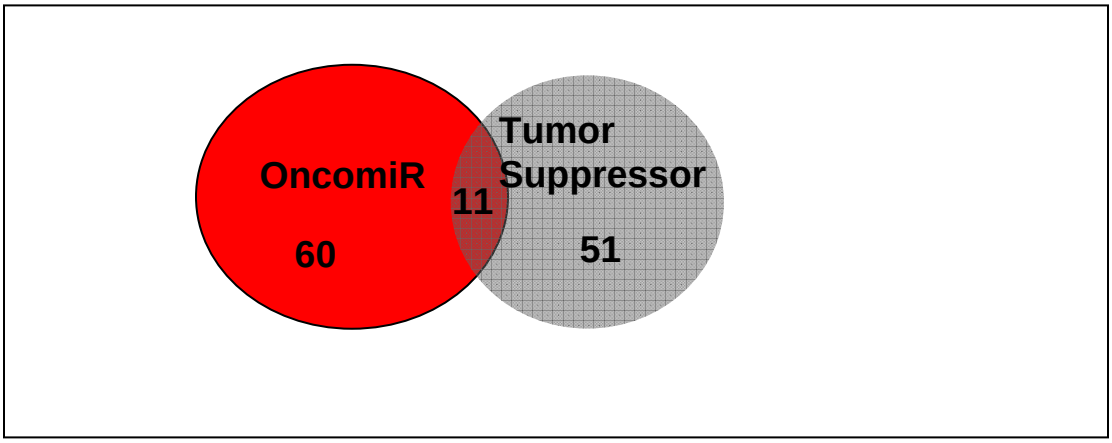

Figure 2-2: microRNA dysregulation in prostate cancer

microRNAs dysregulated during prostate cancer progression were extracted from the miR2disease database along with their potential role in cancer development as defined by their expression profiles [48]. A *Venn* diagram illustrating the numbers of oncomiRs, tumor suppressors, and miRNAs that can function as either oncomiRs or tumor suppressors was created.

Interestingly, there are 11 examples in which the same miRNA displays contrasting behaviors in prostate tumors. These have the potential to act as either oncomiRs or tumor suppressors during tumorigenesis. Their expression level may vary depending upon the degree of cellular de-differentiation. For example hsa-miR-125b (miR-125b) has been reported by several groups to significantly decrease during tumorigenesis. MiR-125b coordinately regulates two members of the human epidermal growth factor receptor family (ErbB2/HER2/ NEU, ErbBB3/HER3) [14, 25, 57, 58]. Decreased expression or loss of miR-125b results in an increase in both ERBB2/ERBB3 protein levels thereby enhancing the invasive potential of the cell leading to tumor formation and progression [59].

Conversely, the androgen independent LNCaP sublines (CDS1 and CDS2) produce higher levels of miR-125b compared to the androgen dependent LnCaP sublines [58]. Treatment of androgen dependent LNCaP cells with synthetic miR-125b allowed them to survive in androgen depleted media. The cellular effects of miR-125b under androgen dependent conditions are mediated through the translational suppression of BAK1 [14]. BAK1, a member of the BCL2 protein family, functions as a pro-apoptotic factor [60]. Suppression of pro-apoptotic factors increases the oncogenic potential of the cell.

A similar finding is observed with hsa-miR-146a, which can function as an oncomiR in many tumors, but in androgen independent tumors functions as a tumor suppressor [25, 61]. Altogether these two examples illustrate how a single miRNA (miR-125b, miR-146a) can function as a tumor suppressor or an oncomiR dependent upon another variable, in these cases androgen dependence. Most likely similar situations could be found for the other overlapping group members.

Protein-protein interaction of prostate cancer miRNA targets show scale free behavior

Nearly every biological process depends upon protein-protein interactions [62]. Disruptions or perturbations in these interactions underlie many human diseases including cancer. Protein- protein interactions are modeled using a system based, network approach and described mathematically. Two protein- protein interaction networks were built with information gathered from the PubMed , Online Mendelian Inheritance in Men, and the US Patent Office databases using the Agilent Literature Search plugin in Cytoscape. Topological network characteristics were measured using CentiScaPe [52, 54, 63].

The first network was built using proven targets of dysregulated miRNAs shown to contribute to the development of prostate cancer. A second similar network of randomly sampled proteins expressed in the prostate, but chosen without regard to miRNA status was compiled. Both the network of dysregulated miRNA protein targets and randomly selected prostate proteins possessed a scale free form (Figure 2-3). However, they differed in the average connectivity as measured by node degree with the miRNA targeted network having a much higher average connectivity measure. Node degree is a measure of interactions among the molecules in a network. In a scale free network, as the node degree increases, the frequency observed decreases, with most nodes having only a few connected neighbors. This functional organization commonly seen in a complex system ensures redundancy in the system resulting in some amount of fault tolerance [46].

Figure 2-3: Targets of miRNAs are more highly connected than randomly chosen proteins

Two shortest path protein-protein interaction networks were built using the Agilent literature search function within Cytoscape 2.8 and topological measures evaluated using CenstiScaPe 2.76. The first network was built using proven targets of miRNAs that are dysregulated during the development of prostate cancer (Red). The other network was built from randomly chosen proteins that are expressed in the prostate but chosen without regard to miRNA status (Blue). Frequency distributions of the node degree for the two shortest path networks are displayed

Figure 2-3: Targets of miRNAs are more highly connected than randomly chosen proteins

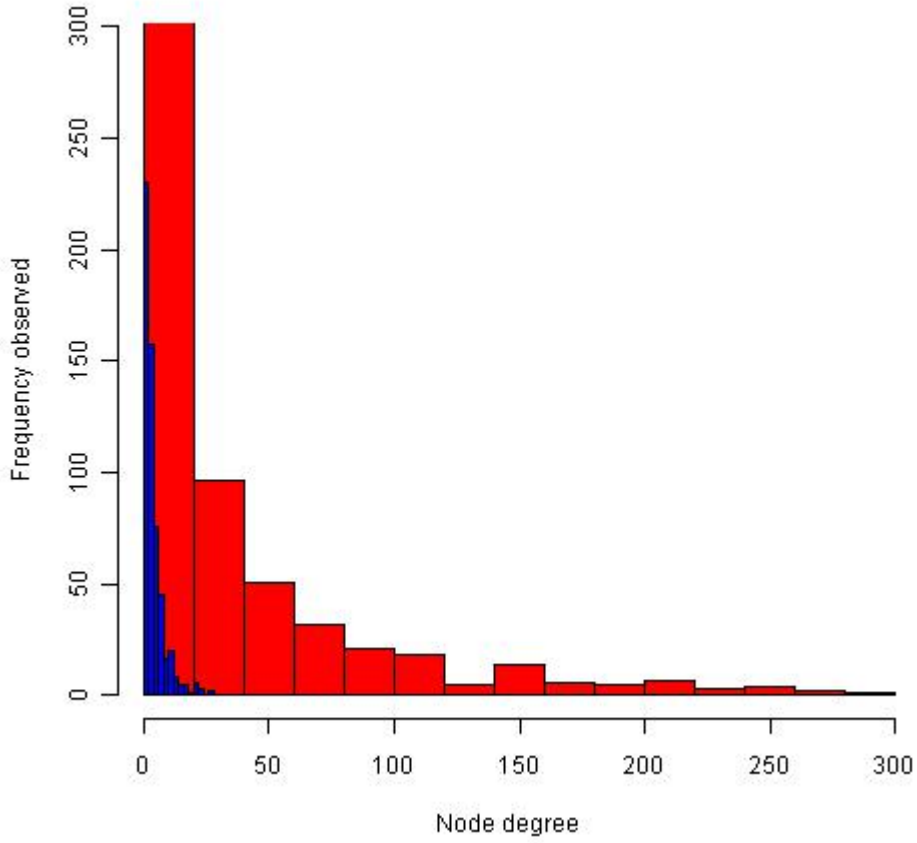

MiRNAs dysregulated in prostate cancer preferentially regulate highly connected proteins

Node degree is one topological measure that can be used to infer the contribution of a protein towards cellular/network stability. Analysis of the average node degree revealed an overall enrichment of highly connected proteins in the prostate cancer miRNA target network not seen in the network of randomly selected prostate proteins ($p <= 0.0001$) (Table 2-1). The average protein in the miRNA targeted network was connected to nearly 30 other proteins. Conversely, the average protein in the randomly chosen network was only connected to approximately 5 others. Of the top candidates in the prostate cancer miRNA targeted network, mitogen-activated protein kinase 14 (MAPK14) was the most connected with a node degree of 290. It is important to note that the node degree represents a maximum protein potential, not all 290 proteins will interact with MAPK14 at the same time. Instead, MAPK14 will interact with a small number of proteins at any one moment and the neighbors change depending upon the needs of the cell. The most highly connected protein in our randomly generated prostate network was only connected to 28 other proteins, a ten-fold difference. A list of prostate cancer miRNA targeted proteins with a node degree over 200 is included in Table 2-2. This list is rich in well known cancer related proteins, many of which are current or proposed drug targets.

Perturbation of these highly connected nodes is more likely to negatively impact network stability [1]. It has been shown that molecules with a higher node degree are essential to the cell and their loss often results in a disease state such as cancer [44, 45]. There is a positive correlation between protein essentiality and connectivity indicating

Table 2-1: Comparison of network node distribution of the prostate cancer miRNA target network and the randomly chosen prostate protein network

Network	Mean Degree	Standard Deviation	Minimum	Maximum
Prostate cancer miRNA target protein	29.80	47.75	1	290
Random prostate protein	4.46	4.24	1	28

Table 2-2: Protein nodes with connectivity degrees greater than 200

Protein	Name	Node degree	Function	Known miRNA
MAPK14	Mitogen activated protein kinase 14	290	Cell proliferation, differentiation, and transcription regulation	hsa-miR-124, hsa-miR-24
SP1	SP1 Transcription Factor	269	Cell growth, differentiation, and apoptosis	hsa-miR-218, hsa-miR-124, hsa-miR-29b
VEGFA	Vascular endothelial growth factor	267	Angiogenesis, vasculogenesis, and vascular endothelial cell growth	hsa-miR-205, has-miR-200b, hsa-miR-126, hsa-miR-93
CASP3	Caspase 3	258	Execution phase of apoptosis	hsa-let-7a, hsa-let-7e
MYC	Transcription factor	254	Cell cycle progression, apoptosis, and cell transformation	hsa-miR-24, hsa-miR-145, hsa-miR-34c-5p, hsa-miR-34a, hsa-miR-34b*, hsa-let-7c
EGFR	Epidermal growth factor receptor	248	Cell proliferation	hsa-miR-1, hsa-miR-7, hsa-miR-16
BCL2	B-cell lymphoma 2	247	Apoptosis	hsa-miR-15, hsa-miR-1, hsa-miR-20a, hsa-miR-34a, hsa-miR-181a, hsa-miR-296-5p, hsa-miR-15a, hsa-miR-153, hsa-miR-17, hsa-miR-15b
CTNNB1	Catenin Beta 1	232	Cell growth regulator and cell adhesion	hsa-miR-155
JUN	Jun proto oncogene	229	Transcription factor, angiogenesis, apoptosis	hsa-miR-15a, hsa-miR-16, hsa-miR-30
TNF	Tumor necrosis factor	217	Cell proliferation, differentiation, apoptosis, lipid metabolism, and coagulation	hsa-miR-146a
FGF2	Fibroblast growth factor 2	216	Cell proliferation, angiogenesis	hsa-miR-16
TP53	Tumor protein 53	213	Cell cycle regulation and apoptosis	hsa-miR-129-5p, hsa-miR-125a-5p, hsa-miR-1285, hsa-miR-125b
PPARG	Peroxisome proliferator activated receptor gamma	213	Regulator of adipocyte differentiation	hsa-miR-27b
ESR1	Estrogen receptor 1	212	Cell growth, differentiation, and sexual reproduction	hsa-miR-302c, hsa-miR-20b, hsa-miR-19b, hsa-miR-18a, hsa-miR-181a, hsa-miR-206, hsa-miR-22, hsa-miR-181b, hsa-miR-193b, hsa-miR-19a
TGFB1	Transforming growth factor beta 1	208	Cell proliferation, differentiation, adhesion, and migration	hsa-miR-141, has-miR-128a
CCND1	Cyclin D1	203	Cell cycle control	hsa-miR-16, hsa-let-7b, hsa-miR-17, hsa-miR-195, hsa-miR-34a, hsa-miR-20a, hsa-miR-15a, hsa-miR-19a, hsa-miR-155, hsa-miR-503

that the more connected a protein is, the greater the likelihood that it is essential to life. Conversely, molecules with a lower number of connecting neighbors are not as likely to disrupt the system when they are perturbed. Disease causing genes are more likely to encode highly connected proteins [64, 65]. This analysis indicated that miRNAs have a strong likelihood of impacting the network structure and dysregulation is more likely to affect essential proteins causing diseases like cancer.

Randomization of the prostate cancer miRNA targeted network was performed to estimate the likelihood that this arrangement arose out of chance. The network was compared to a null model made by a shuffled (50,000 X) version of itself [66]. Shuffling was accomplished using an algorithm that preserves the overall node degree distribution in order to emulate the properties found in the prostate miRNA targeted network. The randomized networks did not result in a mean clustering coefficient (C = 0.029) similar to the protein-protein interaction network (C = 0.621). This measure is evidence that the arrangement of the proteins in this network is not random, but results from clusters of associated proteins, as would be expected in a complex, living system. Randomly generated networks of the same degree and distribution do not maintain this modularity.

OncomiRs regulate more highly connected proteins than tumor suppressors

A one way analysis of variance (ANOVA) revealed statistically significant connectivity differences among the targets of oncomiRs and targets of tumor suppressing miRNAs ($F_{2, 503} = 6.2821$, $p=0.002$). Oncogenic miRNAs showed a regulatory preference towards more highly connected proteins. While the connectivity of an oncomiR target was 39, the average connectivity of a tumor suppressor miRNA target was only 27 other

proteins (Table 2-3). Interestingly, the targets of the 11 miRNAs that can function as tumor suppressors or oncomiRs depending upon a second variable exhibited a much higher average target node degree (61) than either oncomiRs or tumor suppressors alone.

Cancer related proteins in general show greater node degree and higher connectivity than non-cancer associated proteins [67, 68]. The protein products of tumor suppressing genes are known to be more centrally located and more highly connected than the products of oncogenes [69]. In our analysis we found that the connectivity of oncomiR targets was higher than the targets of tumor suppressing miRNAs. It is important to remember that miRNAs are negative regulators of protein translation and the targets of oncomiRs would be tumor suppressive proteins. This analysis confirmed that miRNA dysregulation contributed to the development of prostate cancer.

Highly connected proteins possess more than one miRNA binding site

A comparison of proteins in the prostate cancer miRNA targeted network revealed that there was a positive correlation between protein connectivity and the number of different experimentally proven miRNA binding sites in the 3'-UTR (Figure 2-4). That is, as a protein interacts with a higher number of other proteins, it is more likely to be regulated by multiple miRNAs. MiRNAs may act cooperatively through the simultaneous interaction of multiple miRNA species with the 3'-UTR of a transcript [70]. In the case of vascular endothelial growth factor (VEGFA), multiple distinct binding sites were observed in the 3'-UTR. Transfection with varying combinations of miRNAs resulted in additive levels of translational repression. VEGFA was the third most highly connected protein in our prostate cancer miRNA target network (Table 2-2).

Table 2-3: MicroRNA target connectivity changes with the role of the miRNA

Description	Number of Nodes Regulated by miRNA Type	Node Degree
OncomiR (Expression increases during tumorigenesis)	192	39
Tumor Suppressor (Expression decreases during tumorigenesis)	276	27
Both (Exhibits both behaviors dependent upon a second variable)	37	61

Figure 2-4: Proteins regulated by multiple miRNAs are more likely to be highly connected

Proteins were grouped according to the number of miRNAs that have been proven to regulate their translation. The number of miRNAs that regulate a protein (independent variable) was plotted against the average node degree of the targets (dependent variable) and a best fit linear equation was generated ($y = 17.91 x - 7.9$; $r^2 = 0.831$). Proteins that were regulated by 6-10 miRNA species were grouped into a single group because there were only a few proven examples regulated by more than 6 miRNAs.

Figure 2-4: Proteins regulated by multiple miRNAs are more likely to be highly connected

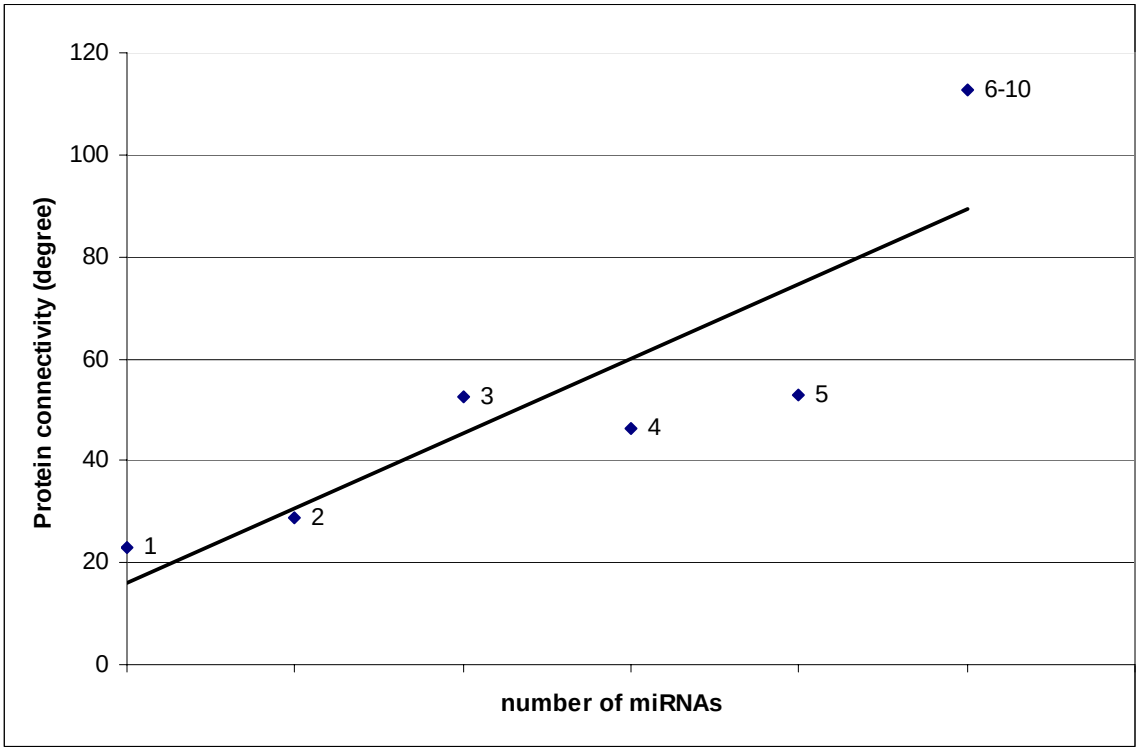

Although not included in table 2-2, another example of a highly connected protein under multiple miRNA regulation is the cyclin dependent kinase inhibitor 1A (CDKN1A). CDKN1A was regulated by the largest number of unique miRNAs (28) and connects to 190 other proteins [71]. Many tumor suppressor pathways are under the control of CDKN1A and its decreased expression increases the likelihood of cancer development [72]. As a potent cell proliferation inhibitor, CDKN1A is an important modulator of the cyclin dependent kinases (CDK) that regulate cell cycle progression through the G1/S checkpoint. Loss of the CDK inhibitor allows the cell to proceed through the cell cycle and diminishes the cell's response to DNA damage. Increased expression of any of the miRNAs that regulate CDKN1A would decrease protein levels and induce oncogenic transformation. This analysis showed that important proteins were regulated by multiple miRNAs and dysregulation of any of these miRNAs could result in a disease state such as cancer.

MiRNAs preferentially regulate highly connected transcription factors

Trans acting factors such as transcription factors and miRNAs control levels of proteins in the cell. However, each differs in their mode of regulation. Transcription factors typically bind up stream of a gene and either potentiate or inhibit transcription. miRNAs have been shown to preferentially bind the 3' UTR of the mRNA transcript affecting protein translation through several mechanisms. Transcription factors that are targeted by miRNAs dysregulated during prostate cancer progression are more highly connected than randomly chosen transcription factors (p-value <0.001) (Figure 2-5). This analysis identifies another mechanism of miRNA regulation. By targeting highly

connected transcription factors, miRNAs can exert a great influence over a large number of proteins. For example, SP1 is one of the most highly connected proteins in our network with a connectivity of 269.

Summary

Cancer is a multifactorial disease that arises from the accumulation of genetic and epigenetic changes that lead to oncogenic transformation causing cells to proliferate uncontrollably. MiRNAs are an important class of translational regulatory agents that affect cell proliferation, differentiation, cell cycle control, and apoptosis. Increased expression of oncomiRs or decreased expression of tumor suppressors leads to uncontrolled cell proliferation, invasion and metastasis.

Because of the scale free design of complex systems and a higher average node degree, miRNA protein targets are more vulnerable to targeted attacks that may lead to catastrophic cellular failures [46]. A single dysregulated miRNA has the potential to induce a significant number of cellular changes by affecting multiple highly connected proteins. It is important to consider that modulation of a single highly connected protein node has the potential to affect hundreds of downstream targets thereby modifying multiple pathways resulting in considerable physiological fluctuation. During the development of prostate cancer, there is wide scale dysregulation of miRNA expression affecting numerous highly connected, essential disease causing proteins and numerous cellular pathways (Figure 2-6).

By combining knowledge of miRNA dysregulation with topological descriptors of a protein-protein interaction network, we may identify important proteins contributing

to tumor progression that have not been previously described. This analysis will be used to identify newer, more relevant indicators of prostate cancer and may offer insights toward the development of targeted molecular therapies. These methods will be used to biologically evaluate the role of miRNA dysregulation in cell lines and human samples.

Figure 2-5: Connectivity of transcription factors

Transcription factors were compiled from the TFCAT curated catalog of transcription factors [55]. Transcription factors targeted by miRNAs dysregulated during tumorigenesis of the prostate were compiled by intersecting the list of miRNA targets with the table of transcription factors using PERL. The process was repeated using the list of randomly associated proteins. Data are presented as a whisker plot that was generated using R and a table of associated values.

Figure 2-5:

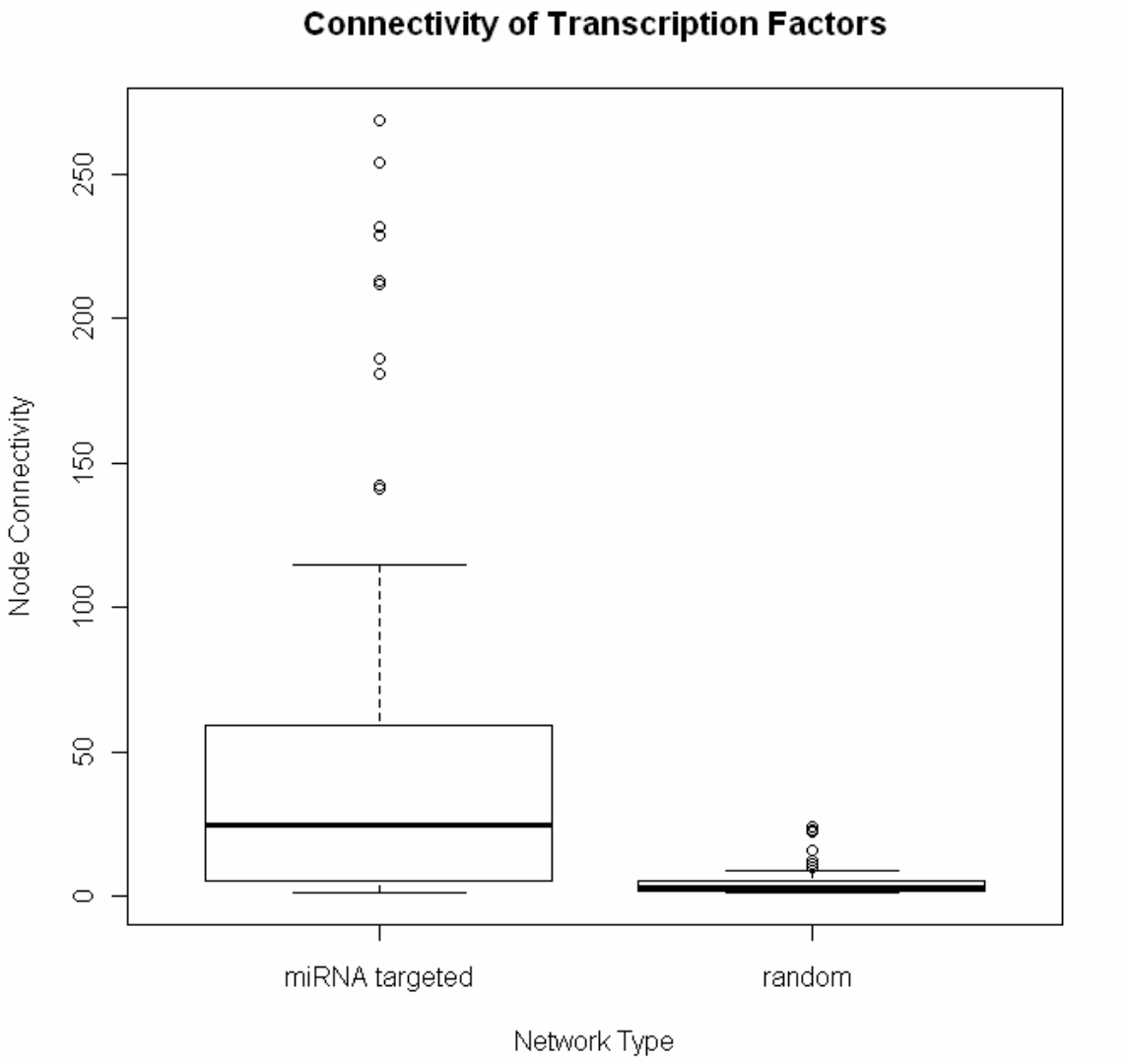

Network Type	Number (467)	Mean connectivity	Standard Deviation	Min	Max
miRNA targeted	112 (24%)	46.01	60.45	1	269
Randomly chosen	122 (26%)	4.34	4.15	1	24

Figure 2-6: Model of miRNA regulation

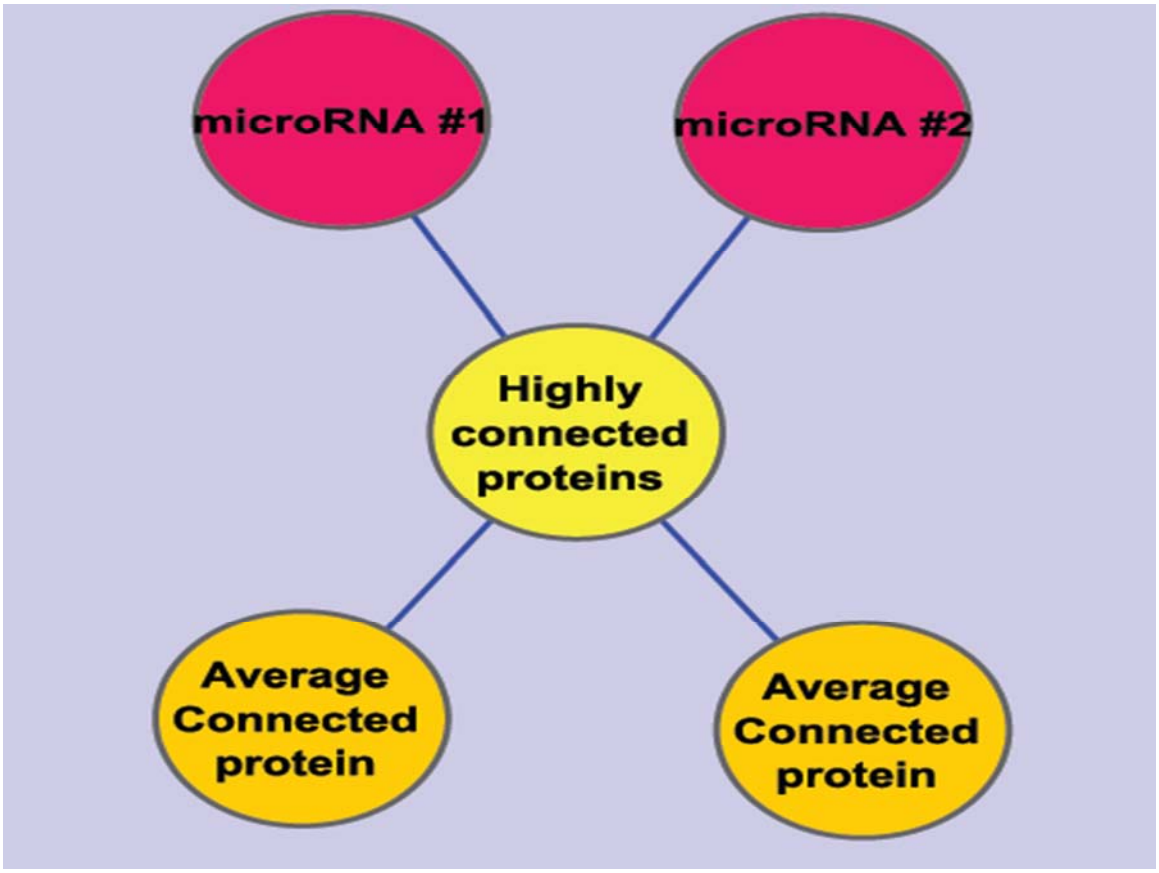

Figure 2-6: Model of miRNA regulation

Using the data obtained from the systems level network analysis a model of miRNA regulation of prostate cancer was created.

Chapter 3

Identification of dysregulated microRNAs contributing to prostate tumorigenesis

Tightly controlled gene regulation is essential to every biological process. Failure to control gene regulation can result in cellular disease or death. Cells have devised many methods for regulating protein levels. The central dogma of biology of one gene, one mRNA, one protein as envisioned by Francis Crick is in need of modification. Complex feedback loops involving RNA splicing, gene regulation at the transcriptional and translational level have been discovered. In order to understand a complex disease phenotype, researchers must consider a greater role for RNA than traditionally envisioned. In the past decade, microRNAs have emerged as an important class of post-transcriptional regulators of protein levels. Nearly every biological process is under the control of at least one miRNA and it is thought that most protein levels are influenced by miRNA expression. Important highly interconnected proteins are often under the control of more than one miRNA [73].

Dysregulation of microRNA expression contributes to a number of pathological conditions and diseases including cancer of the prostate [22]. Conversion of neoplastic growth from benign to metastatic dissemination is a step wise process that likely involves numerous biological macromolecules, often including RNA, protein, and DNA. Accumulating evidence suggests that multiple miRNAs are dysregulated during tumor formation, progression and metastasis [25]. Both miRNA losses and gains of miRNA function have been shown to contribute to the development of neoplasm.

As previously discussed, miRNAs can function as either suppressors of tumor formation or promoters of tumorigenesis (oncomiRs). The increased expression of oncomiRs or loss of tumor suppressors can induce neoplastic transformation. It has been shown that over one hundred miRNAs are dysregulated during the development of

prostate cancer [73]. Comparison of high throughput analyses of miRNA expression in the poorly tumorigenic, non-metastatic P69 cell line and its highly tumorigenic, metastatic variant M12 variant can reveal miRNAs that may contribute to tumorigenicity. As we have shown, miRNAs preferentially regulate highly connected protein targets.

In this study, we propose that our unique combinatorial approach will reveal dysregulated miRNAs contributing to carcinogenesis. Utilizing a prostate cancer cell progression model, we will determine potential miRNAs that may contribute to a cancerous phenotype. Dysregulated miRNAs will be ranked using a unique networks based approach and expression differences will be confirmed by single miRNA analysis. Expression of proposed dysregulated miRNAs will be evaluated using RNA extracted from pure cell populations obtained by LCM in order to validate differential expression from benign to tumorigenic epithelium. The contribution of these miRNAs to controlling P69 and/or M12 cell behavior will be further investigated by a variety of *in vitro* experiments.

Materials and Methods

Cell culture

Cells are cultured at 37° C in RPMI1640 with L-glutamine obtained from Gibco supplemented with 5% fetal bovine serum, 5μg/ml insulin, 5μg/ml transferrin, and 5 μg/ml of selenium (ITS from Collaborative Research Bedford, MA). Inhibition of bacterial contamination was accomplished with the addition of Gentamycin (0.05mg/ml). M12 cells stably transformed with the p-SIREN (M12+miR-17-3p and M12+miR-125b) vector were maintained with Puromycin (100 ng/ml). F6 cells were maintained with

Geneticin (200 μg/ml) [24]. All tissue culture cells were grown in T75 flasks and split when confluent. Cells were pelleted after trypsin (0.25% in EDTA) digestion by centrifugation at 5000 RPM for five minutes. Trypsin inactivated by washing the cells in serum containing media. After washing, cell pellets were flash frozen in liquid nitrogen after washing and stored for at least 24 hours.

Cell pellet RNA extraction

Total RNA was extracted from cell pellets described above using the miRVana™ miRNA isolation kit from Ambion per manufacturer's instructions. Briefly, after cell lysis total RNA was bound to a glass fiber filter and eluted with a proprietary elution buffer. After isolation, RNA concentration was estimated using a Biorad® Smart Spec™ 3000 spectrophotometer, diluted to a concentration of 100ng/ml and stored at -80°C for at least 24 hours.

MicroRNA profiling

Real time PCR profiling was performed using the miRCURY LNA ™ Universal RT microRNA PCR system (Exiqon, Denmark). Human Panel I was used to identify dysregulated miRNAs in the P69 cell line versus its metastatic derivative M12. Duplicate samples were compared using 25ng and 50 ng of RNA as input. Briefly, RNA input was converted to cDNA using supplied reagents and enzymes (4μl of 5x reaction buffer, 9μl of nuclease free water, 2μl enzyme mix, 1μl synthetic RNA spike in, and 5 μl of RNA diluted to 5 ng/ul). The reaction was incubated for 60 minutes at 42° C and the enzyme was heat inactivated for 5 minutes at 95°C. Real time PCR plates were run on an

ABI7900 HT (95°C for 10 mins, 40 cycles at 95°C-10sec, 60°C-1 min, ramp rate 1.6°C/s). Threshold and baseline were set manually according to recommendations in the supplied protocol. After correcting for interplate variability, cycle threshold (CT) values were normalized to the global mean of all miRNA expression. Initial data analysis was performed using Exiqon GenEx software and all values are reported as fold changes relative to P69. miRNAs exhibiting greater than 2-fold expression differences in both sets of arrays were considered to be significant and selected for further analysis.

Ranking of dysregulated miRNAs

Significantly dysregulated miRNAs were ranked according to the sum network connectivity of proven targets. Proven targets of miRNAs were obtained by combining miRecords and Tarbase into a single non-redundant list. A protein-protein interaction network was inferred by using each targeted protein as a search term in the Agilent literature search (v2.76) tool implemented in Cytoscape 2.8 [52, 53]. Network properties were developed using CentiScape. [54].

TaqMan® based miRNA assay

Verification of mature miRNA expression was confirmed using single assays by TaqMan® miRNA assay (Life Technologies, Grand Island, NY). Briefly, cDNA was synthesized in a 25µl reaction volume from 20 ng of total RNA using the TaqMan® MicroRNA Reverse Transcription kit. Reactions were incubated at 16°C for 30 minutes, 42°C for 30 minutes and inactivated at 85°C for 5 minutes. Each cDNA was analyzed in triplicate by quantitative PCR using sequence specific primers in an ABI7300 qRT PCR

system (Applied Biosystems). Each individual assay was performed in a 20µl reaction volume with 1.33µl of cDNA, 1.0µl specific miRNA assay, 10µl TaqMan™ Universal PCR Master Mix II with no AMP Unerase and 7.67µl of nuclease free water. Reactions were incubated in a 96 well plate at 50°C for 2 minutes, followed by 95°C at 95°C and 40 cycles of 95°C for 15 sec/ 60°C for 60 sec.

SYBR green based qRT-PCR

Quantification of mature miRNA expression was carried out using the miRCURY LNA™ Universal RT miRNA PCR (Exiqon, Denmark**).** Synthesis of cDNA was accomplished by incubating 50ng of total RNA in a 20µl reaction volume of 5X reaction buffer (4µl), nuclease free water (9µl), enzyme mix (2µl), synthetic RNA control spike in (1µl) and template RNA (4µl). cDNA reaction was incubated for 60 minutes at 42°C and enzyme inactivated for 5 minutes at 95°C. Following synthesis, the cDNA is diluted 20 fold with nuclease free water. Real time PCR amplification was performed in a 10µl reaction with 4µl of diluted cDNA template, 5µl SYBR® Green Master Mix (Exiqon, Denmark), and 1 µl of PCR primer mix. The reaction was run in an ABI 7300 (Applied Biosystems) at 95°C for 10 min, followed by 40 cycles of 95°C (10 sec), 60°C (60 sec) at a ramp rate of 1.6°C/sec. Melt curve analyses were run on each reaction to verify single product amplification. Threshold and baseline were set manually according to recommendations in the supplied protocol.

qRT-PCR data analysis

Relative quantities of miRNA levels were determined using the 2^{-ddCT} method of Livak et al after normalization with RNU48 as a standard reference [74]. All samples were performed in triplicate and the average cycle threshold (CT) value was determined. The average CT was normalized by subtracting the average CT of RNU48 (dCT). All samples were compared to the parental P69 cell line by subtracting the experimental dCT from the dCT value of the parental cell line (calibrator).

Laser capture microdissection

Human prostate samples were obtained from frozen core samples of radical prostatectomy samples available from VCU's Tissue and Data Acquisition and Analysis Core. All samples were obtained with approval from the VCU institutional review board. All slides were reviewed by a board certified pathologist with expertise in prostate cancer diagnosis. Briefly, 8 μm tissue slices were placed on uncharged glass slides, dehydrated with progressively increasing concentrations of ethanol, stained with hematoxylin and eosin (H&E). Laser capture microdissection was performed using an Arcturus Veritas machine. Areas of interest were captured onto CapSure® Macro LCM caps (Life Technologies, Grand Island, NY). At least ten slides were captured for each patient included in the study.

RNA extraction of LCM samples

Total RNA was extracted from LCM extracts using the PicoPure® RNA Isolation Kit (Life Technologies, Grand Island, NY). The manufacturer's protocol was followed.

Following dissection of tissue, the LCM caps were incubated for 30 minutes at 42°C in 50µl of extraction buffer. Cell extracts were stored at -20°C until ready for RNA extraction. Similar cellular lysates from successive slides were pooled into a single tube and mixed with 1 volume of ethanol (70%). The lysate/ethanol solution was loaded onto a high recovery MiraCol™ column and centrifuged at 100xg for 2 minutes followed by 16,000xg for 30 seconds. RNA was recovered in an 11µl volume. Concentration and quality were measured using an Agilent RNA 6000 Pico kit with the Agilent Bioanalyzer 2100.

Cloning of miR-125b into M12 cells

M12 cells (500,000) were stably transformed with the human miR-125b sequence (as underlined) 5'-GATCCGTCCCTGAGACCCTAACTTGTGATGTTTACCGTTTAAATCACAAGTTAGGGTCTCAGGGA TTCTTTTTTTCTAGAG-3' and its complement 5'-AATTCTCTAGAAAAAAAGAATCCCTGAGACCCTAACTTGTGATTTAAACGGTAAACATCACAAGTTAGGGTCTCAGGGACG-3' into the BamHI and EcoRI cloning sites of the pSIREN vector (BD Biosciecnes, SanJose, CA). Cells were transformed with purified plasmid (2.0 µg) using TransIT-LT1 (4.0 µl) transfection reagent (Mirus BioCorp, Madison, WI). Resistant cells were selected with 400 ng/ml Puramycin.

Migration assay

Cells were detached from the plate using 2.0 ml of CellStripper™ (CellGro®, Manassas, VA) and pelleted at 5000 rpm for 5 minutes. Cells were washed in serum free RPMI 1640 and re-suspended in serum free media at a concentration of $2.5x10^5$cells/ml.

200 µl of cell suspension (50,000 cells) was added to the top chamber of a 6.0µm pore size ThinCert™ tissue culture insert (Greiner, Monroe, NC). 0.5 ml of serum containing media was added to the lower chamber supplemented with 10 ng/ml of EGF (Figure 3-1 A). Cells were incubated at 37°C for 20 hours. Media was removed from both chambers and cells were fixed in 0.025% glutaraldehyde in PBS for 20 minutes after removal of all media from both chambers. Following fixation, inserts were stained with 0.1% crystal violet in PBS for 30 minutes and washed with sterile deionized water. Non-migratory cells were removed from the top surface with a sterile cotton applicator and inserts mounted on a glass microscope slide. Cells were counted in 10 random fields at a 200 X magnification. Data are presented as the mean sum of migratory cells in 10 random fields ± standard error.

Invasion assay

Invasion assays are carried out in a manner similar to the migration assays. At least 30 minutes prior to extracting cells, 60 µl (diluted 1:10) of Culturex® reduced growth factor basement membrane is added to the top chamber of the ThinCert™ tissue culture insert and incubated at 37°C for gelling (Figure 3-1 B). After ensuring that the basement membrane has gelled, the remainder of the protocol is identical to the migration assay. Data are presented as the mean sum of invasive cells in 10 random fields ± standard error.

Figure 3-1: Migration and invasion assay

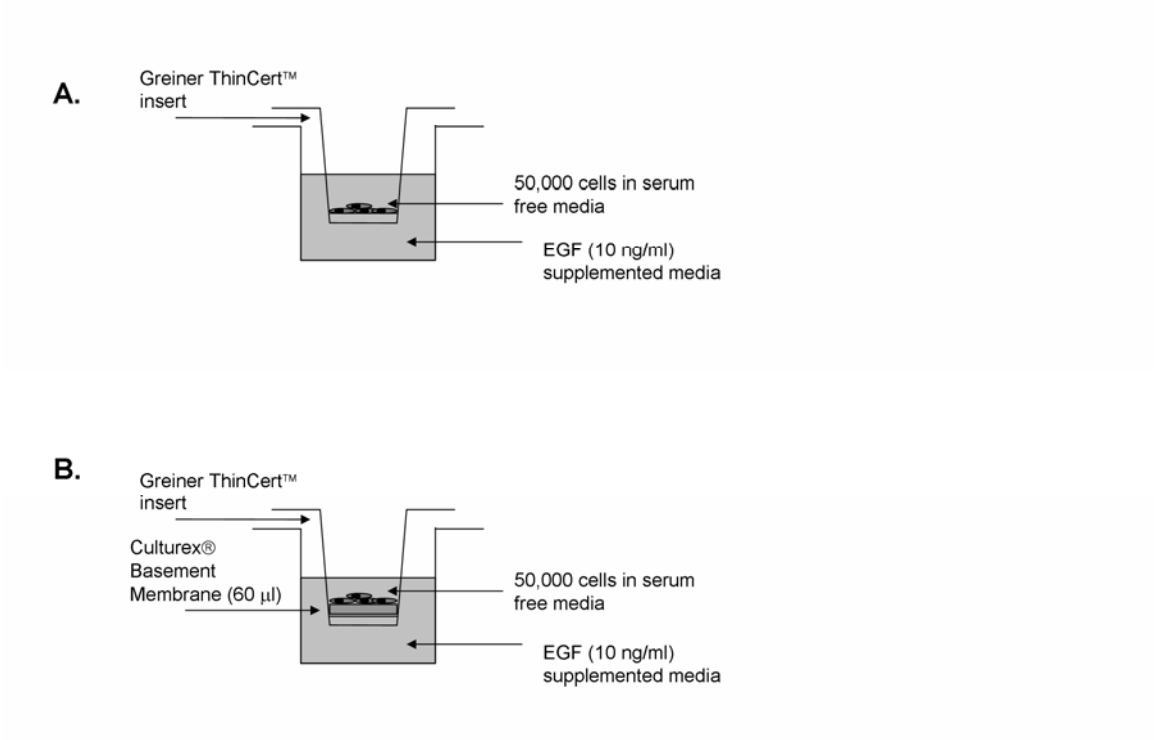

Figure 3-1: Migration and invasion assay

A. Illustration of the experimental setup for an individual well migration assay.
B. Illustration of the experimental setup for an individual well invasion assay.

Results

Identification of miRNAs dysregulated during tumorigenesis

Understanding the molecular perturbations that underlie cancer initiation, progression and metastasis are critical to identify newer, more relevant biomarkers. Many model cell lines have been used to explore prostate cancer progression. Most are derived from metastatic sites and thus may not represent the best model for elucidation of early indicators of cancer formation [75-77] . Rather than being isolated from a metastatic site, these cells were obtained from normal prostate tissue immortalized with SV40 large T antigen (P69) and cycled through male athymic nude mice to obtain the tumorigenic variant (M12) discussed earlier [23]. This unique isogenic model may provide insights to the molecular causes that initiate cancer formation.

Quantification of miRNA levels is difficult. The length of the mature miRNA is 22-23 nucleotides, the same length as traditional PCR primers. Increasing the difficulty is the fact that often miRNAs only differ from one another by a single base. Thus, it is very difficult to design a primer that can discriminate single base differences in such small molecules. The advent of locked nucleic acid (LNA™) modified primers increases the specificity and sensitivity of qRT-PCR for miRNAs.

Utilizing a LNA™ based array panel that profiles the most relevant, currently identified miRNAs (386 miRNAs), we discovered 180 miRNAs that significantly change at least two-fold from the parental P69 cell line to the highly tumorigenic M12 cell line (Table 3-1). Eighty six miRNAs were lost as the tissue becomes more

Table 3-1: miRNAs dysregulated during tumorigenesis

microRNA	Fold Difference	Behavior
hsa-miR-125b	4.76E-06	Tumor Suppressor
hsa-miR-500	0.001	Tumor Suppressor
hsa-miR-127-3p	0.002	Tumor Suppressor
hsa-miR-382	0.003	Tumor Suppressor
hsa-miR-411	0.004	Tumor Suppressor
hsa-miR-299-5p	0.004	Tumor Suppressor
hsa-miR-576-5p	0.004	Tumor Suppressor
hsa-miR-620	0.008	Tumor Suppressor
hsa-miR-409-3p	0.008	Tumor Suppressor
hsa-miR-144	0.012	Tumor Suppressor
hsa-miR-410	0.013	Tumor Suppressor
hsa-miR-548c-3p	0.014	Tumor Suppressor
hsa-miR-136	0.015	Tumor Suppressor
hsa-miR-323-3p	0.015	Tumor Suppressor
hsa-miR-379	0.018	Tumor Suppressor
hsa-miR-583	0.026	Tumor Suppressor
hsa-miR-377	0.031	Tumor Suppressor
hsa-miR-539	0.034	Tumor Suppressor
hsa-miR-487b	0.035	Tumor Suppressor
hsa-miR-376c	0.036	Tumor Suppressor
hsa-miR-325	0.042	Tumor Suppressor
hsa-miR-135b	0.045	Tumor Suppressor
hsa-miR-337-5p	0.054	Tumor Suppressor
hsa-miR-598	0.056	Tumor Suppressor
hsa-miR-99a*	0.061	Tumor Suppressor
hsa-miR-432	0.062	Tumor Suppressor
hsa-miR-20b	0.064	Tumor Suppressor
hsa-miR-597	0.068	Tumor Suppressor
hsa-miR-135a	0.068	Tumor Suppressor
hsa-miR-183	0.072	Tumor Suppressor
hsa-miR-15b	0.079	Tumor Suppressor
hsa-miR-509-3p	0.080	Tumor Suppressor
hsa-miR-376a	0.086	Tumor Suppressor
hsa-miR-19a	0.091	Tumor Suppressor
hsa-miR-495	0.098	Tumor Suppressor
hsa-miR-223	0.111	Tumor Suppressor
hsa-miR-198	0.114	Tumor Suppressor
hsa-miR-302b	0.114	Tumor Suppressor
hsa-miR-185*	0.115	Tumor Suppressor
hsa-miR-346	0.116	Tumor Suppressor
hsa-miR-425*	0.119	Tumor Suppressor
hsa-miR-886-3p	0.134	Tumor Suppressor
hsa-miR-891a	0.138	Tumor Suppressor
hsa-miR-212	0.148	Tumor Suppressor
hsa-miR-514	0.149	Tumor Suppressor
hsa-miR-383	0.150	Tumor Suppressor

microRNA	Fold Difference	Behavior
hsa-miR-493	0.153	Tumor Suppressor
hsa-miR-342-3p	0.160	Tumor Suppressor
hsa-miR-187*	0.168	Tumor Suppressor
hsa-miR-631	0.174	Tumor Suppressor
hsa-miR-369-5p	0.182	Tumor Suppressor
hsa-miR-449a	0.191	Tumor Suppressor
hsa-miR-185	0.209	Tumor Suppressor
hsa-miR-100	0.209	Tumor Suppressor
UniSp6 CP	0.224	Tumor Suppressor
hsa-miR-214	0.242	Tumor Suppressor
hsa-miR-127-5p	0.252	Tumor Suppressor
hsa-miR-572	0.259	Tumor Suppressor
hsa-miR-21	0.260	Tumor Suppressor
hsa-miR-146a	0.264	Tumor Suppressor
hsa-miR-134	0.271	Tumor Suppressor
hsa-miR-302c*	0.280	Tumor Suppressor
hsa-miR-625*	0.287	Tumor Suppressor
hsa-miR-27a	0.300	Tumor Suppressor
hsa-miR-296-5p	0.309	Tumor Suppressor
hsa-miR-335	0.316	Tumor Suppressor
hsa-miR-376b	0.321	Tumor Suppressor
hsa-miR-31	0.323	Tumor Suppressor
hsa-miR-525-5p	0.341	Tumor Suppressor
hsa-miR-191	0.349	Tumor Suppressor
hsa-miR-196b	0.350	Tumor Suppressor
hsa-miR-654-5p	0.365	Tumor Suppressor
hsa-miR-187	0.370	Tumor Suppressor
hsa-miR-339-5p	0.371	Tumor Suppressor
hsa-miR-720	0.374	Tumor Suppressor
hsa-miR-140-3p	0.392	Tumor Suppressor
hsa-miR-146b-5p	0.394	Tumor Suppressor
hsa-miR-181b	0.409	Tumor Suppressor
hsa-miR-506	0.409	Tumor Suppressor
hsa-miR-30b	0.416	Tumor Suppressor
hsa-miR-629	0.426	Tumor Suppressor
hsa-miR-203	0.452	Tumor Suppressor
hsa-miR-449b	0.459	Tumor Suppressor
hsa-miR-27b	0.463	Tumor Suppressor
hsa-let-7a	0.480	Tumor Suppressor
hsa-miR-138	0.490	Tumor Suppressor
hsa-miR-298	2.0	OncomiR
hsa-miR-665	2.1	OncomiR
hsa-miR-126*	2.1	OncomiR
hsa-miR-152	2.1	OncomiR
hsa-miR-423-5p	2.2	OncomiR
hsa-miR-502-5p	2.2	OncomiR
hsa-miR-151-5p	2.2	OncomiR
hsa-miR-324-5p	2.2	OncomiR
hsa-miR-576-3p	2.3	OncomiR

microRNA	Fold Difference	Behavior
hsa-miR-330-3p	2.3	OncomiR
hsa-miR-302a	2.4	OncomiR
hsa-miR-7	2.4	OncomiR
hsa-let-7c	2.5	OncomiR
hsa-miR-615-3p	2.6	OncomiR
hsa-miR-933	2.6	OncomiR
hsa-miR-148a	2.6	OncomiR
hsa-let-7d	2.6	OncomiR
hsa-miR-22	2.7	OncomiR
hsa-miR-33a	2.7	OncomiR
hsa-miR-450a	2.7	OncomiR
hsa-miR-210	2.7	OncomiR
hsa-miR-29c	2.7	OncomiR
hsa-miR-491-5p	2.8	OncomiR
hsa-miR-365	2.8	OncomiR
hsa-miR-30d	2.8	OncomiR
hsa-miR-545	2.8	OncomiR
hsa-miR-602	2.9	OncomiR
hsa-miR-589	2.9	OncomiR
hsa-miR-148b	2.9	OncomiR
hsa-miR-374a	2.9	OncomiR
hsa-miR-668	3.0	OncomiR
hsa-miR-431	3.1	OncomiR
hsa-miR-200a	3.1	OncomiR
hsa-miR-130b	3.2	OncomiR
hsa-miR-32	3.3	OncomiR
hsa-miR-10a	3.3	OncomiR
hsa-miR-204	3.4	OncomiR
hsa-miR-22*	4.1	OncomiR
hsa-miR-486-5p	4.2	OncomiR
hsa-miR-326	4.4	OncomiR
hsa-miR-30c-2*	4.5	OncomiR
hsa-miR-96	4.7	OncomiR
hsa-miR-371-5p	4.7	OncomiR
hsa-miR-181c	4.7	OncomiR
hsa-miR-518e	5.0	OncomiR
hsa-miR-10b	5.2	OncomiR
hsa-miR-188-5p	5.3	OncomiR
hsa-miR-642	5.8	OncomiR
hsa-miR-99a	6.1	OncomiR
hsa-miR-130a	6.4	OncomiR
hsa-miR-888	6.5	OncomiR
hsa-miR-890	7.2	OncomiR
hsa-miR-608	7.8	OncomiR
hsa-miR-370	8.0	OncomiR
hsa-miR-338-3p	8.3	OncomiR
hsa-miR-1	8.5	OncomiR
hsa-miR-518a-3p	8.6	OncomiR
hsa-miR-497	8.7	OncomiR

microRNA	Fold Difference	Behavior
hsa-miR-595	9.5	OncomiR
hsa-miR-124	9.5	OncomiR
hsa-miR-9	9.6	OncomiR
hsa-miR-301b	10.7	OncomiR
hsa-miR-381	10.9	OncomiR
hsa-miR-570	11.3	OncomiR
hsa-miR-518b	11.6	OncomiR
hsa-miR-139-5p	11.7	OncomiR
hsa-miR-196a	12.8	OncomiR
hsa-miR-662	13.2	OncomiR
hsa-miR-105	13.4	OncomiR
hsa-miR-516a-5p	13.6	OncomiR
hsa-miR-873	14.6	OncomiR
hsa-miR-596	14.9	OncomiR
hsa-miR-517a	15.9	OncomiR
hsa-miR-199a-3p	16.5	OncomiR
hsa-miR-217	20.1	OncomiR
hsa-miR-518c*	20.3	OncomiR
hsa-miR-211	26.0	OncomiR
hsa-miR-299-3p	27.5	OncomiR
hsa-miR-33b	29.9	OncomiR
hsa-miR-491-3p	37.8	OncomiR
hsa-miR-498	51.4	OncomiR
hsa-miR-147	54.2	OncomiR
hsa-miR-373*	59.2	OncomiR
hsa-miR-517c	68.4	OncomiR
hsa-miR-451	68.5	OncomiR
hsa-miR-133b	68.9	OncomiR
hsa-miR-524-3p	85.7	OncomiR
hsa-miR-133a	92.9	OncomiR
hsa-miR-551b	152.2	OncomiR
hsa-miR-375	191.0	OncomiR
hsa-miR-153	240.0	OncomiR
hsa-miR-622	365.0	OncomiR
hsa-miR-147b	522.1	OncomiR
hsa-miR-34a	1850.8	OncomiR

tumorigenic, that is they function as potential suppressors of tumor formation. The average expression difference of all tumor suppressors is 100-fold i.e. they are 100-fold higher in the P69 cell line compared to the M12 variant. Expression of the remaining 94 dysregulated miRNAs increases as the tumorigenicity increases (oncomiRs). OncomiRs have an average of 45-fold difference when compared to the P69 cells. The overall number of tumor suppressors and oncomiRs is similar to that found using our global networks approach where we found approximately as many tumor suppressors as oncomiRs. Interestingly, the average connectivity of an oncomiR target is higher than the average target of tumor suppressor miRNAs (Table 2-3). It is reasonable to hypothesize that greater miRNA fold changes are needed to induce phenotypic alterations if the targets are not as highly connected.

Human miR-125b is the most dysregulated tumor suppressor and is essentially lost in the M12 cells. Conversely, hsa-miR-34a is much greater in the M12 cells compared to the P69 cells. As discussed in chapter 2, the miR2disease database lists 111 miRNAs that have been experimentally shown to contribute to the development of prostate cancer [48]. In our model system, 76 of the 111 miRNAs in miR2disease are dysregulated. This suggests that our cell progression model is a relevant indicator of prostate cancer progression and may be useful to assess which miRNAs are causative to prostate cancer and serve as useful biomarkers.

Microarray technology has increased the ability of researchers to simultaneously profile thousands of molecules at a single time point. Because of their power, microarrays have become popular tools among molecular biologists. Important considerations when evaluating array based studies are the validity of the results, and universality of findings

[78]. Repeat experiments are critical to eliminate noise in data. In this study, we profiled two cell lines in duplicate. All miRNAs reported in Table 3-1 were found to be significantly dysregulated in both sets of arrays. The primary goal of microarray analyses is to accurately identify differential molecular regulation affecting biological processes. It is essential that identified miRNAs be validated using traditional techniques such as qRT-PCR. Studies have shown that 71% of mRNAs identified to be dysregulated using microarray were confirmed using qRT-PCR assays [79]. However, the fold difference does not always replicate. This finding suggests that array based methods are valid as screening tools but true expression differences are only accurate using a single assay format.

Network properties for ranking microRNA dysregulation

The cost to confirm every potentially dysregulated miRNA identified in a microarray experiment is prohibitively expensive. Few labs have the financial or physical resources needed to carry out such validation. Therefore, most labs choose a subset of genes, proteins, or miRNAs to validate. Many factors affect the choice of a gene set including relative difference, biological function, availability of reagents, and investigator preference. A traditional approach has been to prioritize molecules with the greatest expression difference as such expression differences are more likely to validate [78].

This approach may overestimate the importance of differential expression. It is reasonable to suspect that smaller changes in some miRNAs may exert a greater influence in tissue behavior, if they modulate the expression of more important proteins. Indeed, our analysis has shown a preference for miRNAs to regulate highly connected

protein nodes (Figure 2-6). Thus a single dysregulated miRNA can affect hundreds of downstream targets by affecting the level of one highly connected protein. In this study we chose a subset of genes for further studies using network properties for proven targets of each miRNA. A total of eight miRNAs were chosen for validation based on their sum network connectivity (Table 3-2).

Dysregulated miRNAs with a range of connectivity indices were chosen (20-1330). Interestingly, two of the miRNAs with the highest connectivity index, were also the two most differentially expressed miRNAs (hsa-miR-125b and hsa-miR-34a). Three miRNAs chosen had a sum connectivity of over 1000 each. When multiple highly connected miRNAs are dysregulated there is a great potential to affect many signaling pathways simultaneously. Hsa-miR-1 has the highest connectivity of all miRNAs in our analysis, potentially influencing 1330 downstream targets. Again, it is important to re-iterate that this index reflects a global potential. It is unlikely that all 1330 proteins are affected at the same time due to both differential protein and miR expression in various cell types. Instead, proteins will interact with one another in a variety of conditions.

Expression profiles comparing levels in M12 and P69 cells of each chosen miRNA were determined using the ddCT method by Livak *et al*. Based on array results, 5 of the miRNAs chosen seem to function as oncomiRs (Figure 3-2). Their expression is higher in the highly tumorigenic, metastatic M12 cell line. As mentioned previously, miR-34a is the most dysregulated oncomiR. Its expression is approximately 1800 times higher in the M12 cell line than it is in the P69 cell line. The sum connectivity of proven protein targets of miR-34a is 1208. As the expression change is quite dramatic, and the connectivity of its targeted proteins is very high, it is reasonable to suspect that

Table 3- 2: Subset of miRNAs chosen for further validation

microRNA	Targets	Degree
hsa-miR-375	Mxi1 Ahr C1QBP YAP JAK2 ADIPOR2 YWHAZ Insm1 USP1 XBP-1 MTPN	20
hsa-miR-127-3p *	BLIMP-1, BCL6	52
hsa-miR-200a	ERBB2IP, ZEB1, ZEB2, ELMO2, SIP1 and 7 others	56
hsa-miR-146a *	CDKN3, BRCA1, MCM10, IRF-5, ROCK1and others	504
hsa-miR-22	PTEN ESR1 BMP7 PPARA MAX	565
hsa-miR-125b *	DICER, ERBB2, ERBB3, CDKN2A, BAK1, UBE21, LIN28, ID3, and others	1194
hsa-miR-34a	CYCLIN D1 BCL2 CCND1 WNT1 E2F3 NOTCH2 MYCN Delta1 CDK6 SIRT1 VEGF c-MET MEK1 AXIN2 MYB JAG1 MYC NOTCH-1	1208
hsa-miR-1	TPM3, PIM-1, HDAC4, c-MET, TPM1, PARG1 and others	1330

*****- potential tumor suppressors

Figure 3-2: Differential expression of oncomiRs determined using Exiqon's miRCURY human panel I

A profile of the miRnome was obtained using the miRCURY ready to use PCR human panel I, V2 (Exiqon, Denmark). The experiment was run in duplicate using 20 and 50 ng RNA as starting material. Manufacturer's protocol was followed and data are presented as the mean expression fold difference of M12 compared to P69. Positive numbers represent an increased expression in M12 cells. Error bars represent the standard deviation of fold changes between the two duplicate assays. Note the broken y axis to depict the discrepancy between miR-22 to miR-34a better.

Figure 3-2: Differential expression of oncomiRs determined using Exiqon's miRCURY human panel I

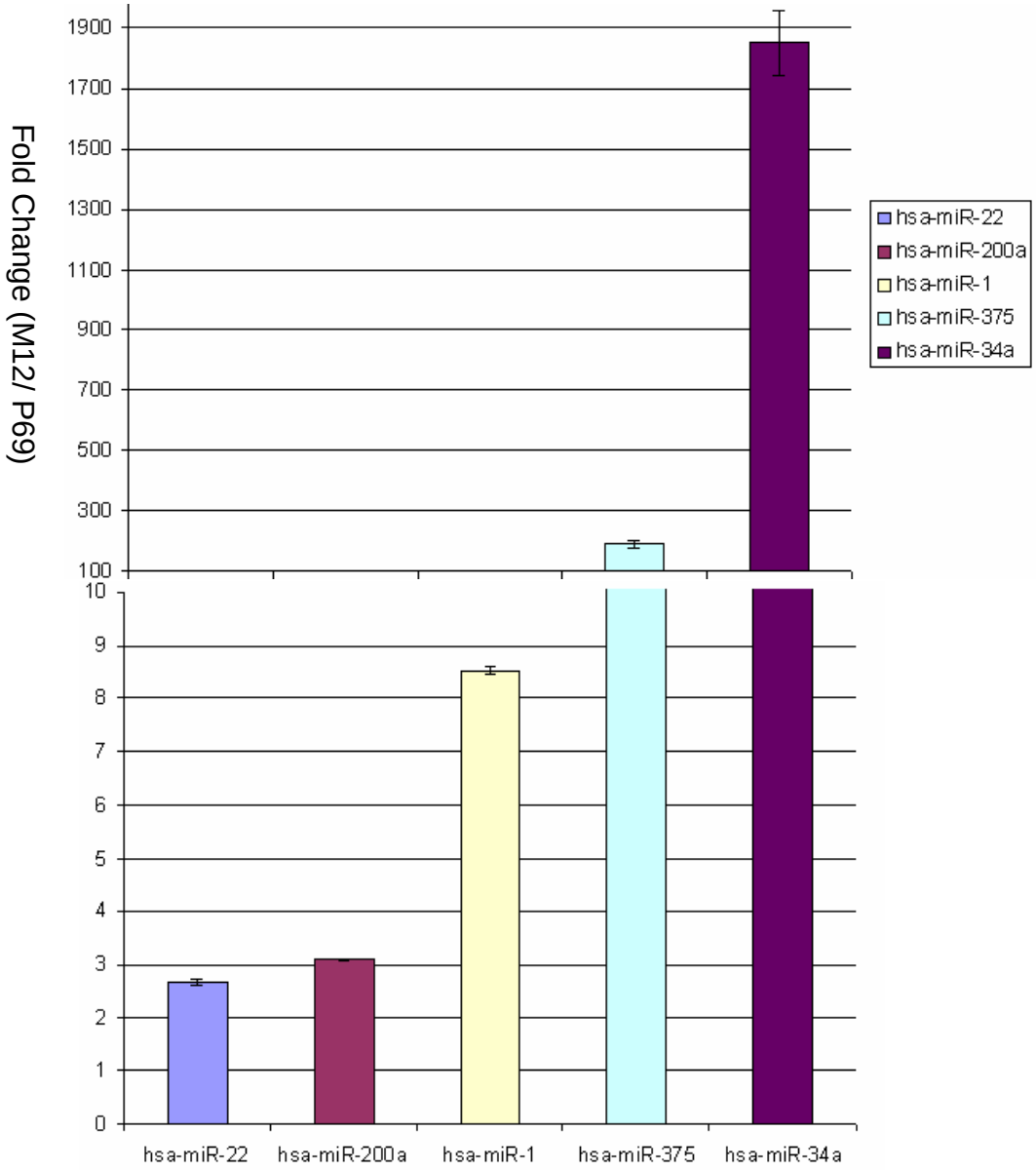

dysregulation of miR-34a may induce an oncogenic event. Even though miR-1 is only 8-fold higher in M12, it is likely to have a great effect on the tumorigenic properties of the cell as it targets a large number of highly connected proteins.

Three of the miRNAs chosen for validation from the array seem to function as tumor suppressors (Figure 3-3). miR-125b is several thousand fold higher in the non-tumorigenic parental cell line (P69). Its expression is nearly undetectable in the M12 subline. HSA-miR-146a is the least differentially expressed tumor suppressor included in our study. Its level is nearly four times higher in the P69 cells.

An additional miRNA was chosen to be validated not because of its connection to the network, but because of other biological interests. miR-127-5p is an alternative transcript that comes off of the same precursor as miR-127-3p. [80]. Many miRNAs have the ability to produce two functional miRNAs from the same pre-miRNA [81]. Although they are produced from the same precursor, miR-127-5p and miR-127-3p do not accumulate at equal levels in the cell. There appears to be a preference towards accumulation of miR-127-5p at the expense of miR-127-3p (Figure 3-4). Note the difference in y-axis scale between Figures 3-3 and 3-4. In the latter figure log transformation was not used in order to optimize the display of differential expression between miR-127-5p and miR-127-3p.

Validation of miRNA dysregulation using locked nucleic acid primers

Since the advent of qRT-PCR, there have been numerous improvements to the process. Several methods exist that allow quantification of the starting cDNA input.

Figure 3-3: Differential expression of tumor suppressors determined using Exiqon's human miRCURY screen panel I

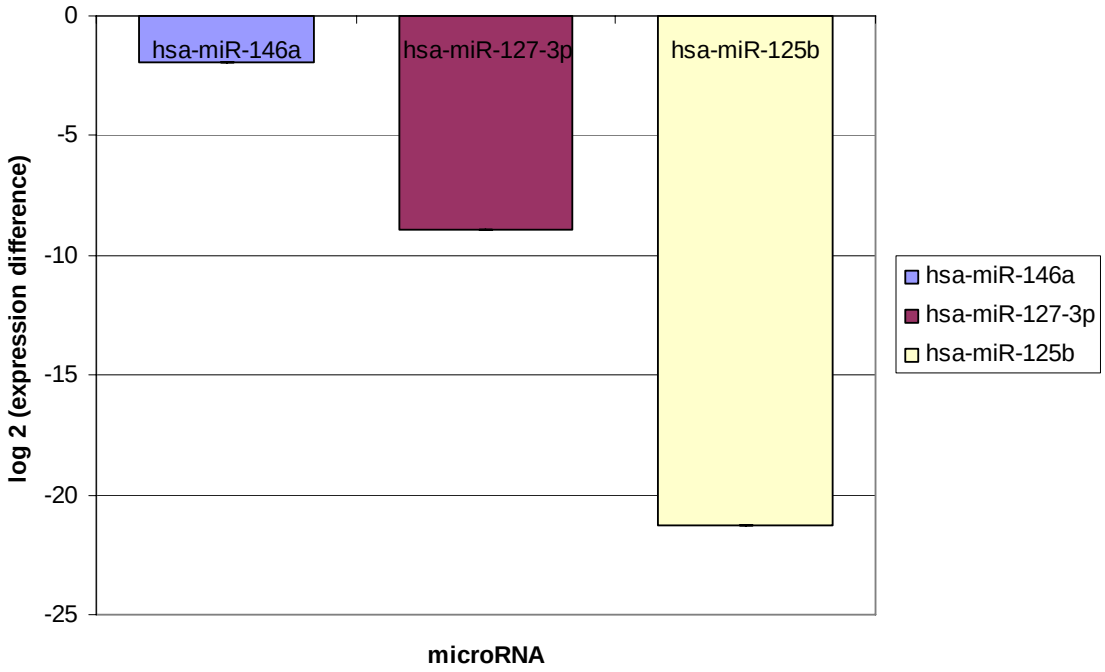

Figure 3-3: Differential expression of tumor suppressors determined using Exiqon's human miRCURY screen panel I.

A profile of the miRnome was obtained using the miRCURY ready to use PCR human panel I, V2 (Exiqon, Denmark). The experiment was run in duplicate using 20 and 50 ng RNA as starting material. Manufacturer's protocol was followed and data are presented as the log transformed mean expression fold difference of M12 compared to P69. Log transformation was used as to reflect the differences in expression. Negative numbers represent a decreased expression in M12 cells. Error bars represent the standard deviation of fold changes between the two duplicate assays.

Figure 3-4: Differential regulation of mature miRNAs produced by same pre-miRNA using miRCURY screen panels

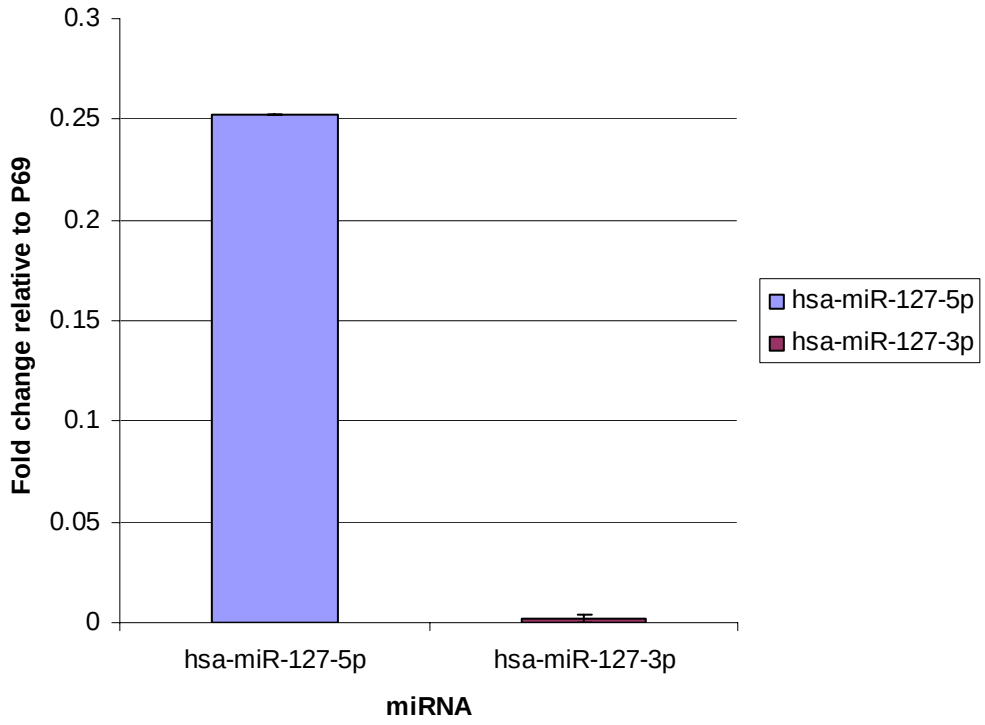

Figure 3-4: Differential regulation of mature miRNAs produced by same pre-miRNA using Exiqon's human miRCURY screen panels

Analysis of the levels of miR-127-5p and miR-127-3p obtained from profile of the entire miRnome. Data was obtained using the miRCURY ready to use PCR human panel I, V2 (Exiqon, Denmark). The experiment was run in duplicate using 20 and 50 ng RNA as starting material. Manufacturer's protocol was followed and data are presented as the mean expression fold difference of M12 compared to P69. Values less than 1 represent an decreased expression in M12 cells. Error bars represent the standard deviation of fold changes between the two duplicate assays.

SYBR green is a DNA intercalating agent that fluoresces when bound to double-stranded DNA [82]. In a qRT-PCR reaction it serves as a reporter and its fluorescence increases exponentially with each cycle of the reaction. The amount of input material is quantified once the reporter activity exceeds an arbitrary threshold (Cycle Threshold, CT). CT values decrease linearly as the amount of starting material is increased. Thus, a sample with more starting material will display a lower CT value.

LNA™ modified probes were used in this study to validate expression differences of the eight miRNAs chosen using our unique networks based approach plus the two additional miRNAs (miR-127-5p, miR-34b). All miRNAs chosen for validation are described by sequence and accession number in Table 3-3 as names often change as miRBase is updated.

Performance of LNA™ modified primers was verified using RNU48 and miR34a as a representative primer set (Figure 3-5). RNU48, traditionally used as a normalization standard, exhibited a linear decrease in CT values as the amount of starting material increased (r^2=0.9985). Normalization is accomplished by subtracting the CT value of RNU48 from the raw CT value of the experimental probe (delta CT). The delta CT of miR-34a decreases linearly as the amount of starting material increased (r^2= 0.9986). As both LNA™ modified probes exhibited the expected linear decrease with extremely good correlation coefficients, it is reasonable to expect that all probes available from the manufacturer will perform in a similar manner. Exiqon advises that each of their primer sets have been validated to specifically bind only a single miRNA and demonstrates the same linear correlation as we observed for RNU48 and miR-34a.

Table 3- 3: Information and sequence for each profiled miRNA

miRNA	Sequence	miR Base Accession Number
hsa-miR-375	UUUGUUCGUUCGGCUCGCGUGA	MIMAT0000728
hsa-miR-127-3p	UCGGAUCCGUCUGAGCUUGGCU	MIMAT0000446
hsa-miR-127-5p	CUGAAGCUCAGAGGGCUCUGAU	MIMAT0004604
hsa-miR-146a	UGAGAACUGAAUUCCAUGGGUU	MIMAT0000449
hsa-miR-22	AAGCUGCCAGUUGAAGAACUGU	MIMAT0000077
hsa-miR-200a	UAACACUGUCUGGUAACGAUGU	MIMAT0000682
hsa-miR-1	UGGAAUGUAAAGAAGUAUGUAU	MIMAT0000416
hsa-miR-125b	UCCCUGAGACCCUAACUUGUGA	MIMAT0000423
hsa-miR-34b	CAAUCACUAACUCCACUGCCAU	MIMAT0004676
hsa-miR-34a	UGGCAGUGUCUUAGCUGGUUGU	MIMAT0000255

Figure 3-5: Verification of locked nucleic acid probes

RNA (20.0 ng) isolated from M12 cells was converted into cDNA using the miRCURY LNA™ Universal RT PCR system (Exiqon, Denmark). cDNA was diluted to an approximate concentration of 0.2 ng/µl, 0.4 ng/µl, and 0.8 ng/µl. Each reaction was performed in triplicate with individual LNA™ modified oligonucleotide primer sets and real time PCR amplification using SYBR Green. RNU48 was used as an endogenous standard (A). The experimental probe (miR-34a) was normalized by subtracting the corresponding CT value of RNU48 (B). Both plots compare CT values to the amount of starting material.

Figure 3-5: Verification of locked nucleic acid probes
A.

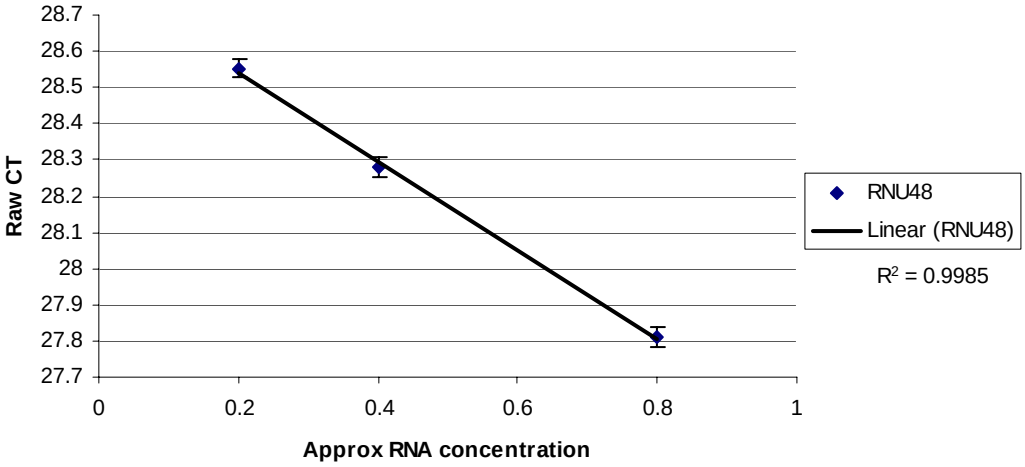

B.

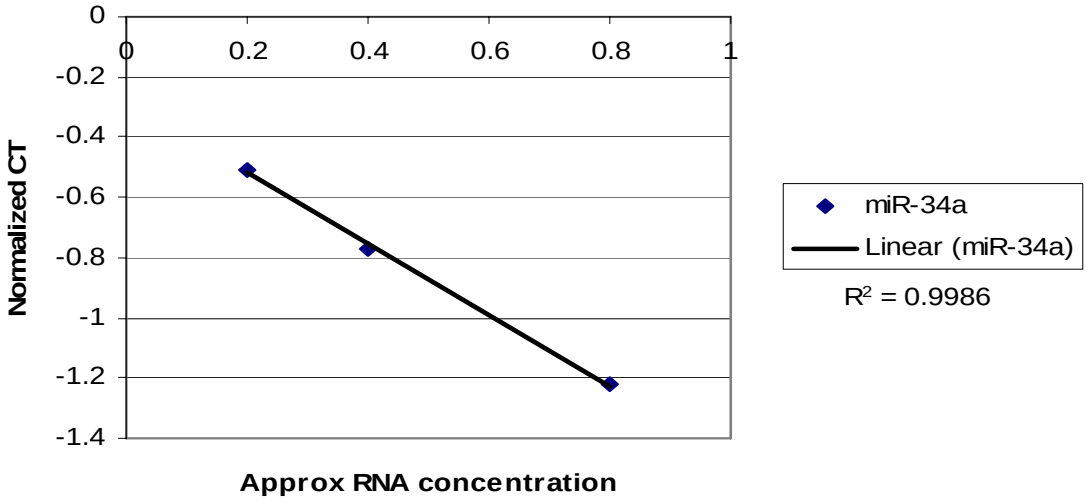

Cancer formation occurs in a step wise process beginning with initiation and ending at metastasis. Along the way, many factors affect and influence the development of cancer. MiRNAs, genes, proteins, and epigenetic mechanisms all contribute during each step of the process. It is important to identify the specific stages of cancer progression that each molecule affects. Utilizing our genetically related prostate cancer progression model, we assayed levels of each dysregulated miRNA in the P69, M2182, and the M12 cell lines. Each step in the progression model was described previously (Figure 1-4). As discussed, array based methods are useful for identifying trends in dysregulation, but true fold changes can only be detected using a single assay format. Results from microarry screens versus single miRNA analyses will be compared in the following section. Where appropriate these results will be correlated to those reported in the literature.

miR-22

Human miR-22 increased during the development of the M12 cells approximately 4-fold (Figure 3-2). Single assay analysis confirms that miR-22 does indeed increase in the M12 subline when compared to the P69 cells (Figure 3-6). Interestingly, the bulk increase occurred during the early phases of tumorigenesis from P69 to M2182. There is only a slight increase in miR-22 from the M2182 cells to the M12 cells.

In the literature, cell lines derived from primary prostate tumor and from distant metastatic sites display increased levels of miR-22 [83]. DU145 cells stably transduced

Figure 3-6: Validation of oncomiRs using single assay format

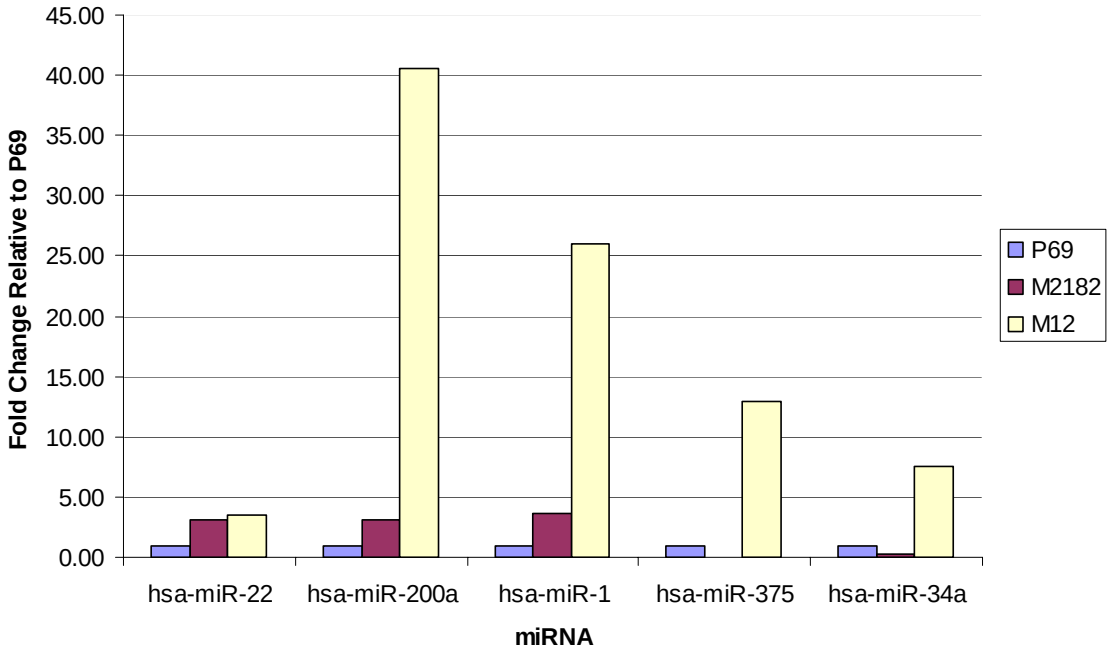

Figure 3-6: Validation of oncomiRs using single assay format

RNA (50ng) was reverse transcribed into cDNA using a universal RT PCR system (Exiqon, Denmark). Each assay was conducted in triplicate with an LNA modified oligonucleotide primer set. SYBR green was used as the fluorescent reporter and the PCR reaction was performed in an ABI7300. Data are presented as the mean fold change between each cell type relative to P69.

with a retroviral vector expressing pri-miR-22 formed a higher number of colonies in soft agar as compared to a nonsense control. Increased expression of miR-22 negatively correlates with the level of PTEN (a known tumor suppressor). In situ hybridization on a prostate tumor microarray slide reveals a majority of prostate tumors express miR-22, while non-tumorigenic tissue does not.

The phosphatase and tensin homog (PTEN) represses the PI3K-AKT pathway which promotes proliferation, invasiveness, and motility [84]. Mutations or deletions of PTEN are common and occur frequently in many cancers including CaP. Dosage-dependent inactivation of PTEN effects tumor progression, invasion and latency. Subtle reductions in PTEN can increase tumorigenic propensity of cells and complete loss of PTEN often gives rise to an aggressive, metastatic phenotype. miR-22, along with other miRNAs, reduces the level of PTEN. Increased expression of miR-22 can lead to a decrease of PTEN levels and accelerate the PI3K/ AKT pathway. Altogether our results agree with these reported findings and support the importance of miR-22 to prostate cancer progression implicating it as a potential oncogenic miRNA.

miR-200a

According to the profiling results, miRNA-200a increases in the M12 subline compared to the P69 cells. In a single assay format using LNA™ primers, we also observed an increase in miR-200a expression as tumorigenicity increased but to a higher level (13-fold) than what was observed in the array (Figure 3-6).

Conversely, most studies seem to find that miR-200a functions as a tumor suppressor with decreased expression upon tumor formation. Multiple studies have

shown that the miR-200 family is essential in maintenance of an epithelial phenotype [85, 86]. Loss of expression of miR-200a induces an epithelial to mesenchymal transition (EMT) through loss of ZEB1/ ZEB2 repression. The EMT is essential for a cell to detach from its neighbors and become motile. There are many markers that indicate a cell has undergone an EMT including increased expression of vimentin and n-cadherin, nuclear localization of β-catenin and loss of e-cadherin [87].

However, there may exist opposite actions for miR-200a that are tumor or tissue type specific. For example, in endometrial endometroid carcinomas (EEC) there is significantly increased expression of all miR-200 family members [88]. Specific inhibition of miR-200a in EEC cell lines decreases proliferation and growth. Although not statistically significant, Lin *et al* observed a tendency towards an increased expression of miR-200a in bladder cancer [89].

Interestingly, we observed a dramatic increase in the level of miR-200a in the highly tumorigenic and metastatic M12 cell line. There is a slight increase in the relative level of miR-200a in the intermediate M2182 cells. Expression of miR-200a exponentially increases from M2182 to the M12 cells which exhibit a more tumorigenic phenotype. Other work in our lab shows M12 cells to be highly invasive and motile [90]. Along with the increased metastatic potential, there is decreased expression of e-cadherin, increased expression of vimentin and nuclear localization of β-catenin proving that M12 cells have undergone an EMT switch.

On the surface, it appears that the results found in this study are contradictory. However, there are numerous targets of miR-200a and it is likely that additional targets remain to be discovered. Regulation of a single target by a miRNA is only partially

understood. It remains to be determined how a miRNA chooses its target when faced with dozens of possibilities. Sequence complementarity, free energy of binding, and mRNA levels may potentially influence which targets are regulated inside of a cell under various conditions. It is becoming clear that multiple types of miRNA interactions are common and it is unlikely that a single miRNA will always serve as either an oncomiR or tumor suppressor in all cell types. Due to this multiplicity of interactions, it is essential to dissect the role of miRNA dysregulation in context of specific types of cancer requiring additional experimentation. In this model of cancer progression, it appears that miR-200a functions as an oncomiR.

miR-1

Predominantly thought to induce cardiac/skeletal muscle differentiation and development, miR-1 also increases during the development of prostate cancer (Figure 3-6) [91]. Similar to miR-200a, the level of miR-1 increases dramatically as the cells progress from an intermediate stage of tumor progression towards a more oncogenic phenotype. Results of the single miRNA assay agree with the overall trend obtained using the mIRCURY array based platform but the fold change observed differed. As seen for miR-200a, analysis of miR-1 using a single assay revealed a much higher fold difference (7-fold) than observed using the array.

There are dozens of targets proven to be regulated by miR-1, the most well described is HDAC4 a histone deacetylase. Androgen insensitivity is commonly observed in most disseminated prostate carcinomas. Localization of HDAC4 in the nucleus of androgen insensitive cancer cell lines was observed and hypothesized to contribute to the

development of the hormone refractive phenotype [92]. In the nucleus, HDAC4 represses genes that induce cellular differentiation. The mechanisms for sequestration of HDAC4 in the nucleus of the androgen insensitive epithelial cells are not well understood. It is possible that accumulation of miR-1 in the cytoplasm by some yet undefined mechanism may play a role in the nuclear localization of HDAC4. Thus miR-1 may be an important oncomiR that drives prostate cancer progession.

miR-375

Exhibiting a greater than 10-fold increase in the M12 subline, miR-375 has been shown by other groups to be of potential interest in the development of prostate cancer [93]. miR-375 accumulates in the cytoplasm of tumor epithelial cells and increases in 82% of patient tumors. In our cell progression model, miR-375 exhibits an interesting behavior. Its expression decreases slightly in the early stages of tumorigenesis and increases as the cells move toward a more tumorigenic, metastatic phenotype (Figure 3-6). The overall observation of miR-375 behavior agrees in both the array and single assay experiments. However, the fold change measured in the array based format was higher than that determined using the single assay experiment reversing the trend seen earlier for miRs-200a and -1. Interestingly, the detection of circulating miR-375 in blood has been suggested as a biomarker for CaP, which would agree with our data suggesting that miR-375 functions as an oncomiR [94].

The X-box binding protein 1 (XBP1) is a basic region-leucine zipper transcription factor involved in the unfolded protein response system [95]. Accumulation of unfolded proteins (ER stress) in the lumen of the endoplasmic reticulum (ER) leads to activation of

pathways that decrease protein expression, increase degradation and protein folding [96]. As ER stress continues to develop, induction of pro-apoptotic pathways occurs. Inadequate responses to ER stress can cause a cell to proliferate uncontrollably. Downregulation of XBP1 inversely correlates with prostate cancer progression ie as XBP1 decreases the Gleason grade of the prostate tumor increases [95]. miR-375 has been shown to target XBP1 causing translational inhibition of the protein leading to increased ER stress. Increased expression of miR-375 may lead to CaP progression.

miR-34a

In our cell model, miR-34a functions as an oncomiR and is approximately 5-fold higher in M12 than in P69 cells (Figure 3-6). Although the miRNA screen and individual assays agree in trend, again there is disagreement in fold differences. The miRNA screen dramatically over estimated the difference of miR-34a between the P69 and M12 cells. Similar to miR-375, earlier stages of pathogenesis display decreased levels of miR-34a. As the cells move toward a more oncogenic state, the level of miR-34a increases.

Traditionally thought to be a tumor suppressor regulated by P53, there is evidence that miR-34a may be highly cell type/tumor type dependent [97, 98]. Nearly 90% of prostate tumors show high levels of miR-34a using an in situ hybridization technique [98]. Knockdown of miR-34a with an antagomir in HeLa cervical cancer and MCF breast cancer cells resulted in decreased proliferation. It is hypothesized that increased expression of miR-34a in tumors may result in an anaerobic metabolic capacity. It is well known that many solid tumors contain hypoxic regions due to structural and functional abnormalities in supporting blood vessels [99]. Increases in the anaerobic potential of

tumors can sustain cell growth and proliferation in spite of the lack of oxygen due to increases in expression of miR-34a. Our analysis suggests that miR-34a acts as an oncomiR in our cell model.

miR-146a

Human miR-146a displays opposing behaviors as the cells become more tumorigenic. In the early stages of oncogenesis (M2182), miR-146a expression increases approximately 2-fold (Figure 3-7). However; as the cells move to the more highly tumorigenic, metastatic phenotype, expression of miR-146a decreases dramatically (60-fold).

Interestingly, a literature search reveals that miR-146a displays contradictory behaviors dependent upon androgen sensitivity [100]. In high grade, hormone refractory prostate cancer, there is a loss of miR-146a expression. There exists an inverse correlation between miR-146a expression and severity of CaP. Increased tumorigenicity is accomplished through the Rho-ROCK1 pathway [101]. ROCK1 is a member of the Rho-GTPase family, driving tumorigenesis by imparting an unlimited proliferative potential, ability to evade apoptosis, and establishment of distant metastastic lesions [102]. Some evidence suggests that ROCK1 may contribute toward the EMT and aid in extravasation of cancer cells from their non-tumorigenic neighbors. Thus loss of miR-146a may induce an oncogenic transformation and miR-146a may be a potential biomarker for CaP progression.

Figure 3-7: Validation of tumor suppressors using single assay format

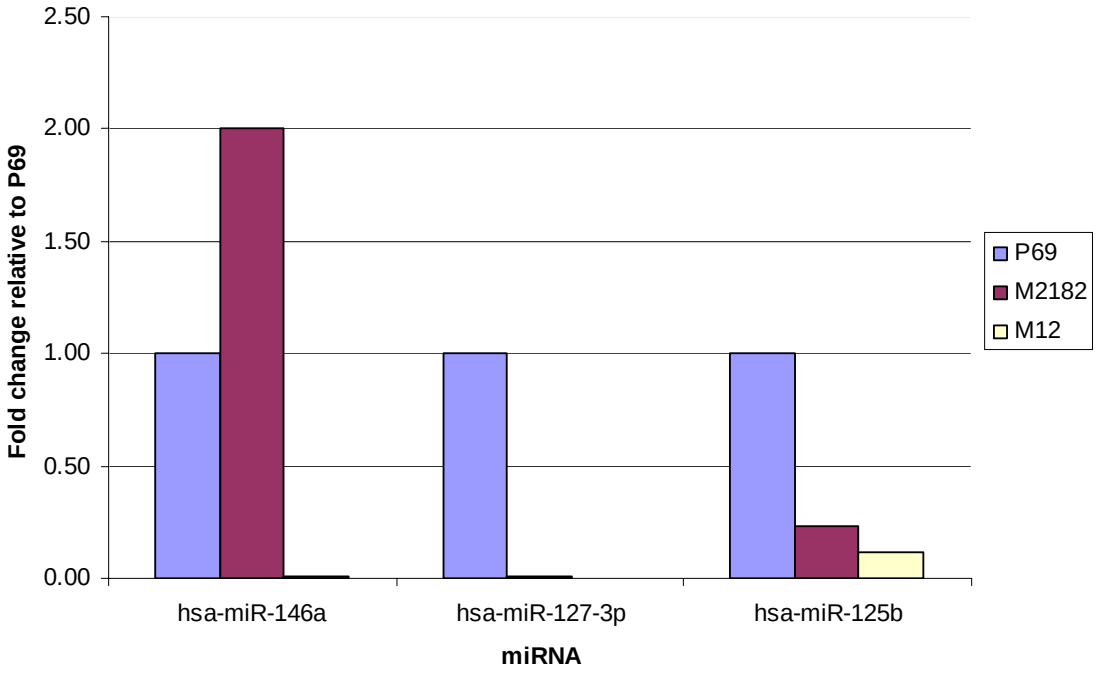

Figure 3-7: Validation of tumor suppressors using single assay format

RNA (50 ng) was reverse transcribed into cDNA using a universal RT PCR system (Exiqon, Denmark). Each assay was conducted in triplicate with an LNA modified oligonucleotide primer. SYBR green was used as the fluorescent reporter and PCR reaction was performed in an ABI7300. Data are presented as the mean fold change between each cell type relative to P69.

miR-127-3p

In our model, the level of miR-127-3p drops dramatically during the early phases of cancer cell progression and is not found to be expressed in the M12 cells (Figure 3-7). Like many miRNAs, miR-127-3p resides in a polycistronic transcript in which all components are under the control of a common promoter. As mentioned, pri-mir-127 gives rise to two fully functional mature miRNAs.

Literature shows that miR-127-3p is a component of the miR-433/miR-127 cluster on chromosome14 that is expressed in the normal, non-tumorigenic prostate gland [103, 104]. Methylation of a specific CpG island in tumor cells silences expression of the mir-127 precursor, while not affecting other members of the cluster. Treatment of the tumor cell with 5'-Aza-CdR results in activation of pri-mir-127 confirming a role for methylation in regulating miR-127-3p expression. miR-127-3p expression correlates with a less tumorigenic, non-metastatic phenotype.

B-cell lymphoma 6 (BCL-6) is a known target of miR-127-3p (Table 3-2) [104]. BCL-6 is a transcriptional repressor best known for its role in the development of lymphoma. However, its expression increases in several solid tumors including tumors of the prostate. A well known target of BCL-6 repression is the programmed cell death 2 (PCD2) gene, that is involved in apoptosis [105]. Induction of BCL-6 protects cells from apoptosis, allowing cells to proliferate in spite of the accumulation of genetic mutations. Decreased expression of miR-127-3p due to promoter methylation leads to accumulation of BCL-6 and subsequent repression of PCD2 allowing cells to escape apoptosis and proliferate uncontrollably. Thus miR-127-3p functions as a tumor suppressor.

miR-127-5p

As pri-mir-127 gives rise to two functional mature miRNAs, it is expected that silencing of the precursor would result in decreases of the level of both mature miRNAs. Our analysis confirms that both levels of miR-127-3p and miR-127-5p decrease as the cells gain tumorigenic properties.

miR125-b

Human miR-125b was greatly decreased in the highly tumorigenic, metastatic M12 cell line (Figure 3-7). In early stages of tumorigenicity, miR-125b levels decrease and continue to decrease as oncogenesis proceeds. Overall from P69 to M12, there is approximately a 20-fold drop in the level of miR-125b. Again, this number does not agree with the fold change found using the miRCURY Human Panel where miR-125b is barely detectable in the M12 variant giving rise to a less accurate number. In spite of this discrepancy, both methods confirm a highly differential expression of miR-125b. There are many proven targets of miR-125b including the epidermal growth factor receptors ErbB2 and ErbB3 [106]. Increased levels of ErbB2/ ErbB3 lead to uncontrolled cellular proliferation and inhibition of apoptosis through activation of the AKT pathway. Patients with metastatic, hormone-refractory CaP all showed an increase in EGFR expression [107]. Overexpression of EGFR receptors has been shown to be associated with poor outcomes from CaP [108].

A recent study that compared matched prostate tumorigenic epithelium to benign epithelium revealed significant down regulation of miR-125b [109]. Decreased expression

of miR-125b can be used as a potential biomarker for the discrimination of malignant from benign epithelium. Due to the evidence of involvement of the EGFR pathway in prostate cancer progression, miR-125b makes an attractive therapeutic target as well. Increasing expression of miR-125b in highly tumorigenic and metastatic prostate cancer cells may decrease tumorigenicity by inhibition of the EGFR family of growth factor receptors. In this cell progression model, miR-125b clearly functions as a tumor suppressor.

Summary of cell line data

Numerous changes occur during the transition from a poorly tumorigenic phenotype to a highly oncogenic state. There are many miRNAs dysregulated as a cell gains increased tumorigenic propensity. In this study, we identified approximately 200 miRNAs with altered expression patterns that may contribute to the development of CaP using an array based format. A subset of these miRNAs was chosen based on their interaction with critical proteins and their expression was analyzed across a cancer progression model. Overall the expression patterns determined using the array based format were confirmed using the single miRNA assay, but in some cases the fold changes did not agree across the two methods. Nevertheless, literature searches confirmed that each miRNA may indeed contribute to cancer progression through the modulation of important cellular pathways. The possible interplay of these pathways in regulating CaP will be further explored below.

Interestingly, two of the chosen miRNAs regulated the PI3K/ AKT pathway. As discussed, loss of miR-125b leads to increased levels of ERBB2/ ERBB3 accelerating

cell proliferation and inhibition of apoptosis (Figure 3-8). Increased expression and accumulation of miR-22 leads to decreased levels of PTEN a known inhibitor of PI3K. Loss of PI3K repression leads to increased cell proliferation and avoidance of apoptosis.

Utilization of *in vitro* models of cancer progression and metastasis has occurred since the advent of the HeLa immortalized cell line. Since that time, hundreds of cell lines have been created that are used to study nearly every form of cancer. CaP has been traditionally studied using three major cell lines and their derivatives (Du145, LnCaP, PC3).

The cell lines used in this research are unique. The primary cell used in this study is derived from non-tumorigenic tissue, not from metastatic lesions. The highly tumorigenic, metastatic sublines were created using *in vivo* selection methods. As such, they are genetically related and offer an insight into the molecular perturbations that underlie tumorigenesis and metastasis. *In vitro* models of cancer progression offer many advantages; they are easy to handle, virtually limitless, essentially homogeneous, and are relatively inexpensive to study [110].

Potential limitations of *in vitro* research include; accumulation of genetic mutations as cells propagate in culture, contamination of cell lines by bacteria, inability to replicate *in vivo* structure, and elimination of environmental cues by separation of cells from their stroma. Although, there are limitations to *in vitro* assays, they still provide an opportunity to elucidate molecular alterations affecting cancer development. For these reasons, it is highly unlikely that a single model system can accurately reflect all aspects of disease progression and it is important to utilize a variety of methods to ensure that findings from cell lines replicate growth of tumor in man. Molecular changes observed in

Figure 3-8: Model of miRNA dysregulation of PI3K/ AKT pathway

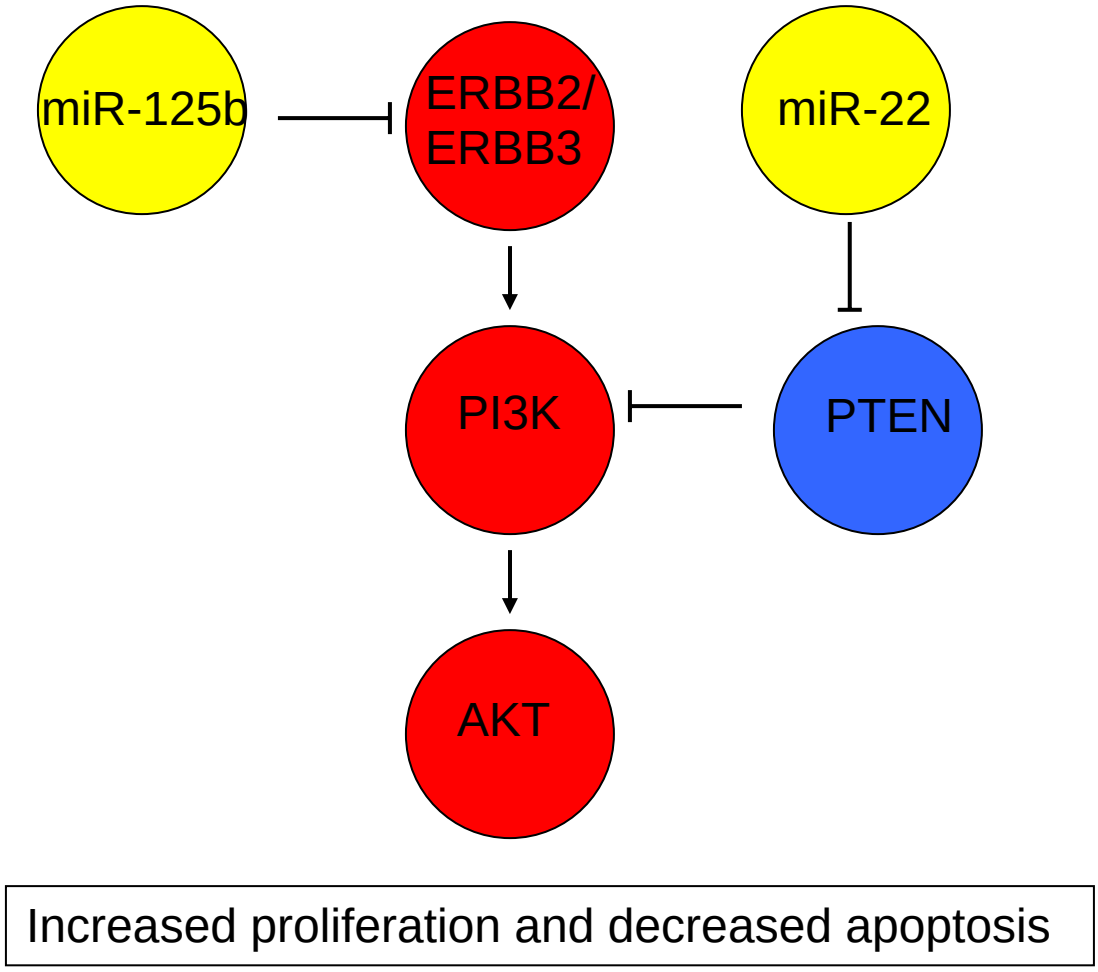

Figure 3-8: Model of miRNA Dysregulation of PI3K/ AKT Pathway

Evaluation of miRNA expression changes using the Exiqon LNA™ miRCURY system revealed the loss of miR-125b with an increase in miR-22 as cells gain tumorigenic potential. The literature shows that mR-125b and miR-22 regulate the PI3K/ AKT pathway. Combined dysregulation of both miRNAs may affect oncogenesis through pathway modulation. Protein nodes in red are known inducers of tumor formation. The node in blue is a well described tumor suppressor, and yellow nodes are miRNAs that inhibit their protein targets.

cell lines must be confirmed in human tissue and its role in prostate cancer defined. It is unclear if many of the observed expression differences are causal or simply as a result of tumorigenic behavior.

Confirmation of miRNA dysregulation in human tumors

Transformation of benign prostate cells to disseminated metastatic lesions can best be understood in the context of the native environment of the prostate gland. Determining molecular changes contributing to pathogenesis in the prostate is complicated by the heterogeneity of the tissue. Relevant cell populations often only comprise a small percentage of whole tissue [111]. Ideally, expression profiling will be carried out in pure cell populations as to minimize the confounding variables contributed by heterogeneous cell populations.

To confirm findings, miRNA dysregulation was assessed in tumors obtained after radical prostatectomy. In consultation with a board certified pathologist (Ema Dragoescu, MD), approximately 25 potential fresh, frozen samples were identified and examined for evidence of prostate cancer. Following prostatectomy, core samples are obtained from the removed prostate. An attempt is made to obtain a representative core sample containing regions of prostate tumor using external palpation. Many of the core samples evaluated did not meet inclusion criteria for this study. Either the amount of tumor was inadequate or there were not enough benign glands for matched comparison. Of the samples evaluated, four were found to be suitable for study inclusion as they contained both benign and tumorigenic epithelial glands. One of the four patients identified was eventually excluded from the study due to an inability to obtain adequate RNA to analyze

as core samples missed most of the tumor. Ideally, additional samples will be profiled in the future. However, one is limited to the number of prostatectomy procedures performed in their facility, patient consent, and adequate levels of tumor in the core samples.

Pure cell populations can only be obtained from a heterogeneous tissue with techniques such as laser capture microdissection [40, 112]. LCM allows for direct visualization of the tissue and extraction of selected cells using UV or IR laser pulses. Selected cells are adhered to a polymer and are utilized for downstream analysis of biological macromolecules.

Although there have been numerous array based studies utilizing human prostate tissue, there is little agreement on specific miRNAs dysregulated during tumorigenesis [90]. A potential reason for disagreement among studies may be contamination of tumor tissue with adjacent smooth muscle, stroma, blood vessel, lymphocytes, and benign epithelium. Whole prostate tissue stained with H&E is visualized microscopically and cells of interest are selected (Figure 3-9a). Often, core samples contain several tissue types. It is not uncommon to find regions of high grade adenocarcinoma located immediately adjacent to benign epithelial glands. Nearly pure populations of the selected cell type are captured onto the polymer cap and residual tissue is left behind (Figure 3-9b and 3-9d). LCM analysis is important as findings from whole tissue may be complicated by the presence of unrelated, contaminating tissue such as prostatic urethra (Figure 3-9c). Previous studies that evaluate miRNA expression using homogenized whole prostate tissue are likely to be contaminated with other tissue types. Cell specific /tumor specific profiles can be obscured when whole tissues are homogenized and extracts are used in downstream applications. LCM is necessary to minimize confounding variables and

Figure 3-9: Laser capture microdissection of human prostate tissue

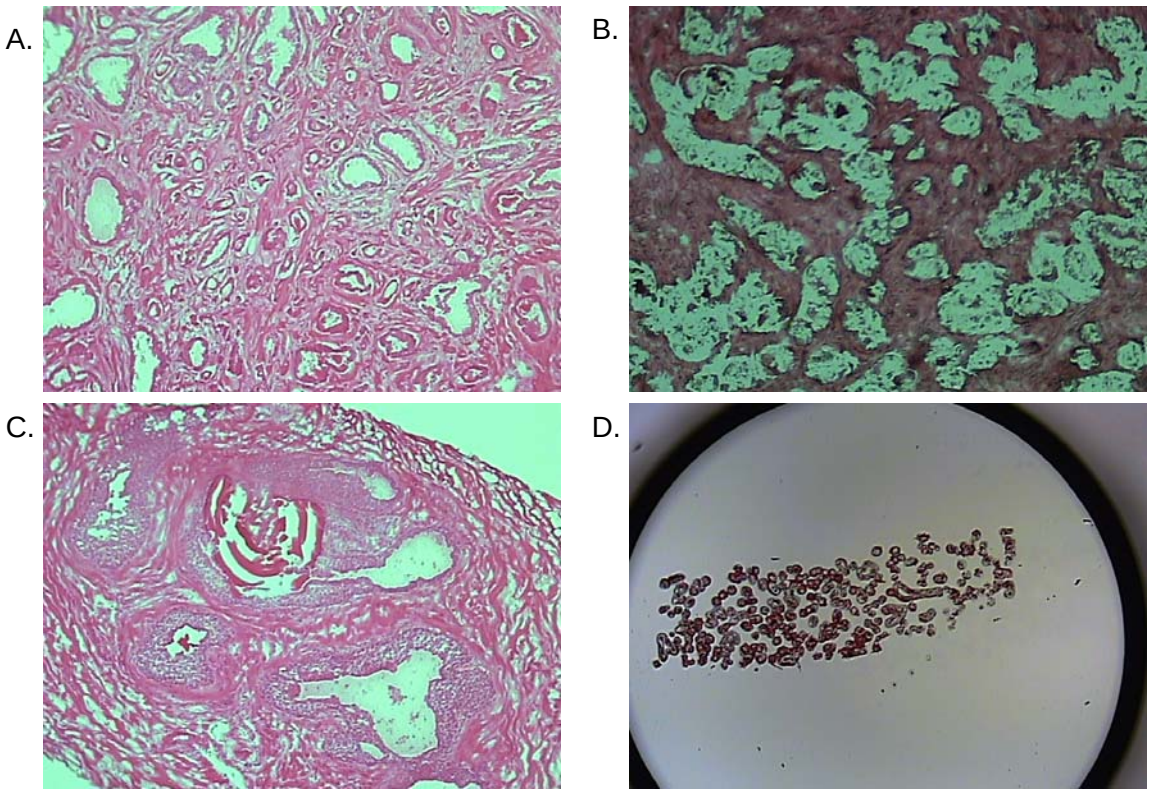

Figure 3-9: Laser capture microdissection of human prostate tissue

Human prostate tissue obtained after prostatectomy was flash frozen in liquid nitrogen. Samples stained with hematoxylin and eosin (H&E) following dehydration with ethanol and xylene were mounted on uncharged glass slides. Representative tissue samples displaying the heterogeneity of prostate tissue are shown (A). Following microdissection, only regions of stroma remained. Epithelial tumor cells were extracted and retained for analysis (B). LCM is required to minimize variation due to tissue heterogeneity. Regions of Prostatic urethra are visible in panel C and if included in a whole tissue sample could complicate analysis (C). Epithelial tumor cells are retained on LCM cap (D).

obtain expression profiles that are truly reflective of the tumorigenic components of the gland. Ideally, different grades of tumor tissue would be separated from one another and their expression profile quantified in isolation. Within the tumor component of tissue, it is normal to find glands of varying grades and stages. This approach assesses differential regulation of miRNA within each distinct phase of tumor progression. However; when using fresh frozen tissue, time is a limiting factor.

In order to obtain RNA that adequately represents the expression profile of the tissue, dissection must be completed within 30 minutes. Due to the time limitation, it is difficult to completely isolate tumor sub-types from one another. Thus in this study, whenever fresh frozen tissue was utilized, all tumor sub-types were grouped together. Future studies will further characterize miRNA dysregulation in tumor sub-types using formalin-fixed paraffin embedded (FFPE) prostate samples. Ideally, fresh frozen samples will be compared to their FFPE counterpart to minimize inter-patient variability. In this study, we have evaluated one FFPE patient sample to profile miR-125b behavior across epithelial sub-types. The expression of other selected miRs was analyzed in the three remaining frozen tissue samples (Figure 3-10 through Figure 3-12).

Evaluation of all proposed oncomiRs revealed that there is not one miRNA in our sub-group that universally increases as cancer progresses (Figure 3-10 – Figure 3-12). It is expected that there will be great variation in the expression profile of miRNAs [113] . Differences in genetic sequence, epigenetic regulation and acquisition of somatic mutations may lead to disease and differential miRNA dysregulation. Some miRNAs demonstrate common patterns of expression that suggest their regulation may be genetically inherited.

Figure 3-10: Evaluation of miRNA dysregulation in patient 09-362-V002

RNA (50ng) was reverse transcribed into cDNA using a universal RT PCR system (Exiqon, Denmark). Each assay was conducted in triplicate with an LNA™ modified oligonucleotide primer set. SYBR green was used as the fluorescent reporter and the PCR reaction was performed in an ABI7300. Data are presented as the mean fold change between tumor cells relative to benign epithelium. OncomiRs predicted to be dysregulated during tumorigenesis are displayed in Panel A. Tumor suppressors are shown in Panel B.

Figure 3-10: Evaluation of miRNA dysregulation in patient 09-362-V002

A.

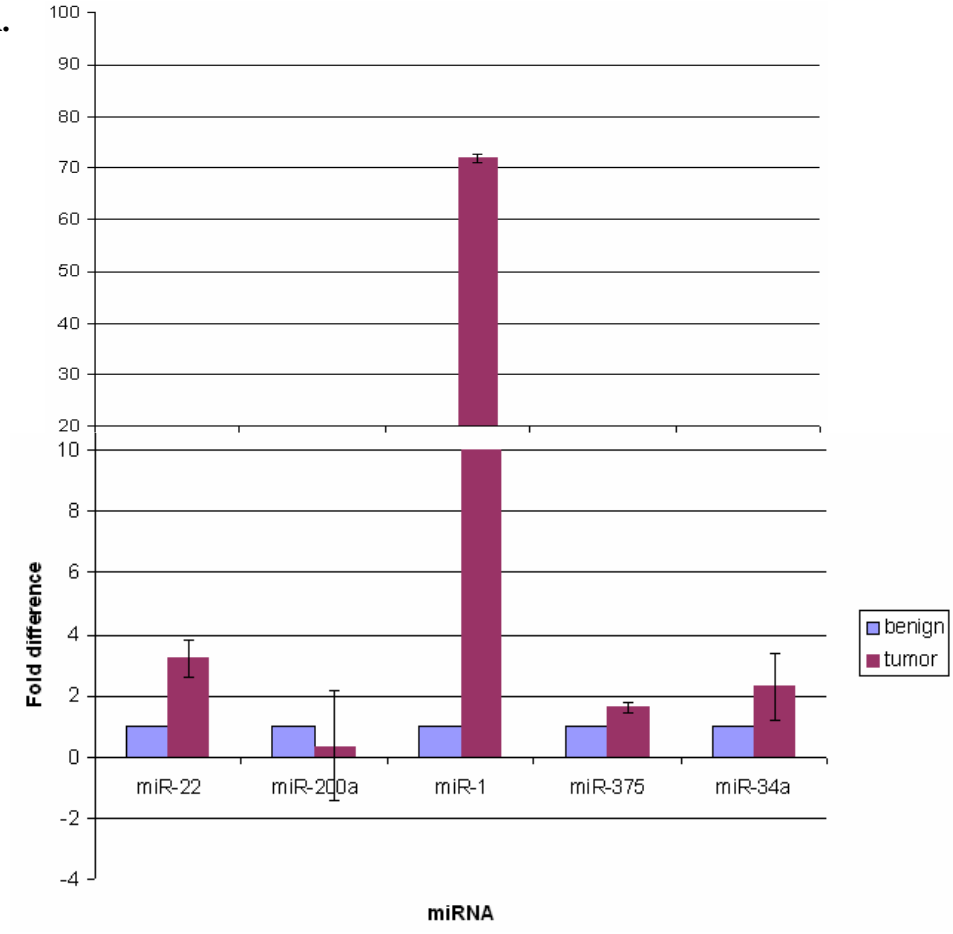

B.

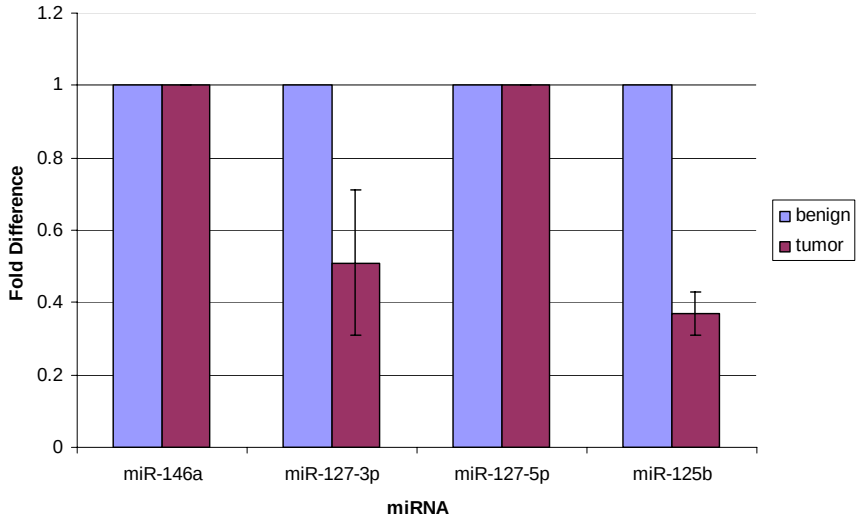

Figure 3-11: Evaluation of miRNA dysregulation in patient 08-347-V007

RNA (50ng) was reverse transcribed into cDNA using a universal RT PCR system (Exiqon, Denmark). Each assay was conducted in triplicate with an LNA™ modified oligonucleotide primer set. SYBR green was used as the fluorescent reporter and the PCR reaction was performed in an ABI7300. Data are presented as the mean fold change between tumor cells relative to benign epithelium. OncomiRs are displayed in panel A and tumor suppressors are shown in panel B.

Figure 3-11: Evaluation of miRNA dysregulation in patient 08-347-V007

A.

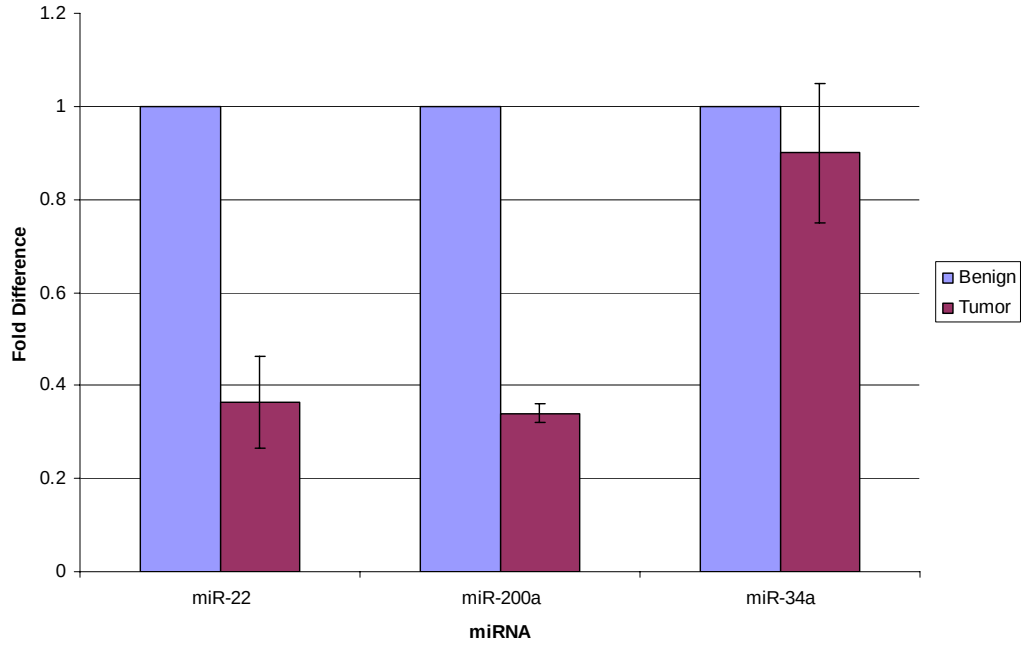

B.

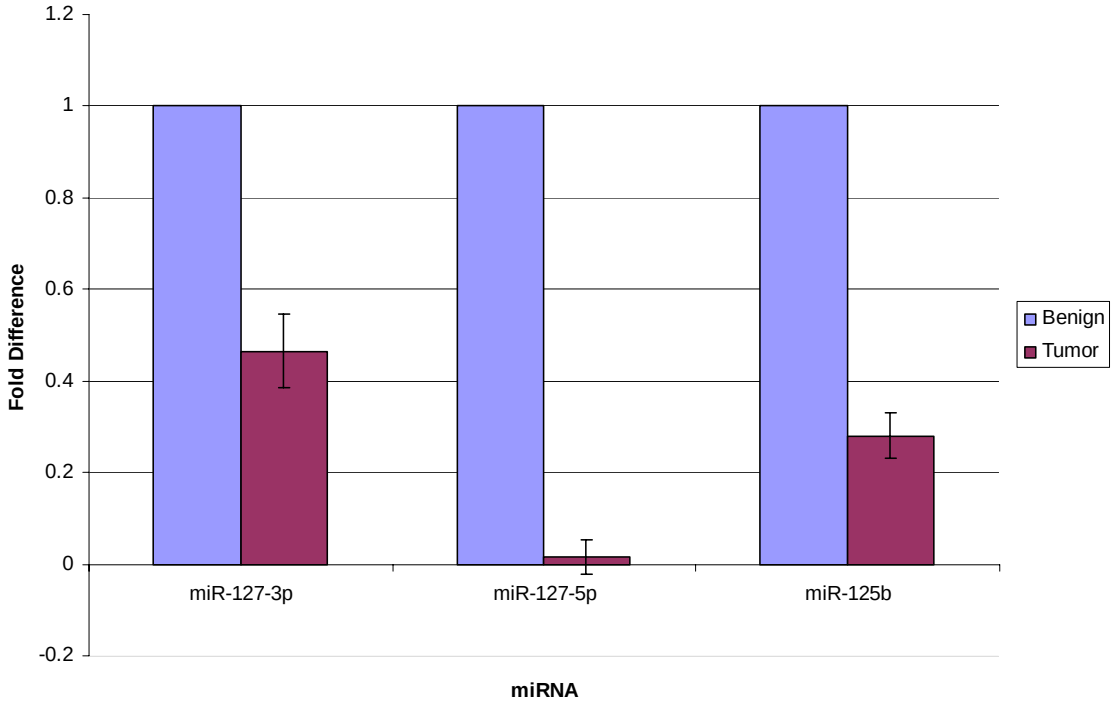

Figure 3-12: Evaluation of miRNA dysregulation in patient 09-225-V002

RNA (50ng) was reverse transcribed into cDNA using a universal RT PCR system (Exiqon, Denmark). Each assay was conducted in triplicate with an LNA™ modified oligonucleotide primer set. SYBR green was used as the fluorescent reporter and the PCR reaction was performed in an ABI7300. Data are presented as the mean fold change between tumor cells relative to benign epithelium. OncomiRs are displayed in panel A and tumor suppressors are shown in panel B.

Figure 3-12: Evaluation of miRNA dysregulation in patient 09-225-V002

A.

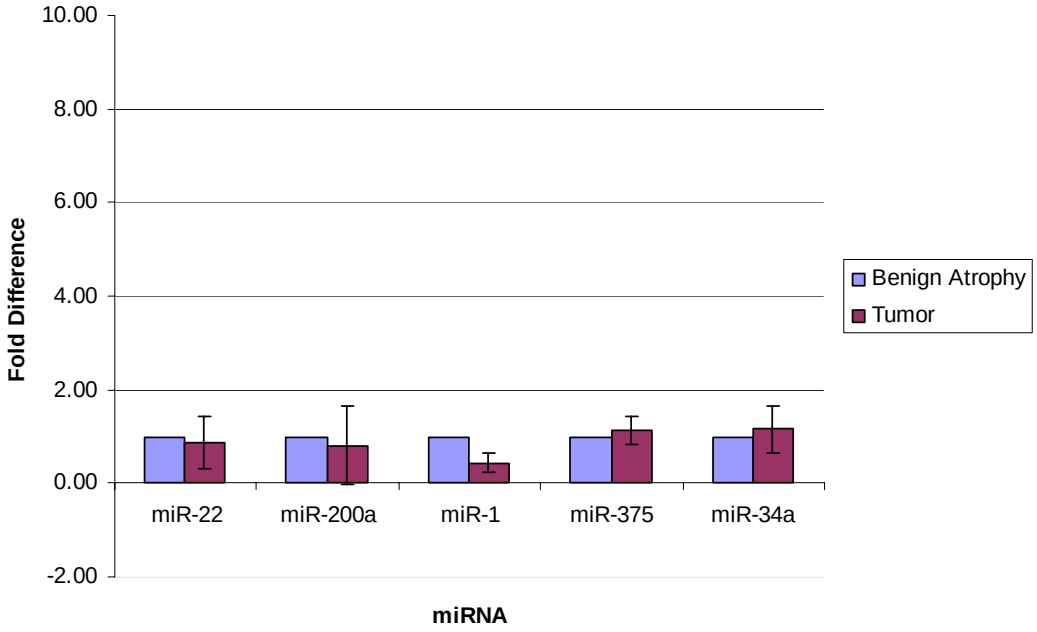

B.

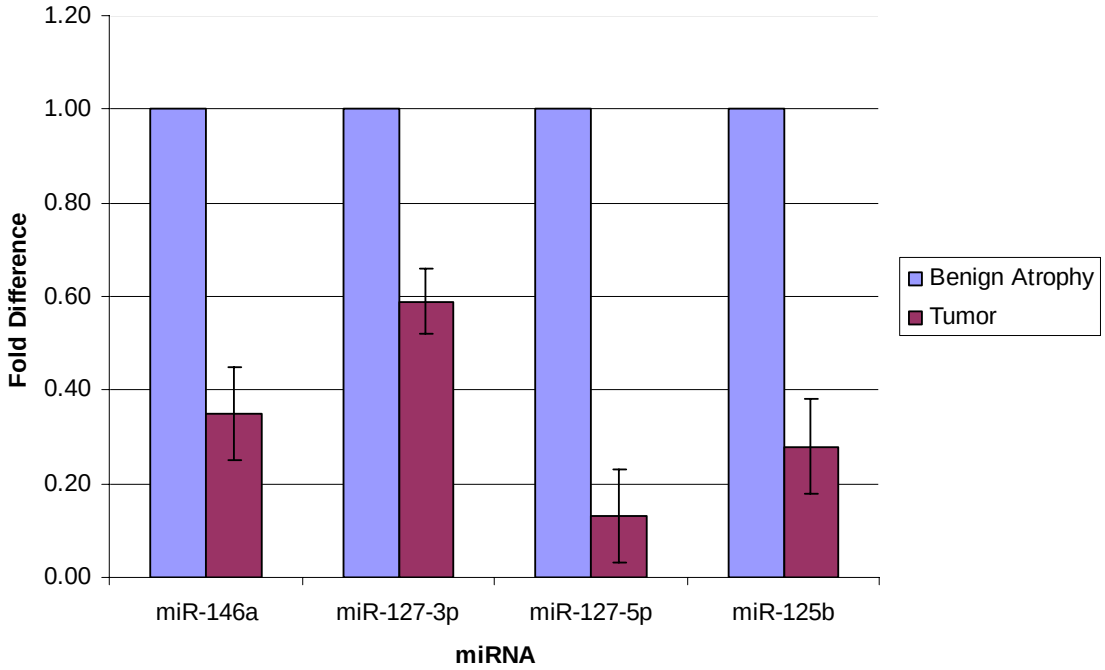

It has been shown that some miRNAs differ in their expression patterns between African-American and Caucasians demonstrating that different human populations vary in their global miRNA expression patterns. Due to the high degree of variance, it is essential that researchers profile a large number of patients to identify key miRNAs that may contribute to CaP progression. However, at this point we only had three samples to profile and some interesting circumstances are discussed below which could contribute to the lack of universal findings.

Due to technical limitations in acquiring use of the LCM facility, one sample remained stored at -80° C after mounting onto slides for an extended period of time ie 6 months (08-347-V007). Thus, RNA extracted from this patient may be of dubious quality and not accurately reflect all miRNA changes (Figure 3-11). Due to limited RNA availability not all miRNAs could be assessed.

Another patient (09-225-V002) presented with an interesting morphological condition. The glands of the prostate were atrophied. Although the attending pathologist described the condition as benign, the miRNA expression profile suggests otherwise. There is essentially no difference in oncomiR expression between the atrophied glands and the tumor epithelium (Figure 3-12). It is possible that prostatic atrophy is not a benign lesion but may be an early form of cancer. Consistent with this hypothesis, literature shows that other authors have demonstrated that atrophied glands have increased production of proliferative markers, and decreased levels of apoptosis [114]. Prostatic atrophy seems to be a pre-cursor to prostatic intraepithelial neoplasia and prostate carcinoma and is not the same as normal prostatic epithelium.

One patient (09-362-V002) exhibited expected increased expression for all proposed oncomiRs with the exception of miR-200a (Figure 3-10). As discussed, there are opposing roles for miR-200a that are likely to be tumor type dependent and this discrepancy is justifiable. We put the most stock in this sample, as it was freshly prepared. Cells were captured and RNA was extracted within 4 days. Moreover, the tissue illustrated little abnormalities in cell type composition. In addition, we obtained significant yields of high quality RNA from this individual as attested by analysis of sample composition on a bioanalyzer. However, these results need to be confirmed with additional human samples.

Profiling of tumor suppressors in human tissue

Contrary to our analysis of oncomiRs, all of the tumor suppressors identified in our cell progression model were confirmed in each patient sample analyzed (Figure 3-10 – Figure 3-12). miR-127-3p and miR-127-5p both function as tumor suppressors; however, there remains some form of differential regulation. Although differential expression was observed in the cell lines, human samples showed a reverse trend with higher levels of the 3p strand. miR-127-3p showed 3-4-fold higher expression levels when compared to miR-127-5p in human tumor samples.

miR-125b showed significantly decreased expression (~5-fold) in all human samples analyzed thus far. Again this fold change is not as significant as estimated using the array based platform, but remains exciting nonetheless. As discussed, miR-125b is one of two miRNAs chosen that regulate the PI3K/AKT pathway leading to increased cell proliferation and apoptosis inhibition. Loss of miR-125b results in increased

expression of ERBB2/ERBB3, two members of the family of epidermal growth factor receptors. Anther study has shown widespread, but not universal downregulation of miR-125b during the development of prostate cancer [115].

This analysis indicates that it is easier to lose expression of a tumor suppressing miRNA rather than increase expression of oncomiRs. Loss of miRNA expression can be brought about by a number of events. Pre-cursor miRNAs are cleaved into their mature functional molecule by Drosha and Dicer processing. Differential expression of Drosha and Dicer could account for some of the loss of miRNAs in tumor tissue [116]. Literature shows that Dicer levels are differentially regulated in various prostate tumors. [117]

Furthermore, over half of miRNA genes are located in regions of the genome that are sensitive to loss of heterozygosity (LOH). Epigenetic modifications have been shown to effect numerous miRNAs as well. Often hypermethylation of miRNA promoters inhibits expression of the pri-mirna thus decreasing the overall level of mature miRNA available.

An ideal biomarker would be able to distinguish malignant cells from benign cells before histological changes occur as therapy is more likely to be successful. The loss of miR-125b in the tumor cells may be a potential indicator of cancer initiation and progression. In order to determine if miR-125b decreases in the early stages of cancer development, analysis of FFPE archived prostate samples was used to measure miR-125b in various types of prostate epithelium (Figure 3-13). Dissection of FFPE samples is not time limited and provides an ideal opportunity to more finely resolve changes that occur during tumor progression.

Interactions between cells and their microenvironment contribute to the maintenance of tissue homeostasis [118]. Intricate intercellular signaling networks between the stroma and epithelium help to maintain normal tissue integrity. Communication failure within either the stromal cells or the epithelial cells may induce oncogenic transformation and contribute to cancer initiation or progression. Generation of a reactive stroma is generally thought to occur during early phases of tumor progression [119]. Identification of miRNA changes driving the switch from normal to reactive stroma may result in a unique early indicator of prostate cancer. A slight increase in the level of miR-125b is observed in the stroma of this sample compared to benign epithelial tissue (Figure 3-13).

Benign prostatic hyperplasia (BPH) is a common disorder that will affect nearly all men at some point in their life. BPH normally occurs in two distinct phases [120]. During the first phase of disease progression, there is microscopic evidence that the glandular cells of the prostate increase in size. The second phase of BPH progression results in dysuria caused by macroscopic growth of the prostate gland resulting in partial obstruction of the prostatic urethra. It is generally thought that the presence of BPH does not increase a patient's risk of developing CaP. The level of miR-125b decreases in BPH cells when compared to normal benign epithelium (Figure 3-13). However, there is a great range of miR-125b levels in BPH cells as evident by the large standard deviation. It would be interesting to determine if BPH glands located closer to tumor cells display an altered miRNA expression portrait.

Figure 3-13: Evaluation of miR-125b expression in various epithelial subtypes

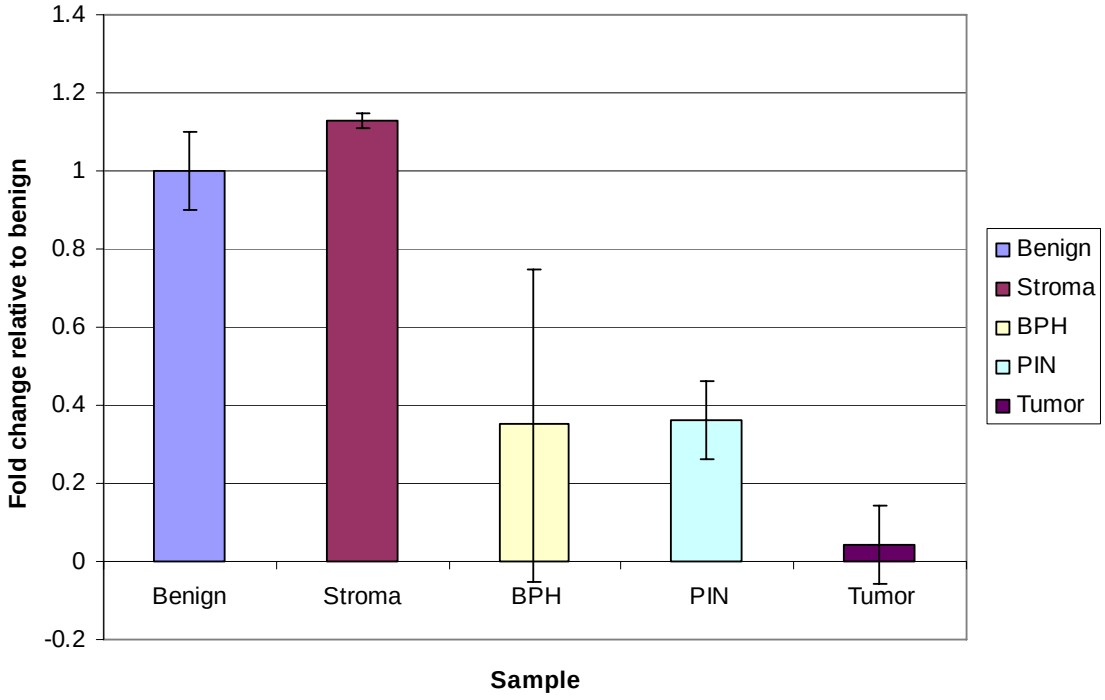

Figure 3-13: Evaluation of miR-125b expression in various epithelial subtypes

A single FFPE prostate sample mounted in 10µm slices onto 20 slides was dissected with LCM into various epithelial subtypes and stroma. Using the PicoPure RNA extraction kit, total RNA was obtained and quantity estimated using an Agilent Bioanalyzer 2100 with the RNA Pico chip. RNA (20 ng) was converted into cDNA using the TaqMan® microRNA Reverse Transcription Kit (Life Technologies, Grand Island, NY). Q-PCR was performed with specific primers against miR-125b using the TaqMan® Universal Master Mix II with no Amp unerase (Life Technologies, Grand Island, NY). CT values were normalized using levels of the endogenous control (RNU48) and reported as fold differences using the ddCT method of Livak et al [74].

Prostatic intraepithelial neoplasia (PIN) is considered to be a pre-cursor for the development of prostate carcinoma [121]. PIN is characterized by increased proliferation of basal cells in the prostate gland without invasion into the underlying stroma. Many of the genetic changes that drive prostate cancer occur early in pathogenesis and are evident in PIN cells. Expression of the EGFR members ERBB2/ ERBB3 increase as the cells transition from a benign phenotype to PIN cells [122]. As ERBB2/ ERBB3 are targeted by miR-125b, it is reasonable to suspect that miR-125b decreases as the cells transition. Our analysis confirms this hypothesis. miR-125b decreases 3- 4-fold when compared to the benign epithelium (Figure 3-13). This finding indicates the miR-125b may be useful to identify early pre-cancerous lesions and subsequent decreases in the level of miR-125b may help identify progressive tumor growth.

In order for a tumor cell to set up a distant metastatic lesion, it must detach from its neighbors and invade the surrounding basement membrane. Numerous proteins have been implicated in the ability of a cell to acquire metastatic potential [123]. Two proteins that affect the PI3K/ AKT pathway have been shown to impact the metastatic potential of a cell. Over-expression of ERBB2/ ERBB3 has been shown to increase a cell's ability to become motile and invasive. Loss or reduction of PTEN has a similar phenotypic effect.

Due to the combinatorial analysis implicating ERBB2/ ERBB3 as potential drivers of tumorigenesis negatively regulated by miR-125b whose level is reduced as tumorigenicity increases, it is reasonable to suspect that restoration of miR-125b would inhibit tumorigenic potential. Many studies have used miRNA overexpression as a means to identify function of the miRNA [124]. Literature shows that the enforced expression of miR-125b impacts a cells ability to invade and migrate through the stroma of the prostate

tissue [125]. Proof of this concept also exists in breast cancer where it was shown that increased expression of miR-125b in SKBR3 cells inhibits the ability of cells to migrate and invade through the down regulation of ERBB2/ERBB3 [106]. Down-regulation of miR-125b is found in many solid tumors and promotes anchorage independent proliferation, cell migration and invasion. Loss of miR-125b seems to be an important step in the attainment of an oncogenic state.

In Vitro metastasis assays

Stable transformation of M12 cells with a pSIREN vector expressing the pre-mir-125b sequence negatively affected the ability of M12 cells to migrate (Figure 3-14). After transfection and selection, restoration of expression was confirmed by qRT- PCR and the level of miR-125b was found to be 3-fold higher than the original M12 cells (Figure 3-15). It is important to note that this fold of expression change is physiologically relevant. Most human tumors profiled in this study had a 3 - 5-fold drop in the level of miR-125b. Enforced overexpression of a miRNA past physiological levels may not reveal accurate results.

Previous studies have demonstrated that restoration of a tumor suppressing miRNA (hsa-miR-17-3p) limits the ability of M12 cells to migrate in a Transwell assay [90]. It is known that miR-17-3p downregulates the intermediate filament protein, vimentin, which is known to increase in highly tumorigenic, metastatic cells. M12 cells stably expressing mature miR-17-3p were used as a positive control to compare our miR-125b expressing cells. Like miR-17-3p, restoration of miR-125b expression inhibited cellular migration approximately 3- 4-fold.

Figure 3-14: Migration assay

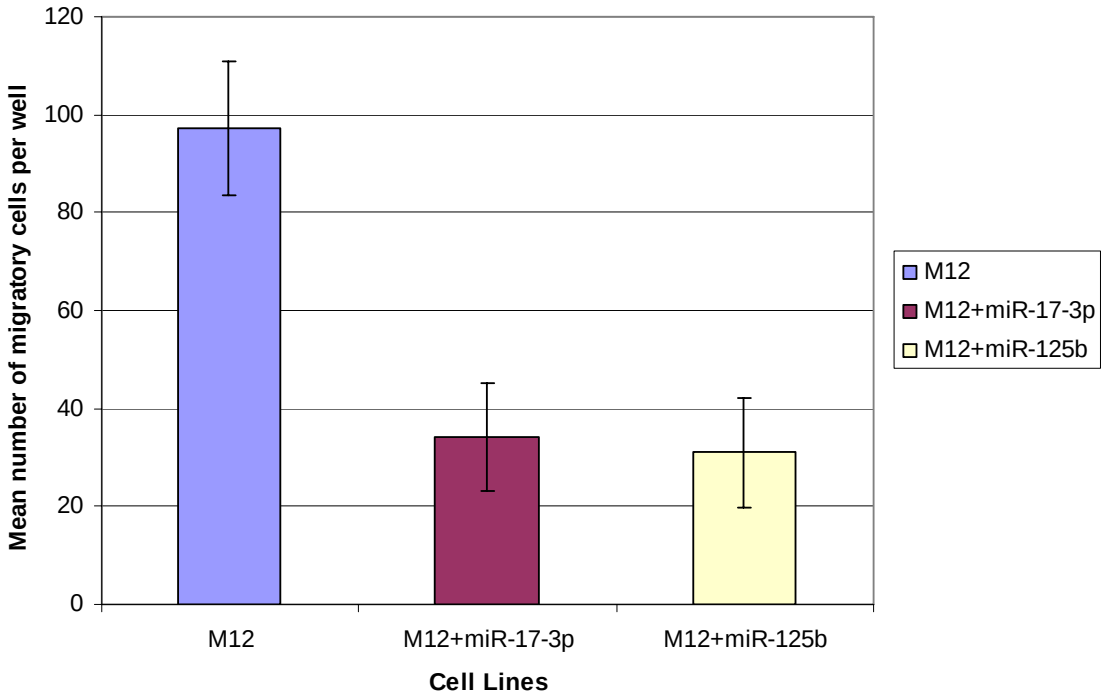

Figure 3-14: Migration assay

Cells (50,000) were plated in serum free media in the top chamber of a ThinCert™ tissue culture insert. Bottom chamber contained 500 µl of RPMI 1640, 5% FBS, supplemented with 10 ng/ml of EGF as a chemotractant agent. Cells were incubated for 20 hours and fixed with 0.025% glutaraldehyde for at least 20 minutes. Cells visualized by staining with 0.1% crystal violet in PBS for 30 minutes and the membrane was mounted on a glass slide. Cells were plated in triplicate across three wells and counted in 10 random fields. Total number of migratory cells was estimated by summing up each of the individual fields. The mean sum of the well is presented, along with the standard error.

Figure 3-15: Restoration of miR-125b in M12 cells

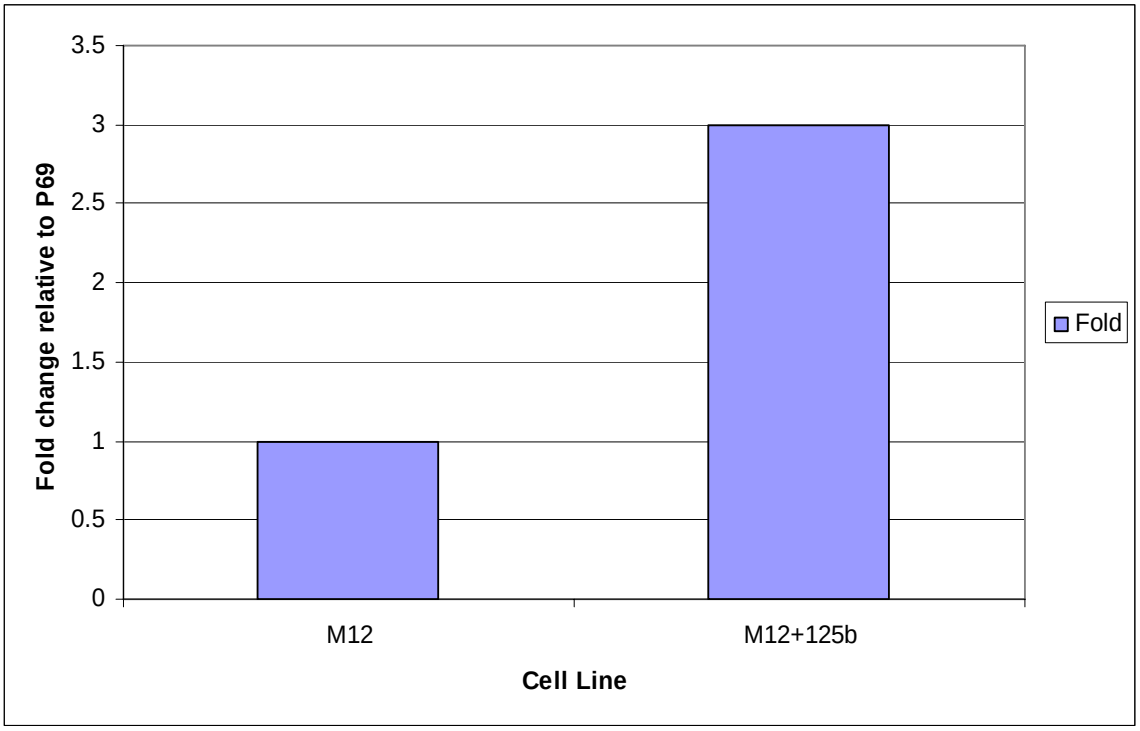

Figure 3-15: Restoration of miR-125b in M12 cells

M12 cells (500,000) were stably transformed with the human miR-125b sequence. Cells were transformed with purified plasmid (2.0 μg) using TransIT-LT1 (4.0 μl) transfection reagent (Mirus BioCorp, Madison, WI). Resistant cells were selected with 400 ng/ml Puramycin. Increased expression of miR-125b was verified by TaqMan™ qRT-PCR analysis.

Secondary tumor sites are a culmination of a metastatic cascade of events in which the tumor cell becomes motile and invades the basement membrane [126]. Restoration of miR-125b reduces the motility of cancer cells as evidenced by the Transwell assay shown in Figure 3-14. Invasion of a cell through the basement membrane is critical to the ability of a tumor to disseminate to other organs. The invasive potential of M12 cells with restored miR-125b was assessed using Transwell chambers coated with reduced growth factor basement membrane. Untreated M12 cells were highly invasive. M12 cells with restored miR-125b had a 75% lower invasive ability than M12 cells (Figure 3-16). Again the results are quite similar to M12 cells with restored expression of miR-17-3p.

Together these assays suggest that restoration of miR-125b negatively impacts a tumor cell's ability to metastasize. As most patients that die from prostate cancer, die from metastatic lesions, inhibition of metastasis may prolong the lives of patients suffering from prostate cancer. Targeted delivery of miR-125b to prostate cancer cells may offer a unique therapeutic alternative to limit morbidity and mortality associated with the disease. These analyses demonstrate that progressive loss of miR-125b increases the metastatic potential of tumor cells.

Figure 3-16: Invasion assay

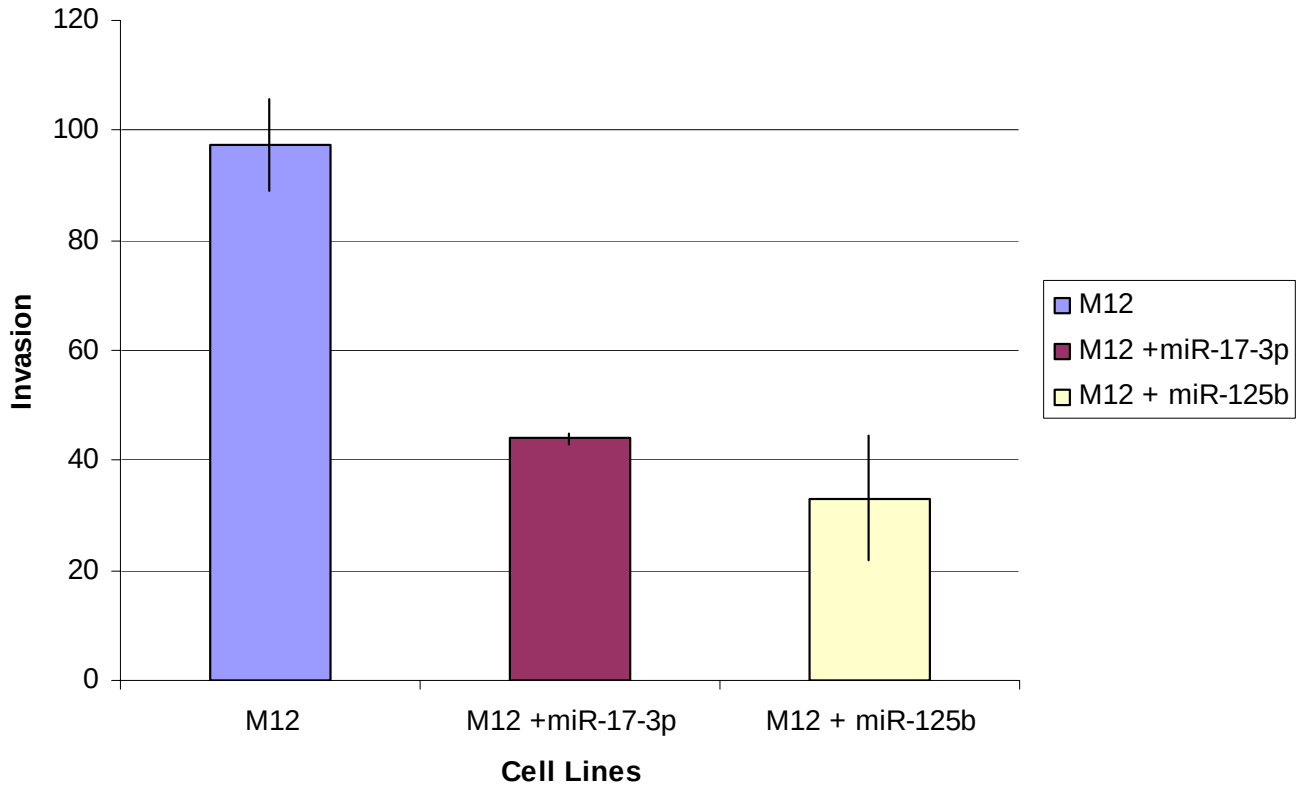

Figure 3-16: Invasion assay
Cells (50,000) were plated in serum free media in the top chamber of a ThinCert™ tissue culture insert. Bottom chamber contained 500µl of RPMI 1640, 5% FBS, supplemented with 10ng/ml of EGF as a chemotractant agent. Membrane was coated with Culturex® growth factor reduced basement membrane (60µl). Cells were incubated for 20 hours and fixed with 0.025% glutaraldehyde for at least 20 minutes. Cells visualized by staining with 0.1% crystal violet in PBS for 30 minutes and the membrane was mounted on a glass slide. Cells were plated in triplicate across three wells and counted in 10 random fields. Total number of migratory cells was estimated by summing up each of the individual fields. The mean sum of the well is presented, along with the standard error.

Chapter 4

Reverse phase microArray identifies key proteins regulating cell growth

Reason for proteomics

Proteins have long been considered the workhorse of biological molecules. They are involved in nearly every cellular process from regulation of cell growth to initiation of apoptosis. Aberrant protein signaling pathways influence many processes that aid in tumorigenesis [37]. Traditionally, gene array profiling has been used to distinguish genes that are dysregulated during the development of disease. It was traditionally thought that mRNA expression reflected actual protein levels. Knowledge of post-transcriptional control affecting mRNA translation challenges this traditional theory. It is now known that most genes are influenced by at least one miRNA. Thus, mRNA expression correlates poorly with protein levels.

A more useful comparison would be miRNAs to protein levels, since protein synthesis is the direct target for miRNA regulation. It is true that some miRNA targeting results in mRNA degradation, but the more common outcome is a halt of translation. Although both methods of attack results in decreased protein levels, differences in mRNA expression correlate poorly with protein levels. Actually, few mRNAs have been shown to be degraded by miRNA binding. Obviously, direct measurement of protein content via a proteomic approach would be a better indicator of overall miRNA regulation than gene arrays. Unfortunately, gene arrays have been inappropriately used for this purpose, as they are freely available, relatively inexpensive and easily applied even by a novice. Proteomic arrays, on the other hand, require considerable expertise, a bevy of well characterized optimized antibodies and are not easily duplicated by the

novice. However, in order to identify proteins contributing to the development of CaP, one must utilize a high throughput proteomic method

Identifying key proteins that are dysregulated during tumorigenesis may reveal common pathways that are altered during cancer progression. Cellular fate is determined by minute fluctuations in the proteome of the cell [37]. The reverse phase protein microarray (RPMA) immobilizes hundreds of cellular lysates onto a nitrocellulose glass slide in a miniature dilution curve [112]. The slide is probed with an antibody to the protein of interest and the level of the protein is accurately determined. This method requires one slide for each antibody of interest. In this capacity, we have been assisted by Drs. Lance Liottta and Emmanuel Petricoin III from George Mason University, leaders of this technology. Ultimately, the method is high throughput allowing a researcher to quantify hundreds of proteins across hundreds of samples.

Materials and Methods

Cell culture

Cells are cultured at 37° C in RPMI1640 with L-glutamine obtained from Gibco supplemented with 5% fetal bovine serum, 5 μg/ml insulin, 5 μg/ml transferrin, and 5 μg/ml of selenium (ITS from Collaborative Research Bedford, MA). Inhibition of bacterial contamination was accomplished with the addition of Gentamycin (0.05 mg/ml). M12 cells stably transformed with the p-SIREN (M12+miR-17-3p and M12+miR-125b) vector were maintained with Puromycin (100 ng/ml). F6 cells were maintained with Geneticin (200 μg/ml) [24]. All tissue culture cells were grown in T75 flasks and split when

confluent. Cells were pelleted after trypsin (0.25% in EDTA) digestion by centrifugation at 5000 RPM for five minutes. After washing, cell pellets were flash frozen in liquid nitrogen after washing and stored for at least 24 hours. Three representative cell pellets were harvested during three serial passages for a total of 9 samples analyzed for each sample type was sent to the George Mason University Center for Applied Proteomics and Molecular Medicine. Overall, a total of 12 cell types were sent for RPMA analysis. All cell types were variants of the progression model described and many were designed to overexpress miRNAs of interest.

Reverse phase microarray

RPMA experiments were conducted at the George Mason University Center for Applied Proteomics and Molecular Medicine under the supervision of Dr Emmanuel Petricoin III. It is important to note that the cell pellets used for RNA extraction for miRNA profiling were also used for proteomics analysis. This approach minimizes variation from culture to culture. Briefly, cell pellets were lysed in a tissue extraction buffer and spotted on the nitrocellulose coated glass slide. Each lysate was spotted in a miniature dilution curve (1:1, 1:2, 1:4, 1:8, and 1:16) to ensure accurate quantification of each protein measured. Overall, the cellular lysate was spotted onto 111 slides and each incubated with a unique antibody. Data were returned to our group on a Microsoft Excel spreadsheet containing each cell type analyzed with each antibody of interest.

Statistical analysis

Using Microsoft Excel, a two sample equal variance T-test was used to test for significant differences among the P69 cells and M12 cells. The significance value was set at $\alpha = 0.05$.

Results

Significantly different proteins

Although there were a total of 12 cell types sent for RPMA evaluation, this study focuses on the P69 and M12 variants. It was found that there were 17 significantly dysregulated proteins between P69 and M12 cells (Table 4-1). Comparing the set of dysregulated proteins to our subset of miRNAs dyesregulated during tumorigenesis revealed several proteins regulated in part by miR-125b. Due to our proven interest in miR125b, we have concentrated on these targeted proteins first. Loss of miR-125b causes an increase during the transformation to a more tumorigenic phenotype of ErbB2 (2-fold) / ErbB3 (2.1-fold) and PI3K (1.5-fold) (Figure 4-1). As mentioned previously, activation of the PI3K/ AKT pathway increases cellular proliferation, invasion and metastasis. Activation of the PI3K/ AKT pathway plays a central role in the development of an oncogenic phenotype [127]. AKT activation is an essential survival mechanism in many cell types and is found in numerous forms of cancer including CaP.

Table 4-1: Statistically significant proteomics changes determined using RPMA

Protein	Fold change
Receptor Tyrosine Kinase	
ErbB2	1.8
ErbB3	2
p-ErbB3	1.3
p-PI3K	1.4
p-BAD	1.7
p c-KIT	700
Cell Cycle	
p27	0.7
Cyclin B1	0.6
Apoptosis	
p-BCL2	1.2
Cytochrome C	0.4
Caspase 7	1.5
Others	
Androgen Receptor	1.7
p-c-KIT	700
CD44	0.2
p-GSK3A/B	1.2

Figure 4-1: Model of AKT activation in prostate cancer

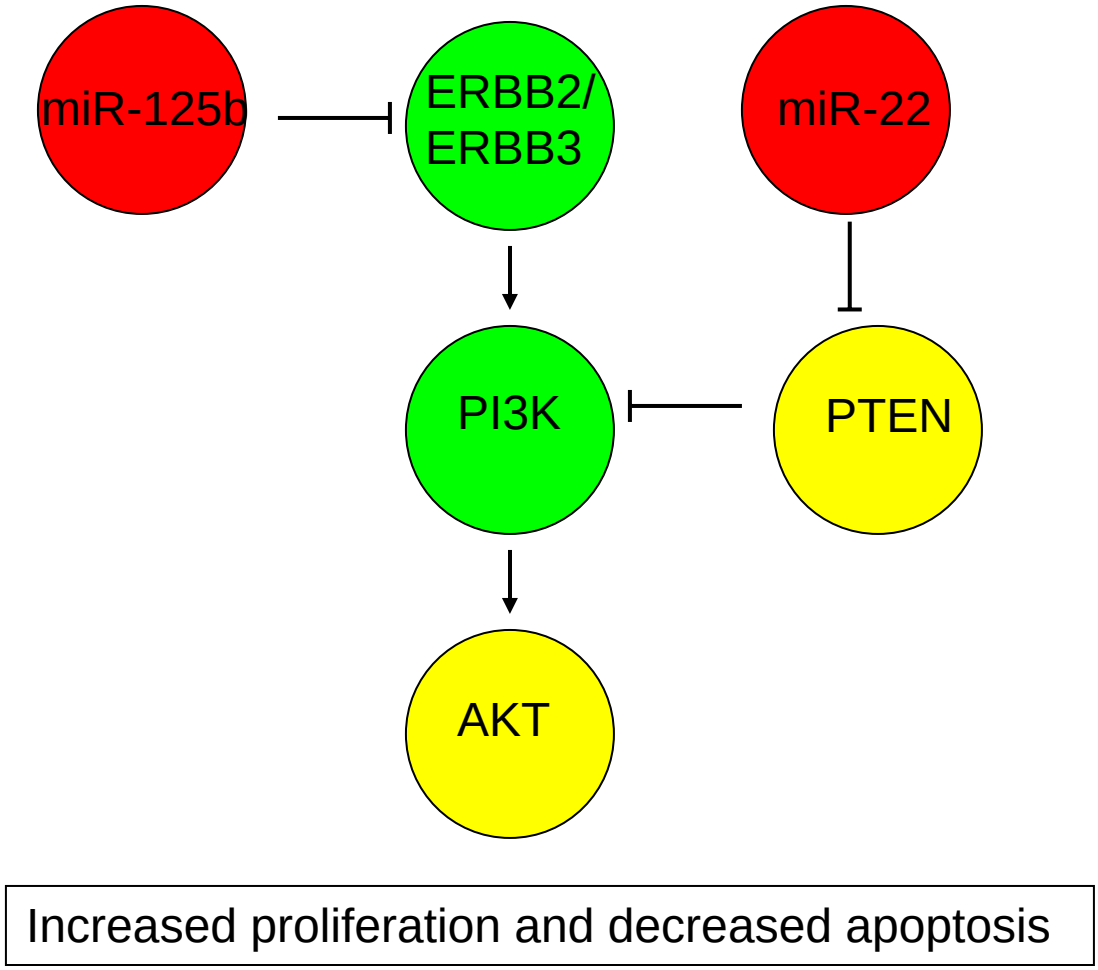

Figure 4-1: Model of AKT activation in prostate cancer

Combinatorial analysis of miRNA expression profiling and reverse phase proteomics reveals activation of the PI3K/ AKT pathway. Inhibition of miR-125b leads to increased expression of ERBB2/ ERBB3, thereby accelerating proliferation and inhibiting apoptosis. Nodes in red have been shown to be lost during prostate cancer development. Nodes in green increases as the tumor became more oncogenic. Nodes in yellow were not either not statistically significant or were not able to be assessed in the current study as antibodies were not included.

Literature shows that dysregulated PI3K activity is a major contributor to oncogenic transformation [128]. Increased activity of PI3K increases phosphorylation of AKT and affects a number of downstream targets that impart oncogenic potential. Proteomics analysis shows that increased expression of both ErbB2 and ErbB3 lead to a statistically significant increase in the phosphorylation of PI3K (p-value = 0.002) (Figure 4-2). AKT is activated by phosphorylation of two potential residues, serine-473 and threonine-308. Although not statistically significant, our results show a trend toward increased phosphorylation of serine-473. It is possible that with an increased sample number, we may be able to further resolve differences between samples and statistically show an increase in AKT activation.

AKT activation causes phosphorylation of BAD, a BCL-2 family member that induces apoptosis. Apoptosis results from the interaction of BAD and the BCL-Xl protein. In absence of phosphorylation, BAD induces cell death by phosphorylation of either serine-112 or serine-136 [129]. Phospho-BAD binds to 14-3-3 protein which sequesters BAD and inhibits apoptosis. Our analysis shows an increase in the phosphorylation of BAD, but not an increase in the basal expression of BAD. Taken together this data demonstrates that ErbB2/ ErbB3 accumulation activates the PI3K/ AKT pathway and inhibits apoptosis through phosphorylation of BAD.

RAS protein is a membrane bound protein that exists in 2 states of activation [130]. When a GDP molecule is bound to the cytoplasmic side of the protein, RAS is inactive. GTP binding activates the RAS molecule and initiates a

Figure 4-2: Pathways increased during prostate tumorigenesis

Analysis of RPMA data revealed that common members of the PI3K/ AKT pathway are activated during conversion of P69 cells to the more tumorigenic M12 variant. Overexpression of ErBB2/ ErbB3 and p-MET can also lead to activation of the RAS oncogenic pathway. Protein nodes in green were shown to be significantly upregulated during tumorigenesis (p-value <0.05). Proteins in yellow were not statistically significant.

Figure 4-2: Pathways increased during prostate tumorigenesis

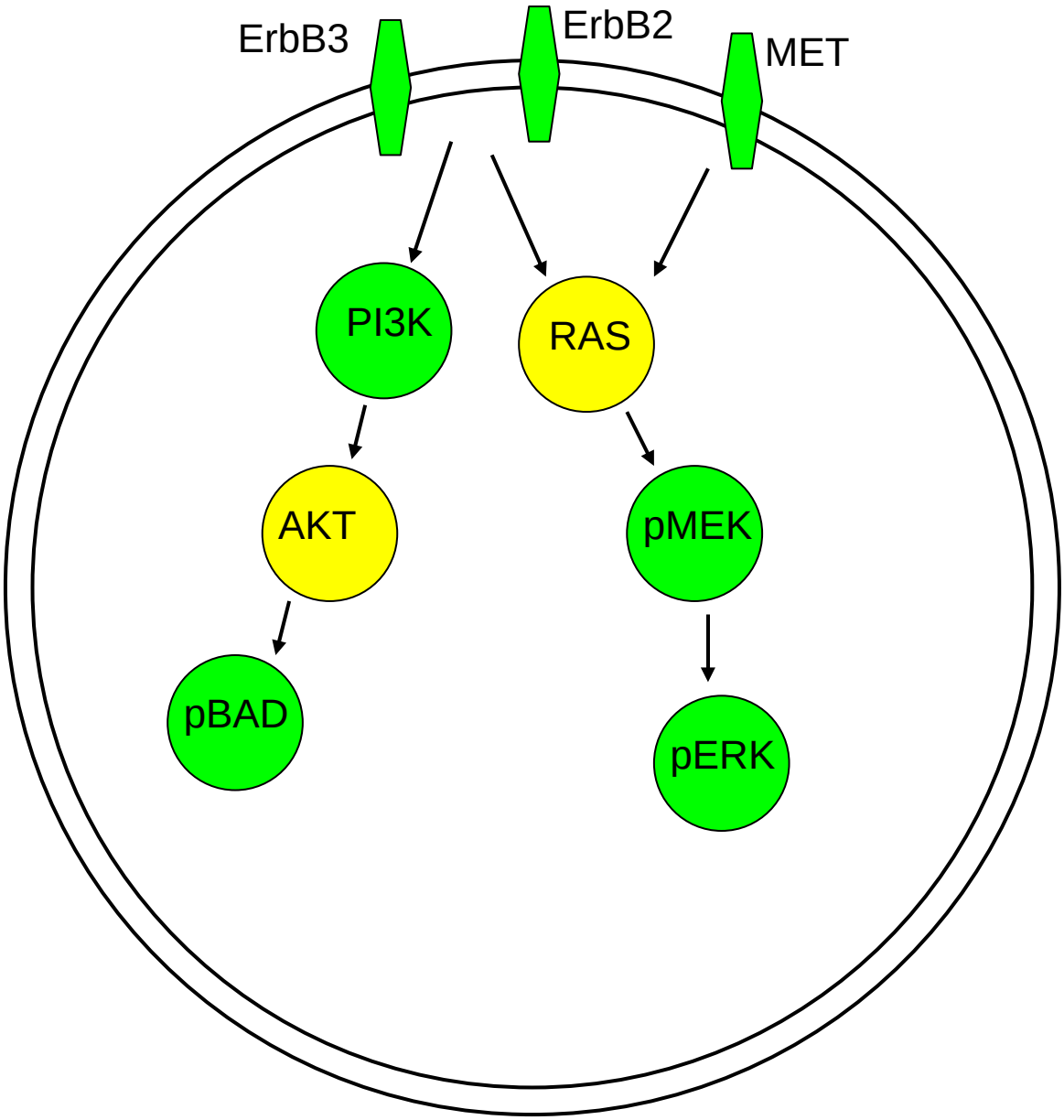

series of events inside of the cell that ultimately results in cell proliferation, cellular differentiation, cell survival, and an increase in cell motility.

ErbB2/ ErbB3 phosphorylation recruits the growth-factor-receptor-bound-protein 2 (GRB2) bound to SOS to the plasma membrane [130]. SOS recruitment to the membrane brings it in close proximity to the RAS molecule. Due to their proximity, a nucleotide exchange occurs between the two proteins activating RAS. RAS activation sets off a cascade of events, ultimately ending in phosphorylation of ERK. The phosphorylation of MEK1 is an intermediate step in the activation of ERK. ERK can affect numerous targets in the nucleus. Transcription factors regulated by p-ERK affect proliferation, differentiation, cell survival and motility.

Our data show that downstream targets of RAS such as p-MEK and p-ERK are more active in the highly tumorigenic, metastatic M12 variant. There is approximately 5-fold more p-ERK present in the M12 variant than there is in the P69 parental cell (p-value=0.03). Over expression and activation of the EGFR receptors (ErbB2/ErbB3) activate two downstream pathways that independently affect proliferation, apoptosis, and mobility. Targeted therapies against only one pathway are likely to be ineffective. However, re-expression of miR-125b may be a viable alternative that can inhibit both the PI3K/AKT and the MAPK/ ERK pathways through repression of ErbB2 and ErbB3.

Chapter 5

Summary and discussion

Prostate cancer is a leading cause of death of men in the United States; it is estimated that 1 in 6 men will be affected by prostate carcinoma at some point in their life. Cancer development is a multifactorial process influenced by age, ethnicity, and sexual factors. These factors influence a person's risk of developing prostate cancer. Traditionally, CaP was diagnosed with a digital rectal exam followed by transrectal biopsy of the gland. The advent of the PSA biomarker increased the likelihood of a man's compliance with active screening methods. However, as it has become clear that the PSA test is not a reliable indicator of prostate cancer formation, there has become a need to develop more accurate biomarkers. Diagnostic rates have declined in the last few years, particularly in the African-American population and in persons without a college education. It is known that African-Americans have a much higher death rate from prostate cancer than their Caucasian counterparts. Biomarkers that are non-invasive and can indicate early tumor formation are critically needed to minimize death and suffering from this disease.

In recent years, miRNAs have gained attention as important mediators of numerous cellular processes. Differential regulation has been observed in the development of numerous pathologies including cancer. This study has shown that miRNAs tend to regulate highly connected proteins and transcription factors affecting numerous downstream cellular pathways when dysregulated. Additionally, we have demonstrated that highly connected proteins are more likely to be regulated by more than one miRNA. Thus, dysregulation of even a single miRNA may impact intracellular stability and induce oncogenic transformation.

MiRNA dysregulation is a wide spread problem occurring during the development of prostate cancer. Using a unique genetically related prostate cancer cell progression model, we identified approximately 200 miRNAs that potentially influence cancer initiation, progression and metastasis. Initial profiling was accomplished with the Exiqon miRCURY LNA™ based array platform. As miRNAs influence post-transcriptional regulation of proteins, we identified key highly connected proteins using an innovative networks approach. Dysregulated miRNAs were ranked according to the sum connectivity of their proven targets. A subset of miRNAs was chosen for evaluation across all variants of the cancer progression model (5 oncomiRs, 3 tumor suppressors). Although all were identified to be dysregulated using the miRCURY array, several did not agree in estimated fold changes to single miRNA analyses. We conclude that array based platforms are ideal to determine gross regulation differences but true fold changes are only detectable with a single assay format.

miRNA changes were assessed using pure cell populations obtained after microdissection of human prostate tumor samples. Interestingly, only the identified tumor suppressors were universally confirmed in all of the human samples included in the study. One patient sample showed that many of the proposed oncomiRs increased during tumorigenesis but not all. This finding suggests that increased expression of oncomiRs may be tumor type dependent but loss of tumor suppressors is more universal. There are many mechanisms in which a tumor suppressor may be lost including epigenetic modification.

Our unique combinatorial approach integrated a bioinformatically driven networks method with high throughput miRNA screening and reverse phase proteomics

to identify key miRNAs and pathways associated with prostate cancer progression. This approach indicated that miR-125b may be an essential miRNA that drives prostate cancer progression as it is lost during the conversion of benign cells toward a more oncogenic state. At this point, our analysis focused in on miR-125b because of its regulation of the PI3K/ AKT pathway and its known involvement in cancer progression and initiation of metastasis. However, much of the knowledge regarding miR-125b dysregulation was discovered in breast cancer. Previous researchers have demonstrated that miR125b inhibits translation of the ERBB2/ ERBB3 members of the epidermal growth factor receptor family [106]. Analysis of miR-125b expression across epithelial subtypes showed that its level began decreasing in early pre-cancerous lesions (PIN) and the level continued to decline as the cancer progressed. .

Support of a potential role of miR-125b affecting the PI3K/ AKT pathway was found using a reverse phase proteomics array in which we observed an increase in ERBB2/ ERBB3 and PI3K. The loss of miR-125b results in an increase in the level of ERBB2/ERBB3 and increased activation of PI3K. Stable restoration of miR-125b in M12 cells decreased metastatic capability as evidenced by decreased cell migration and invasion through a basement membrane.

Various human tumors demonstrate progressive loss of miR-125b, suggesting that miR-125b may be a common tumor suppressor in numerous types of cancers [131]. However, there have been conflicting findings with some studies showing an increase in the level of miR-125b, while others have shown that miR-125b decreases in prostate cancer development. As discussed previously, miR-125b is dependent upon androgen sensitivity during the development of CaP.

There has been a large amount of effort in determining the role of miR-125b and ErbB2/ ErbB3 in breast cancer. Numerous reports have shown that loss of miR-125b in breast cancer decreases chances of survival and increases the likelihood of metastasis [131]. Two potential CpG rich islands were located within 2000 bp upstream of miR-125b. One of the potential CpG islands was shown to be heavily methylated in highly tumorigenic cell lines and invasive breast cancer tissue. Treatment with 5-AZA-Cr restored expression of miR-125b. Taken together these data demonstrate that hypermethylation of the promoter of miR-125b decreases its expression in breast cancer.

Although there is ample evidence that loss of miR-125b occurs frequently in the development of breast cancer and its loss directly affects the levels of ErbB2/ErbB3. There is little evidence in prostate cancer for a role of miR-125b. Our study clearly demonstrates that in androgen independent sublines, miR-125b functions as a tumor suppressor. Similar to the study conducted by Ozen et al, our study found that miR-125b decreased in all prostate cancer tumors analyzed [115]. Findings of this study confirm that miR-125b functions as a suppressor of tumor formation in the prostate gland and increases coordinately the levels of ErbB2/ErbB3 activating the PI3K/AKT and RAS oncogenes pathways. Taken together, these data suggest that loss of miR-125b may be an ideal biomarker for the identification of prostate cancer and potentially be used as a therapy to inhibit metastatic potential.

References

1. Zhu, X., Gerstein, M. & Snyder, M. Getting connected: analysis and principles of biological networks. *Genes Dev.* **21**, 1010-1024 (2007).

2. Hoffman, R. M. *et al*. Racial and ethnic differences in advanced-stage prostate cancer: the Prostate Cancer Outcomes Study. *J. Natl. Cancer Inst.* **93**, 388-395 (2001).

3. http://apps.nccd.cdc.gov/uscs/.

4. Catto, J. W. *et al*. Suitability of PSA-detected localised prostate cancers for focal therapy: experience from the ProtecT study. *Br. J. Cancer* **105**, 931-937 (2011).

5. Hankey, B. F. *et al*. Cancer surveillance series: interpreting trends in prostate cancer--part I: Evidence of the effects of screening in recent prostate cancer incidence, mortality, and survival rates. *J. Natl. Cancer Inst.* **91**, 1017-1024 (1999).

6. Haile, R. W. *et al*. A review of cancer in U.S. Hispanic populations. *Cancer. Prev. Res. (Phila)* **5**, 150-163 (2012).

7. Mordukhovich, I. *et al*. A review of African American-white differences in risk factors for cancer: prostate cancer. *Cancer Causes Control* **22**, 341-357 (2011).

8. Jones, B. A. *et al*. Explaining the race difference in prostate cancer stage at diagnosis. *Cancer Epidemiol. Biomarkers Prev.* **17**, 2825-2834 (2008).

9. Brooks, D. D., Wolf, A., Smith, R. A., Dash, C. & Guessous, I. Prostate cancer screening 2010: updated recommendations from the American Cancer Society. *J. Natl. Med. Assoc.* **102**, 423-429 (2010).

10. SEER*Stat Database: Incidence - SEER 9 Regs Research Data, Nov 2011 Sub (1973-2009) (2011).

11. Catalona, W. J. *et al*. Measurement of prostate-specific antigen in serum as a screening test for prostate cancer. *N. Engl. J. Med.* **324**, 1156-1161 (1991).

12. Lee, R. C., Feinbaum, R. L. & Ambros, V. The C. elegans heterochronic gene lin-4 encodes small RNAs with antisense complementarity to lin-14. *Cell* **75**, 843-854 (1993).

13. Hammond, S. M. MicroRNAs as oncogenes. *Curr. Opin. Genet. Dev.* **16**, 4-9 (2006).

14. DeVere White, R. W., Vinall, R. L., Tepper, C. G. & Shi, X. B. MicroRNAs and their potential for translation in prostate cancer. *Urol. Oncol.* **27**, 307-311 (2009).

15. Baskerville, S. & Bartel, D. P. Microarray profiling of microRNAs reveals frequent coexpression with neighboring miRNAs and host genes. *RNA* **11**, 241-247 (2005).

16. Lee, Y., Jeon, K., Lee, J. T., Kim, S. & Kim, V. N. MicroRNA maturation: stepwise processing and subcellular localization. *EMBO J.* **21**, 4663-4670 (2002).

17. Lee, Y. *et al*. The nuclear RNase III Drosha initiates microRNA processing. *Nature* **425**, 415-419 (2003).

18. Pillai, R. S. MicroRNA function: multiple mechanisms for a tiny RNA? *RNA* **11**, 1753-1761 (2005).

19. Elbashir, S. M., Harborth, J., Lendeckel, W., Yalcin, A. & Weber, K. T. Duplexes of 21-nucleotide RNAs mediate RNA interference in cultured mammalian cells. *Nature* **411**, 494-498 (2001).

20. Liu, J. *et al*. Argonaute2 is the catalytic engine of mammalian RNAi. *Science* **305**, 1437-1441 (2004).

21. Calin, G. A. *et al*. Human microRNA genes are frequently located at fragile sites and genomic regions involved in cancers. *Proc. Natl. Acad. Sci. U. S. A.* **101**, 2999-3004 (2004).

22. Esquela-Kerscher, A. & Slack, F. J. Oncomirs - microRNAs with a role in cancer. *Nat. Rev. Cancer.* **6**, 259-269 (2006).

23. Bae, V. L., Jackson-Cook, C. K., Brothman, A. R., Maygarden, S. J. & Ware, J. L. Tumorigenicity of SV40 T antigen immortalized human prostate epithelial cells: association with decreasedepidermal growth factor receptor (EGFR) expression. *Int. J. Cancer* **58**, 721-729 (1994).

24. Astbury, C., Jackson-Cook, C. K., Culp, S. H., Paisley, T. E. & Ware, J. L. Suppression of tumorigenicity in the human prostate cancer cell line M12 via microcell-mediated restoration of chromosome 19. *Genes Chromosomes Cancer* **31**, 143-155 (2001).

25. Porkka, K. P. *et al*. MicroRNA expression profiling in prostate cancer. *Cancer Res.* **67**, 6130-6135 (2007).

26. Castoldi, M. *et al*. A sensitive array for microRNA expression profiling (miChip) based on locked nucleic acids (LNA). *RNA* **12**, 913-920 (2006).

27. Castoldi, M., Schmidt, S., Benes, V., Hentze, M. W. & Muckenthaler, M. U. miChip: an array-based method for microRNA expression profiling using locked nucleic acid capture probes. *Nat. Protoc.* **3**, 321-329 (2008).

28. Braasch, D. A. & Corey, D. R. Locked nucleic acid (LNA): fine-tuning the recognition of DNA and RNA. *Chem. Biol.* **8**, 1-7 (2001).

29. Tang, X. *et al*. Detection of microRNAs in prostate cancer cells by microRNA array. *Methods Mol. Biol.* **732**, 69-88 (2011).

30. Ambs, S. *et al*. Genomic profiling of microRNA and mRNA reveals deregulated microRNA expresion in prostate cancer. *Cancer Res.* **68**, 6162-6170 (2008).

31. Croce, C. M. Causes and consequences of microRNA dysregulation in cancer. *Nat. Rev. Genet.* **10**, 704-714 (2009).

32. Ota, A. *et al*. Identification and characterization of a novel gene, C13orf25, as a target for 13q31-q32 amplification in malignant lymphoma. *Cancer Res.* **64**, 3087-3095 (2004).

33. Volinia, S. *et al*. A microRNA expression signature of human solid tumors defines cancer gene targets. *Proc. Natl. Acad. Sci. U. S. A.* **103**, 2257-2261 (2006).

34. Folini, M. *et al*. miR-21: an oncomir on strike in prostate cancer. *Mol. Cancer.* **9**, 12 (2010).

35. Coppola, V., De Maria, R. & Bonci, D. MicroRNAs and prostate cancer. *Endocr. Relat. Cancer* **17**, F1-17 (2010).

36. Thomas, R. K. *et al*. High-throughput oncogene mutation profiling in human cancer. *Nat. Genet.* **39**, 347-351 (2007).

37. Grubb, R. L. *et al*. Signal pathway profiling of prostate cancer using reverse phase protein arrays. *Proteomics* **3**, 2142-2146 (2003).

38. Sheehan, K. M. *et al*. Use of reverse phase protein microarrays and reference standard development for molecular network analysis of metastatic ovarian carcinoma. *Mol. Cell. Proteomics* **4**, 346-355 (2005).

39. Shi, X. B., Tepper, C. G. & White, R. W. MicroRNAs and prostate cancer. *J of Cell Mol Med* **12**, 1456-1465 (2008).

40. Espina, V. *et al*. Laser-capture microdissection. *Nat. Protoc.* **1**, 586-603 (2006).

41. Kitano, H. Systems biology: a brief overview. *Science* **295**, 1662-1664 (2002).

42. Ahn, A. C., Tewari, M., Poon, C. S. & Phillips, R. S. The limits of reductionism in medicine: could systems biology offer an alternative? *PLoS Med.* **3**, e208 (2006).

43. Van Regenmortel, M. H. Reductionism and complexity in molecular biology. Scientists now have the tools to unravel biological and overcome the limitations of reductionism. *EMBO Rep.* **5**, 1016-1020 (2004).

44. Batada, N. N., Hurst, L. D. & Tyers, M. Evolutionary and physiological importance of hub proteins. *PLoS Comput. Biol.* **2**, e88 (2006).

45. Liang, H. & Li, W. H. Gene essentiality, gene duplicability and protein connectivity in human and mouse. *Trends Genet.* **23**, 375-378 (2007).

46. Barabasi, A. L. & Oltvai, Z. N. Network biology: understanding the cell's functional organization. *Nat. Rev. Genet.* **5**, 101-113 (2004).

47. Yook, S. H., Oltvai, Z. N. & Barabasi, A. L. Functional and topological characterization of protein interaction networks. *Proteomics* **4**, 928-942 (2004).

48. Jiang, Q. *et al*. miR2Disease: a manually curated database for microRNA deregulation in human disease. *Nucleic Acids Res.* **37**, D98-104 (2009).

49. Papadopoulos, G. L., Reczko, M., Simossis, V. A., Sethupathy, P. & Hatzigeorgiou, A. G. The database of experimentally supported targets: a functional update of TarBase. *Nucleic Acids Res.* **37**, D155-8 (2009).

50. Xiao, F. *et al*. miRecords: an integrated resource for microRNA-target interactions. *Nucleic Acids Res.* **37**, D105-10 (2009).

51. Boguski, M. S. & Schuler, G. D. ESTablishing a human transcript map. *Nat. Genet.* **10**, 369-371 (1995).

52. Vailaya, A. *et al*. An architecture for biological information extraction and representation. *Bioinformatics* **21**, 430-438 (2005).

53. Cline, M. S. *et al*. Integration of biological networks and gene expression data using Cytoscape. *Nat. Protoc.* **2**, 2366-2382 (2007).

54. Scardoni, G., Petterlini, M. & Laudanna, C. Analyzing biological network parameters with CentiScaPe. *Bioinformatics* **25**, 2857-2859 (2009).

55. Fulton, D. L. *et al*. TFCat: the curated catalog of mouse and human transcription factors. *Genome Biol.* **10**, R29 (2009).

56. Lu, J. *et al*. MicroRNA expression profiles classify human cancers. *Nature* **435**, 834-838 (2005).

57. Schaefer, A. *et al*. Diagnostic and prognostic implications of microRNA profiling in prostate carcinoma. *Int. J. Cancer* **126**, 1166-1176 (2010).

58. Shi, X. B. *et al*. An androgen-regulated miRNA suppresses Bak1 expression and induces androgen-independent growth of prostate cancer cells. *Proc. Natl. Acad. Sci. U. S. A.* **104**, 19983-19988 (2007).

59. Scott, G. K. *et al*. Coordinate suppression of ERBB2 and ERBB3 by enforced expression of micro-RNA miR-125a or miR-125b. *J. Biol. Chem.* **282**, 1479-1486 (2007).

60. Safran, M. *et al*. GeneCards 2002: towards a complete, object-oriented, human gene compendium. *Bioinformatics* **18**, 1542-1543 (2002).

61. Lin, S. L., Chiang, A., Chang, D. & Ying, S. Y. Loss of mir-146a function in hormone-refractory prostate cancer. *RNA* **14**, 417-424 (2008).

62. Stelzl, U. *et al*. A human protein-protein interaction network: a resource for annotating the proteome. *Cell* **122**, 957-968 (2005).

63. Smoot, M. E., Ono, K., Ruscheinski, J., Wang, P. L. & Ideker, T. Cytoscape 2.8: new features for data integration and network visualization. *Bioinformatics* **27**, 431-432 (2011).

64. Goh, K. I. *et al*. The human disease network. *Proc. Natl. Acad. Sci. U. S. A.* **104**, 8685-8690 (2007).

65. Zanzoni, A., Soler-Lopez, M. & Aloy, P. A network medicine approach to human disease. *FEBS Lett.* **583**, 1759-1765 (2009).

66. Milo, R. *et al*. Network Motifs: Simple Building Blocks of Complex Networks. *Science* **298**, 824-827 (2002).

67. Rambaldi, D., Giorgi, F. M., Capuani, F., Ciliberto, A. & Ciccarelli, F. D. Low duplicability and network fragility of cancer genes. *Trends in Genetics* **24**, 427-430 (2008).

68. Sun, J. & Zhao, Z. A comparative study of cancer proteins in the human protein-protein interaction network. *BMC Genomics* **11 Suppl 3**, S5 (2010).

69. Hernandez, P. *et al*. Evidence for systems-level molecular mechanisms of tumorigenesis. *BMC Genomics* **8**, 185 (2007).

70. Hua, Z. *et al*. MiRNA-directed regulation of VEGF and other angiogenic factors under hypoxia. *PLoS One* **1**, e116 (2006).

71. Wu, S. *et al*. Multiple microRNAs modulate p21Cip1/Waf1 expression by directly targeting its 3' untranslated region. *Oncogene* **29**, 2302-2308 (2010).

72. Gartel, A. L. & Tyner, A. L. The role of the cyclin-dependent kinase inhibitor p21 in apoptosis. *Mol. Cancer. Ther.* **1**, 639-649 (2002).

73. Budd, W. T., Weaver, D. E., Anderson, J. & Zehner, Z. E. microRNA dysregulation in prostate cancer: network analysis reveals preferential regulation of highly connected nodes. *Chem. Biodivers* **9**, 857-867 (2012).

74. Livak, K. J. & Schmittgen, T. D. Analysis of relative gene expression data using real-time quantitative PCR and the $2^{-(\text{Delta DeltaC(T}}_{\text{))Method}}$. *Methods* **25**, 402-408 (2001).

75. Stone, K. R., Mickey, D. D., Wunderli, H., Mickey, G. H. & Paulson, D. F. Isolation of a human prostate carcinoma cell line (DU 145). *Int. J. Cancer* **21**, 274-281 (1978).

76. Thalmann, G. N. *et al*. Androgen-independent cancer progression and bone metastasis in the LNCaP model of human prostate cancer. *Cancer Res.* **54**, 2577-2581 (1994).

77. Horoszewica, J. S. *et al*. LNCaP model of human prostatic carcinoma. *Cancer Res.* **43**, 1809-1818 (1983).

78. Chuaqui, R. F. *et al*. Post-analysis follow-up and validation of microarray experiments. *Nat. Genet.* **32 Suppl**, 509-514 (2002).

79. Rajeevan, M. S., Vernon, S. D., Taysavang, N. & Unger, E. R. Validation of array-based gene expression profiles by real-time (kinetic) RT-PCR. *J. Mol. Diagn.* **3**, 26-31 (2001).

80. Griffiths-Jones, S. miRBase: microRNA sequences and annotation. *Curr. Protoc. Bioinformatics* **Chapter 12**, Unit 12.9.1-10 (2010).

81. Griffiths-Jones, S. The microRNA Registry. *Nucleic Acids Res.* **32**, D109-11 (2004).

82. Ponchel, F. *et al*. Real-time PCR based on SYBR-Green I fluorescence: an alternative to the TaqMan assay for a relative quantification of gene rearrangements, gene amplifications and micro gene deletions. *BMC Biotechnol.* **3**, 18 (2003).

83. Poliseno, L. *et al*. Identification of the miR-106b~25 microRNA cluster as a proto-oncogenic PTEN-targeting intron that cooperates with its host gene MCM7 in transformation. *Sci. Signal.* **3**, ra29 (2010).

84. He, L. Posttranscriptional regulation of PTEN dosage by noncoding RNAs. *Sci. Signal.* **3**, pe39 (2010).

85. Schliekelman, M. J. *et al*. Targets of the tumor suppressor miR-200 in regulation of the epithelial-mesenchymal transition in cancer. *Cancer Res.* **71**, 7670-7682 (2011).

86. Korpal, M. & Kang, Y. The emerging role of miR-200 family of microRNAs in epithelial-mesenchymal transition and cancer metastasis. *RNA Biol.* **5**, 115-119 (2008).

87. Lee, J. M., Dedhar, S., Kalluri, R. & Thompson, E. W. The epithelial-mesenchymal transition: new insights in signaling, development, and disease. *J. Cell Biol.* **172**, 973-981 (2006).

88. Lee, J. W. *et al*. The expression of the miRNA-200 family in endometrial endometrioid carcinoma. *Gynecol. Oncol.* **120**, 56-62 (2011).

89. Lin, T. *et al*. MicroRNA-143 as a tumor suppressor for bladder cancer. *J. Urol.* **181**, 1372-1380 (2009).

90. Zhang, X. *et al*. MicroRNA-17-3p is a prostate tumor suppressor in vitro and in vivo, and is decreased in high grade prostate tumors analyzed by laser capture microdissection. *Clin. Exp. Metastasis* **26**, 965-979 (2009).

91. Chen, J. F. *et al*. The role of microRNA-1 and microRNA-133 in skeletal muscle proliferation and differentiation. *Nat. Genet.* **38**, 228-233 (2006).

92. Halkidou, K., Cook, S., Leung, H. Y., Neal, D. E. & Robson, C. N. Nuclear accumulation of histone deacetylase 4 (HDAC4) coincides with the loss of androgen sensitivity in hormone refractory cancer of the prostate. *Eur. Urol.* **45**, 382-9; author reply 389 (2004).

93. Wach, S. *et al*. MicroRNA profiles of prostate carcinoma detected by multiplatform microRNA screening. *Int. J. Cancer* **130**, 611-621 (2012).

94. Brase, J. C., Wuttig, D., Kuner, R. & Sultmann, H. Serum microRNAs as non-invasive biomarkers for cancer. *Mol. Cancer.* **9**, 306 (2010).

95. Takahashi, S. *et al*. Down-regulation of human X-box binding protein 1 (hXBP-1) expression correlates with tumor progression in human prostate cancers. *Prostate* **50**, 154-161 (2002).

96. Rutkowski, D. T. & Kaufman, R. J. A trip to the ER: coping with stress. *Trends Cell Biol.* **14**, 20-28 (2004).

97. He, L. *et al*. A microRNA component of the p53 tumour suppressor network. *Nature* **4478**, 1130-1134 (2007).

98. Dutta, K. K. *et al*. Association of microRNA-34a overexpression with proliferation is cell type-dependent. *Cancer. Sci.* **98**, 1845-1852 (2007).

99. Vaupel, P., Kelleher, D. K. & Hockel, M. Oxygen status of malignant tumors: pathogenesis of hypoxia and significance for tumor therapy. *Semin. Oncol.* **28**, 29-35 (2001).

100. Lin, S. L., Chiang, A., Chang, D. & Ying, S. Y. Loss of mir-146a function in hormone-refractory prostate cancer. *RNA* **14**, 417-424 (2008).

101. Baltimore, D., Boldin, M. P., O'Connell, R. M., Rao, D. S. & Taganov, K. D. MicroRNAs: new regulators of immune cell development and function. *Nat. Immunol.* **9**, 839-845 (2008).

102. Vega, F. M. & Ridley, A. J. Rho GTPases in cancer cell biology. *FEBS Lett.* **582**, 2093-2101 (2008).

103. Song, G. & Wang, L. MiR-433 and miR-127 arise from independent overlapping primary transcripts encoded by the miR-433-127 locus. *PLoS One* **3**, e3574 (2008).

104. Saito, Y. & Jones, P. A. Epigenetic activation of tumor suppressor microRNAs in human cancer cells. *Cell. Cycle* **5**, 2220-2222 (2006).

105. Baron, B. W. *et al*. The human programmed cell death-2 (PDCD2) gene is a target of BCL6 repression: implications for a role of BCL6 in the down-regulation of apoptosis. *Proc. Natl. Acad. Sci. U. S. A.* **99**, 2860-2865 (2002).

106. Scott, G. K. *et al*. Coordinate suppression of ERBB2 and ERBB3 by enforced expression of micro-RNA miR-125a or miR-125b. *J. Biol. Chem.* **282**, 1479-1486 (2007).

107. DiLorenzo, G. *et al*. Expression of epidermal grwoth factor receptor correlates with disease relapse and progression to andronge-independence in human prostate cancer. *Clin. Cancer Res.* **8**, 3438-3444 (2002).

108. Canil, C. M. *et al*. Randomized phase II study of two doses of gefitinib in hormone-refractory prostate cancer: a trial of the National Cancer Institute of Canada-Clinical Trials Group. *J. Clin. Oncol.* **23**, 455-460 (2005).

109. Schaefer, A. *et al*. Diagnostic and prognostic implications of microRNA profiling in prostate carcinoma. *Int. J. Cancer* **126**, 1166-1176 (2010).

110. Burdall, S. E., Hanby, A. M., Lansdown, M. R. & Speirs, V. Breast cancer cell lines: friend or foe? *Breast Cancer Res.* **5**, 89-95 (2003).

111. Paweletz, C. P. *et al*. Reverse phase protein microarrays which capture disease progression show activation of pro-survival pathways at the cancer invasion front. *Oncogene* **20**, 1981-1989 (2001).

112. Paweletz, C. P., Liotta, L. A. & Petricoin, E. F.,3rd. New technologies for biomarker analysis of prostate cancer progression: Laser capture microdissection and tissue proteomics. *Urology* **57**, 160-163 (2001).

113. Calin, G. A. & Croce, C. M. MicroRNA-cancer connection: the beginning of a new tale. *Cancer Res.* **66**, 7390-7394 (2006).

114. De Marzo, A. M., Marchi, V. L., Epstein, J. I. & Nelson, W. G. Proliferative inflammatory atrophy of the prostate: implications for prostatic carcinogenesis. *Am. J. Pathol.* **155**, 1985-1992 (1999).

115. Ozen, M., Creighton, C. J., Ozdemir, M. & Ittmann, M. Widespread deregulation of microRNA expression in human prostate cancer. *Oncogene* **27**, 1788-1793 (2008).

116. Lujambio, A. & Esteller, M. CpG island hypermethylation of tumor suppressor microRNAs in human cancer. *Cell. Cycle* **6**, 1455-1459 (2007).

117. Chiosea, S. *et al*. Up-regulation of dicer, a component of the MicroRNA machinery in prostate adenocarcinoma. *Am. J. Pathol.* **169**, 1812-1820 (2006).

118. Sung, S. Y. & Chung, L. W. Prostate tumor-stroma interaction: molecular mechanisms and opportunities for therapeutic targeting. *Differentiation* **70**, 506-521 (2002).

119. Tuxhorh, J. A. *et al*. Reactive stroma in human prostate cancer: Induction of myofibroblast phenotype and extracellular matrix remodeling. *Clin. Cancer Res.* **8**, 2912-2923 (2002).

120. Isaacs, J. T. & Coffey, D. S. Etiology and disease process of benign prostatic hyperplasia. *Prostate Suppl.* **2**, 33-50 (1989).

121. Klink, J. C., Miocinovic, R., Magi Galluzzi, C. & Klein, E. A. High-grade prostatic intraepithelial neoplasia. *Korean J. Urol.* **53**, 297-303 (2012).

122. Bostwick, D. G., Liu, L., Brawer, M. K. & Qian, J. High-grade prostatic intraepithelial neoplasia. *Rev. Urol.* **6**, 171-179 (2004).

123. Sahai, E. Mechanisms of cancer cell invasion. *Curr. Opin. Genet. Dev.* **15**, 87-96 (2005).

124. Krutzfeldt, J., Poy, M. N. & Stoffel, M. Strategies to determine the biological function of microRNAs. *Nat. Genet.* **38 Suppl**, S14-9 (2006).

125. Lee, Y. S. & Dutta, A. MicroRNAs in cancer. *Annu. Rev. Pathol.* **4**, 199-227 (2009).

126. Repesh, L. A. A new in vitro assay for quantitating tumor cell invasion. *Invasion Metastasis* **9**, 192-208 (1989).

127. Shukla, S. *et al*. Activation of PI3K-Akt signaling pathway promotes prostate cancer cell invasion. *Int. J. Cancer* **121**, 1424-1432 (2007).

128. Chang, F. *et al*. Involvement of PI3K/Akt pathway in cell cycle progression, apoptosis, and neoplastic transformation: a target for cancer chemotherapy. *Leukemia* **17**, 590-603 (2003).

129. Datta, S. R. *et al*. Akt phosphorylation of BAD couples survival signals to the cell-intrinsic death machinery. *Cell* **91**, 231-241 (1997).

130. Downward, J. Targeting RAS signalling pathways in cancer therapy. *Nat. Rev. Cancer.* **3**, 11-22 (2003).

131. Zhang, Y. *et al*. miR-125b is methylated and functions as a tumor suppressor by regulating the ETS1 proto-oncogene in human invasive breast cancer. *Cancer Res.* **71**, 3552-3562 (2011).

Vita

William Thomas Budd was born August 27, 1973 in Alexanderia, Virginia and is a citizen of the United States of America. He graduated in 1991 from Orange County High School in Orange, Virginia. He graduated Magna Cum Laude from Virginia Commonwealth University with a Bachelors of Science in Bioinformatics in 2009. At Virginia Commonwealth University, he has taught Introduction to Life Science and Applications in Bioinformatics. At ECPI University, he has taught Anatomy and Physiology. Publications include a December 2009 study entitled "MicroRNA-17-3p is a Prostate Tumor Suppressor *In Vitro* and *In Vivo*, and is Decreased in High Grade Prostate Tumors as Analyzed by Laser Capture Microdissection" published in Clinical and Experimental Metastasis. Another paper recently published in Chemistry and Biodiversity was entitled "MicroRNA Dysregulation in Prostate Cancer: Biological Networks Analysis Reveals Preferential Regulation of Highly Connected Protein Nodes".